FE-2028-8

# KINETICS AND MECHANISM OF DESULFURIZATION AND DENITROGENATION OF COAL-DERIVED LIQUIDS

Seventh Quarterly Report, December 21, 1976—March 20, 1977

By
Bruce C. Gates
James R. Katzer
Jon H. Olson
Harold Kwart
Alvin B. Stiles

November 1977
(TIC Issuance Date)

Work Performed Under Contract No. EX-76-C-01-2028

Departments of Chemical Engineering and Chemistry
University of Delaware
Newark, Delaware


## U. S. DEPARTMENT OF ENERGY

## DISCLAIMER

## NOTICE

FE-2028-8
Distribution Category UC-90d

# KINETICS AND MECHANISM OF DESULFURIZATION AND DENITROGENATION OF COAL-DERIVED LIQUIDS



Seventh Quarterly Report for Period

December 21, 1976, to March 20, 1977

Prepared by:

Bruce C. Gates, James R. Katzer,
Jon H. Olson, Harold Kwart, and Alvin B. Stiles

Departments of Chemical Engineering and Chemistry
University of Delaware
Newark, Delaware 19711



Date Published

April 6, 1977

Prepared for

Fossil Energy
Energy Research and Development Administration
Washington, D.C.

Under Contract No. E(49-18)-2028

TABLE OF CONTENTS

## LIST OF TABLES

## LIST OF FIGURES

LIST OF FIGURES (cont)

LIST OF FIGURES (cont)

## I. ABSTRACT

Three high-pressure flow microreactors and two batch autoclave reactors have been used to study the reaction networks and kinetics of (1) catalytic hydrodesulfurization of dibenzothiophene and methyl-substituted dibenzothiophenes and (2) catalytic hydrodenitrogenation of acridine. The catalysts were commercial, sulfided $CoO-MoO_3/\gamma-Al_2O_3$ and commercial, sulfided $NiO-MoO_3/\gamma-Al_2O_3$.

At 300°C and 104 atm, dibenzothiophene reacts to give $H_2S$ and biphenyl in high yield. Methyl-substituted dibenzothiophenes react similarly, and each reaction is first-order in the sulfur-containing compound. Two methyl groups near the sulfur atom (in the 4 and 6 positions) reduce the reactivity tenfold, whereas methyl groups in positions further removed from the sulfur atom increase reactivity about twofold. These results are consistent with steric and inductive effects.

In acridine conversion, a large amount of hydrogenation precedes nitrogen removal. Breaking of the carbon-nitrogen bond is evidently part of the slowest reaction in the network. The Ni-Mo catalyst is about twice as active as the Co-Mo catalyst for ring hydrogenation, and the two catalysts are about equally active for breaking the carbon-nitrogen bond.

Aged catalysts taken from the H-Coal$^R$ process and containing coke and deposits of mineral matter were examined in experiments with dibenzothiophene hydrodesulfurization and quinoline hydrodenitrogenation. The activity of the used catalyst was reduced 20-fold for hydrodesulfurization of dibenzothiophene and fivefold for hydrodenitrogenation of quinoline. Most of the loss of hydrodesulfurization activity was associated with the mineral deposits and not with the coke.

## II. OBJECTIVES AND SCOPE

The major objectives of this research are as follows:

i) To develop high-pressure liquid-phase microreactors for operation in pulse and steady-state modes to allow determination of quantitative reaction kinetics and catalytic activities in experiments with small quantities of reactants and catalyst.

ii) To determine reaction networks, reaction kinetics, and relative reactivities for catalytic hydrodesulfurization of multi-ring aromatic sulfur-containing compounds found in coal-derived liquids.

iii) To determine reaction networks, reaction kinetics, and relative reactivities for catalytic hydrodenitrogenation of multi-ring aromatic nitrogen-containing compounds found in coal-derived liquids.

iv) To obtain quantitative data characterizing the chemical and physical properties of aged hydroprocessing catalysts used in coal liquefaction processes and to establish the mechanisms of deactivation of these hydroprocessing catalysts.

v) To develop reaction engineering models for predicting the behavior of coal-to-oil processing and of catalytic hydroprocessing of coal-derived liquids and to suggest methods for improved operation of hydrosulfurization and hydrodenitrogenation processes.

vi) In summary, to recommend improvements in processes for the catalytic hydroprocessing of coal-derived liquids.

## SCOPE

A unique high-pressure, liquid-phase microreactor is being developed for pulse (transient) and steady-state modes of operation for kinetic measurements to achieve objectives ii) through iv). The relative reactivities of the important types of multi-ring aromatic compounds containing sulfur and nitrogen are being measured under industrially important conditions (300-450°C and 500-4000 psi). The reaction networks and kinetics of several of the least-reactive multi-ring aromatic sulfur-containing and nitrogen-containing compounds commonly present in coal-derived liquids will be determined. Catalyst deactivation is an important aspect of the commercial scale upgrading of coal-derived liquids. Accordingly, the chemical and physical properties of commercially aged coal-processing catalysts are being determined to provide an understanding of catalyst deactivation; these efforts can lead to improved catalysts or procedures to minimize the problem. To make the results of this and related research most useful to ERDA, reaction engineering models of coal-to-oil processing in trickle-bed and slurry-bed catalytic reactors including deactivation will be developed to predict conditions for optimum operation of these processes. Based on the integrated result of all of the above work, recommendations will be made to ERDA for improved catalytic hydrodesulfurization and hydrodenitrogenation processing.

## III. SUMMARY OF PROGRESS TO DATE

This summary is organized to parallel the task statements of the contract. A milestone chart is provided at the end of this section.

### Microreactor Development

Three continuous-flow, liquid-phase, high-pressure microreactors have been built and operated under this contract. The work in this report confirms the success of these microreactors; the data from the batch autoclave runs are effectively identical to data from the flow microreactors. This task has been completed.

### Catalytic Hydrodesulfurization

The hydrodesulfurization of dibenzothiophene (DBT) has been examined with a liquid-phase, high-pressure microreactor and in batch, stirred-autoclave experiments. The range of data collected thus far shows that the reaction network is slightly more complex than the direct reduction of DBT to hydrocarbon products; the reaction is first order in the concentration of DBT. The principal product of the reaction is biphenyl; phenylcyclohexane and bicyclohexane have been identified tentatively as the other two hydrocarbon reaction products.

The relative rates of hydrodesulfurization of a variety of the important compounds in coal-derived liquids have been determined. The compounds include methyl-substituted dibenzothiophenes, which evidently are among the least reactive compounds in hydrodesulfurization. The relative rate constants for the various reactants are the following: BT, very large; DBT, 1; 4-MeDBT, 0.16; 4,6-diMeDBT, 0.10; 3,7-diMeDBT, 1.7; and 2,8-diMeDBT, 2.6. These results are largely explained by steric effects. Groups located near the S atom restrict its interaction with a surface anion vacancy and lower the reactivity. Inductive effects explain the higher reactivities of the compounds having methyl substituents where they exert no steric influence.

### Catalytic Hydrodenitrogenation

The hydrodenitrogenation of quinoline has been studied to yield a nearly complete identification of the reaction network and partial identification of the rate parameters in this network. The network under catalytic conditions is as follows:

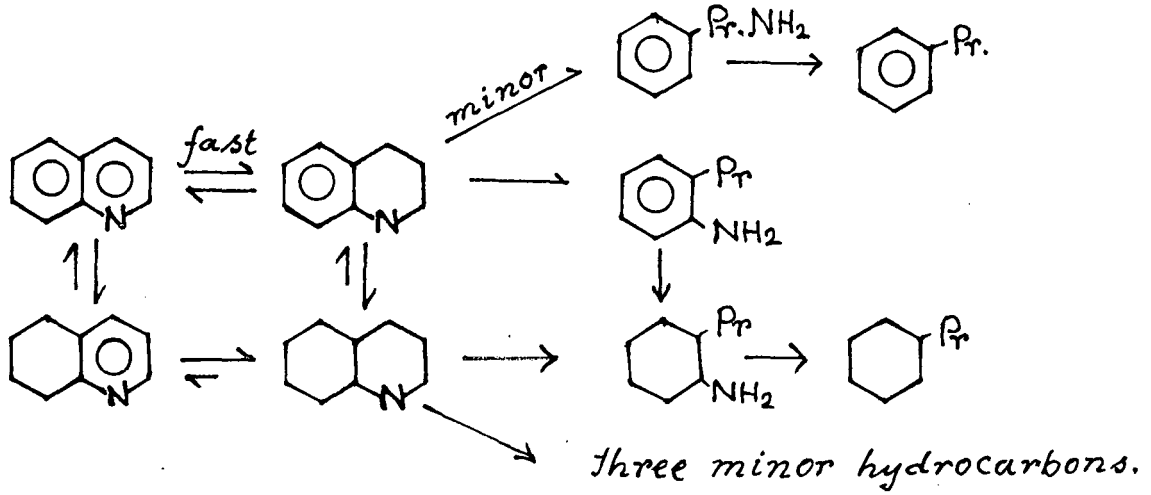


This network shows that usually both the benzene and pyridine rings are saturated before the C-N bond in the (now) piperidine ring is broken. Thus, the HDN of quinoline requires a large consumption of hydrogen before the N atom is removed from the hydrocarbon backbone.

The total rate of HDN shows a maximum with respect to hydrogen partial pressure. However, the only individual reaction in the network which decreases in rate with hydrogen partial pressure is the conversion of 1,2,3,4-tetrahydroquinoline to ortho-n-propylaniline; therefore, this reaction dominates the overall network at high pressure.

In hydrodenitrogenation of acridine, a large amount of hydrogenation precedes nitrogen removal, and the carbon-nitrogen bond breaking is the rate-determining process. In the presence of Co-Mo/$\gamma$-$Al_2O_3$ catalyst, heteroaromatic ring hydrogenation is favored, and with a Ni-Mo/$\gamma$-$Al_2O_3$ catalyst, aromatic ring hydrogenation is favored. For both acridine and quinoline, little effect of replacing Co with Ni could be detected in the nitrogen removal reaction, although Ni-Mo/$\gamma$-$Al_2O_3$ is twice as active as Co-Mo/$\gamma$-$Al_2O_3$.

## Catalyst Deactivation

A variety of physical techniques have been used to identify the aging processes for catalysts used in synthetic liquid fuel processes. Catalyst samples from three processes have been examined: a proprietary fixed-bed process, Synthoil, and H-Coal$^R$. The spent fixed-bed catalysts show the formation of an external crust which appears to be formed by columnar grain growth combined with the deposition of coal mineral matter, particularly clays and rutile. This external crust is absent from the H-Coal$^R$ catalyst. The interior of the catalyst is altered by several processes: coking, reactive deposition of mineral matter, passive deposition of mineral matter, and crack enhancement. These four processes are found in catalysts from all three processes. Coking fills the micropore volume of the catalyst. Reactive deposition of mineral matter penetrates about 200 μm from the outer surface into the interior of the catalyst. The concentration profile is approximately exponentially decreasing from the surface. Passive cementing occurs within 50 μm of the surface unless the cracks have been enlarged by grain growth; this deposition yields irregular concentration profiles. Finally, grain growth can occur inside the catalyst near the surface and tends to increase these cracks. When the surface cracks become a significant portion of the pore volume, passive deposition can penetrate further into the interior of the catalyst.

The activity of aged catalyst from the H-Coal$^R$ process has been measured in batch experiments with dibenzothiophene and with quinoline. The activity was reduced 20-fold for HDS of dibenzothiophene and five-fold for HDN of quinoline. Burning off of carbonaceous deposits increased the activity of the aged catalyst only three-fold for dibenzothiophene HDS, which implies that irreversibly deposited inorganic matter was responsible for most of the loss of catalytic activity.

## Microreactor Engineering

The use of moments as a tool in interpreting pulse data from microreactors has been extended to fairly complex reaction networks. This work is now complete. The complex data for quinoline and acridine reactions have been reduced to rate parameters by extension of nonlinear regression analysis.

## TIME PLAN* AND MILESTONE CHART**

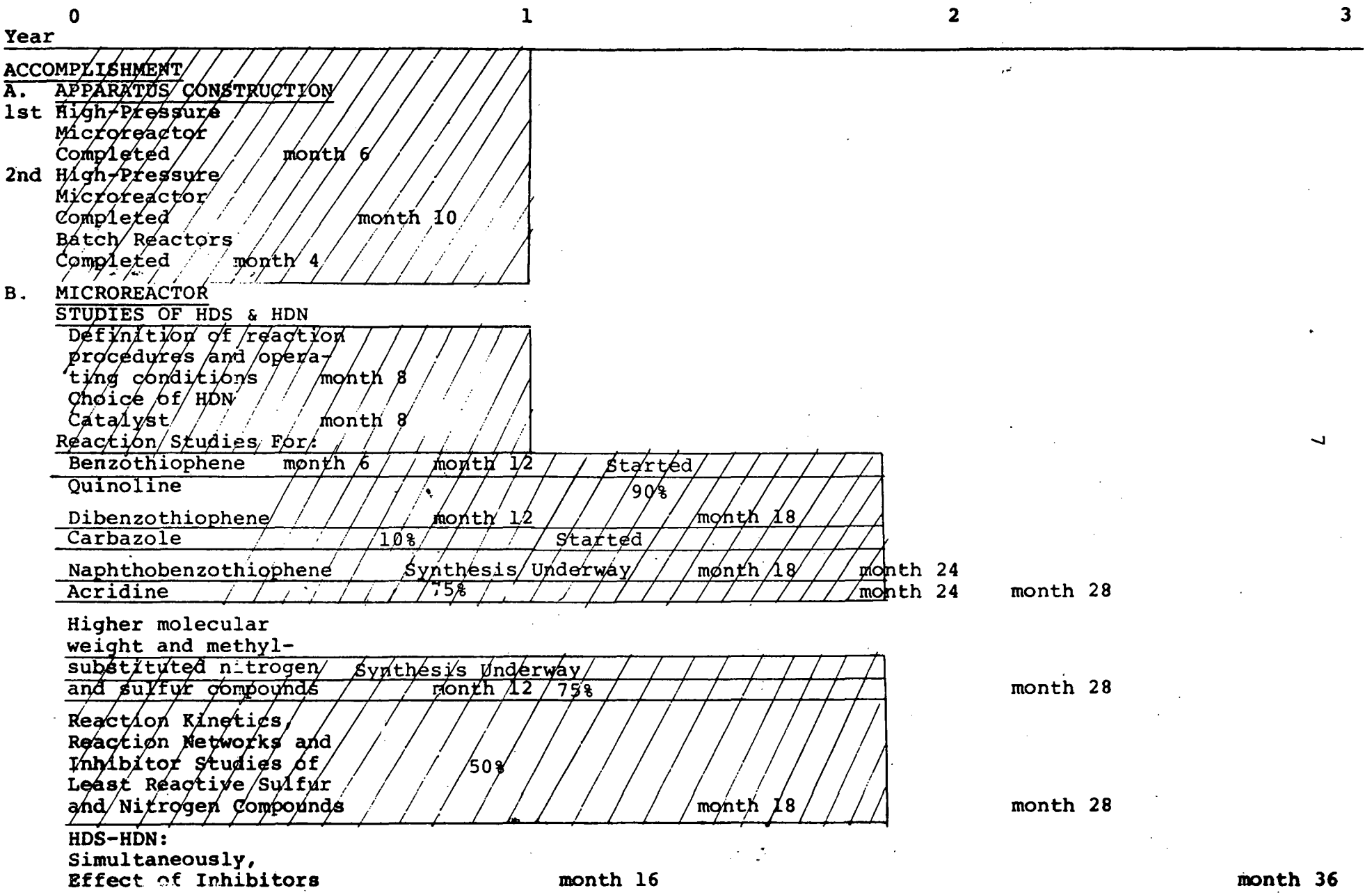

## TIME PLAN* AND MILESTONE CHART** (cont)

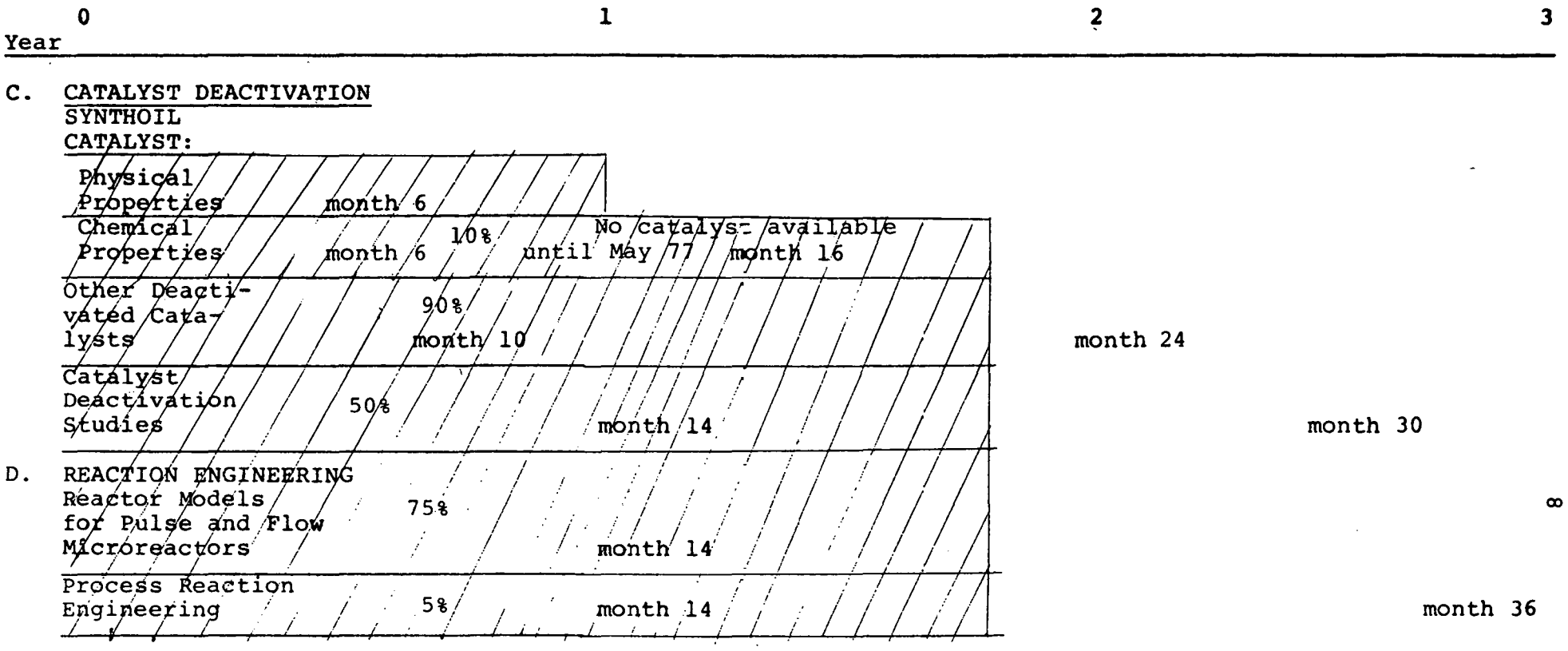


*Time Plan and Milestone Chart as Presented in Proposal.

**Hatching indicates that activity indicated is under active investigation; number in hatched region indicates the precentage completed; crosshatching indicates that the task has been completed.

CUMULATIVE EXPENDITURES*

| Item | Quarter | | | | | | |
|---|---|---|---|---|---|---|---|
| | First | Second | Third | Fourth | Fifth | Sixth | Seventh |
| Personnel | $5,807 | $20,740 | $37,396 | $53,418 | $91,593 | $112,666 | $132,669 |
| Travel | 28 | 528 | 1,152 | 1,152 | 1,521 | 2,458 | 3,140 |
| Supplies & Expense | 4,674 | 10,007 | 19,582 | 25,735 | 37,291 | 42,341 | 51,589 |
| Occupancy & Maintenance | 6,110 | 9,208 | 10,108 | 10,634 | 13,755 | 13,920 | 14,396 |
| Equipment | 610 | 17,978 | 30,704 | 34,930 | 50,614 | 54,013 | 54,013 |
| Information Processing | -- | -- | -- | 97 | 154 | 375 | 1,180 |
| Transfers (Overhead) | -- | 10,202 | 20,035 | 38,710 | 75,839 | 93,287 | 113,830 |



*Includes encumbrances

# IV. DETAILED DESCRIPTION OF TECHNICAL PROGRESS

## A. HYDROPROCESSING MICROREACTOR DEVELOPMENT

The first high-pressure microreactor continues to be used in routine operation for study of the relative reactivities of dibenzothiophene and methyl-substituted dibenzothiophenes. The construction of the third high-pressure unit has been completed. The equipment has been tested and its performance checked and compared to that of the first microreactor.

## B. CATALYTIC HYDRODESULFURIZATION

### 1. Experimental

#### a. Third high-pressure flow microreactor

The third microreactor is operational. The unit has been tested in experiments to confirm the results obtained with the first microreactor, and it is to be used in the next period to study dibenzothiophene (DBT) hydrodesulfurization kinetics.

Reproducibility experiments performed with the microreactor have been carried out under the same conditons described in section (b) below for the first microreactor. Some modifications of the standard conditions were then made to decrease the conversion level to the differential range and allow direct determination of reaction rates (Table 1).

#### b. First high-pressure flow microreactor

The microreactor operating conditions were the same as reported in the fifth and sixth quarterly reports in this series and are summarized below:

- Catalyst: HDS 16A; mass: 25 mg, volume of reactor bed: 0.325 $cm^3$, length of bed: 4.1 cm; catalyst particle size = 149-178 μm.
- Pretreatment: catalyst sulfided *in situ* with 10% $H_2S$ in $H_2$ for 2 hours at 400°C.
- Liquid flow rate: 1.2 to 7.2 $cm^3/hr$
- $H_2$ saturation pressure: 1000 psig
- Reaction temperature: 300°C
- Reactant mixture: 0.12 wt % DBT in *n*-hexadecane carrier oil

Reactivities of biphenyl and hexahydroDBT, possible intermediates in the HDS network for DBT, have been determined using the following reactant mixtures:

~0.1 wt % biphenyl in *n*-hexadecane
~0.126 wt % hexahydroDBT in *n*-hexadecane

TABLE 1

MODIFICATION OF THE STANDARD CONDITION
REALIZED WITH THE THIRD MICROREACTOR

| | Catalyst Weight, mg | Alundum Weight, mg | Bed Height, cm | Bed Volume, $cm^3$ |
|---|---|---|---|---|
| First unit | 25 | 625 | 4.1 | 0.325 |
| Third unit | 10 | 280 | 2.0 | 0.158 |

## 2. Analytical

In addition to the glc analysis described in previous reports, work was begun in this quarter on glc/ mass spectrometer identification of reaction intermediates and products. The technique includes dry column chromatography to concentrate and separate the products followed by glc/mass spectrometry to identify the individual product peaks. Simultaneous analysis of the concentrated product samples is done by glc alone using both FID and FPD sulfur-specific detectors. The large quantities of product in hexadecane necessary for dry column work (1-200 $cm^3$) are obtained most readily from the batch experiments or by collecting liquid from the flow reactors during several days of operation.

## 3. Results and Discussion

### a. Comparison between the first and third microreactors

The data from two initial runs in microreactor No. 3 are shown in Figure 1. The data indicate a satisfactory reproducibility and good operation of the new microreactor at the standard operating conditons established with microreactor No. 1. The DBT conversion level was the same in both microreactors (see Figure 3 of the sixth quarterly report). Likewise, data from both reactors taken at various liquid flow rates and otherwise the same standard conditions give nearly equal rate constant and good fits assuming first-order kinetics in DBT (for the limited number of points taken). These results confirm the proper operation of the third microreactor and substantiate the results being obtained from the first reactor.

### b. Reaction network for DBT HDS

The reaction network for hydrodesulfurization of DBT proposed in the fourth quarterly report is:

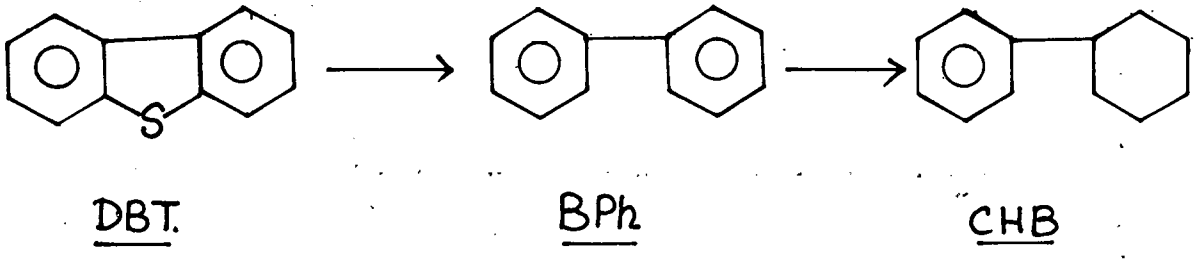


During the past quarter, dry column chromatography and mass spectrometry of samples of previous runs and two runs with biphenyl and hexahydrodibenzothiophene as reactants have added information relative to the DBT network. The reactant-product

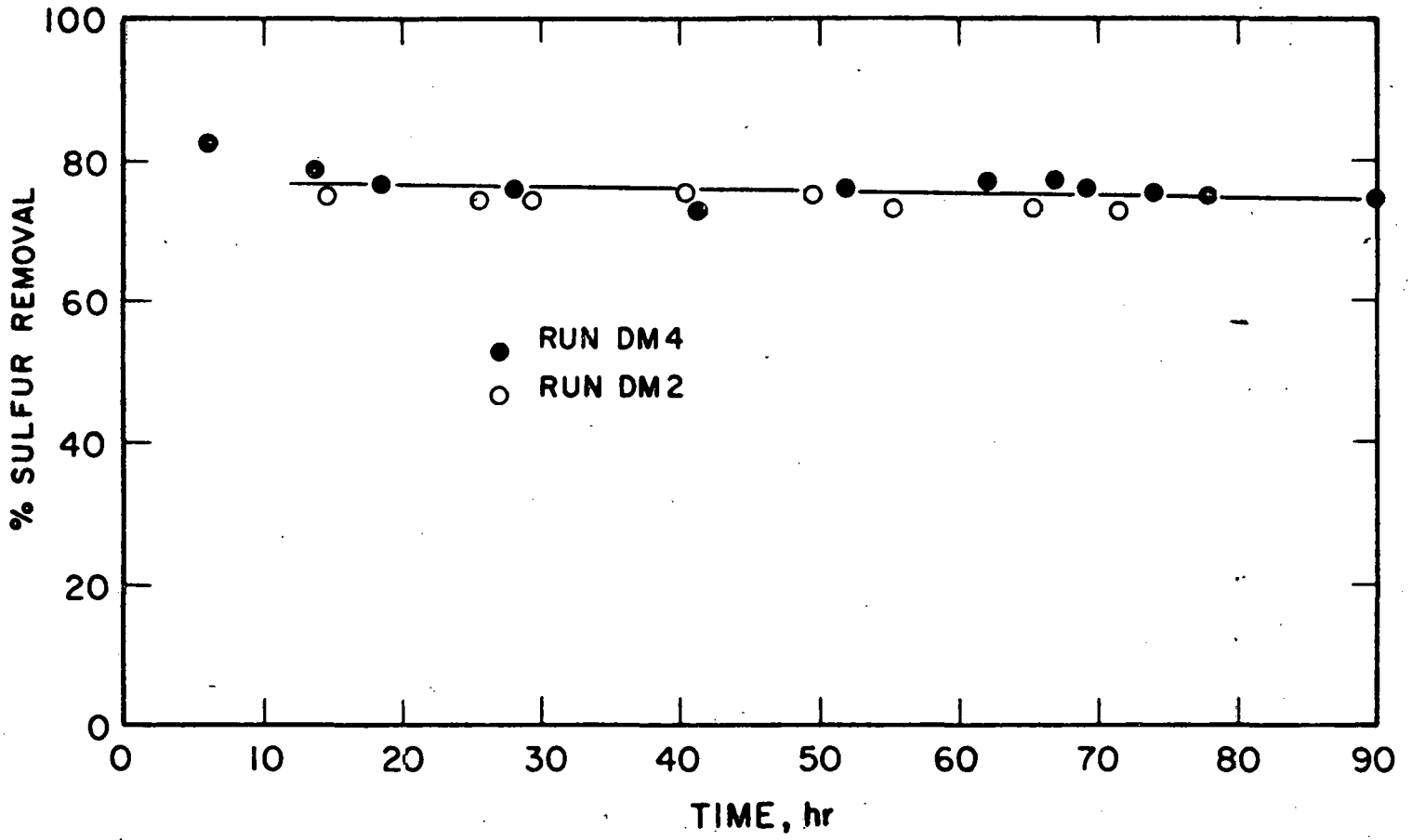


Figure 1. Reproducibility of DBT HDS activity in microreactor No. 3 under standard operating conditions.

mixture remaining from the batch runs Nos. 8 and 9 (see the sixth quarterly report) were concentrated by means of dry column chromatography and analyzed on the glc/mass spectrometer, with FID and FPD detectors. A second sulfur-containing compound (probably tetrahydrodibenzothiophene) was observed. The major product was identified as biphenyl as expected, and a minor product was found, which is judged likely to be cyclohexylbenzene. No other hydrogenated compounds with or without sulfur were found. From the run with biphenyl + $H_2$ in n-hexadecane feed analyzed by glc with the FID detector only, the percent conversion was observed to be less than 10, and the only product was cyclohexylbenzene (CHB). The concentration of CHB produced from biphenyl (BPh) present as the feed at a concentration of about 0.10 wt % was almost half that produced during the HDS of DBT in which the concentration of BPh as a product from DBT is somewhat less. This indicates that BPh is probably not the only precursor of CHB.

When 6-hydrodibenzothiophene (6-HDBT) was reacted under the same standard conditions, the major product was CHB with at least two minor products, one of which was BPh. Again what appears to be tetrahydroDBT was observed, this time in relatively large amounts, whereas 6-HDBT was not detectable by the FPD sulfur-specific detector. Further analytical work is in progress.

## B.1 RELATIVE REACTIVITIES OF METHYL-SUBSTITUTED DIBENZOTHIOPHENES

### 1. Introduction

Thiophenes and related compounds are among the most abundant sulfur-containing residues in coal hydrogenation products (Akhtar et al., 1974). Sharkey et al. (1966) found 14 substituted thiophenic compounds which are liberated from coal during the Synthoil liquefaction hydrodesulfurization process. One of the most stable of these is evidently dibenzothiophene:

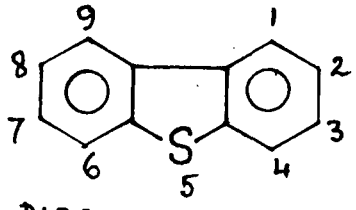


DIBENZOTHIOPHENE

Because of the large number of methyl groups in the aromatic coal-derived liquids, methyl-substituted dibenzothiophenes are expected to represent a class of thiophenic compounds that are expected to be both abundant and relatively unreactive. They are therefore of primary interest in this work.

Almost no quantitative studies have been reported of reactivities (or relative reactivities) of these compounds under the conditions of the Synthoil process or other potential commerical processes. Frye and Mosby (1967) studied the hydrodesulfurization of components in petroleum light catalytic cycle oil, boiling range about 450° to 600°K. They reported a gas chromatographic analysis showing the sulfur analysis of the feed and the products from desulfurization (Figure 2). Three compounds related to dibenzothiophene appear in the gas chromatogram of the feed. They are, respectively, dibenzothiophene itself, methyl-substituted dibenzothiophenes, and (probably) dimethyldibenzothiophene. No information about the positions of the methyl substituents on the aromatic rings was given. Figure 2 indicates low reactivities of methyldibenzothiophene and (presumably) dimethyldibenzothiophene, relative to dibenzothiophene.

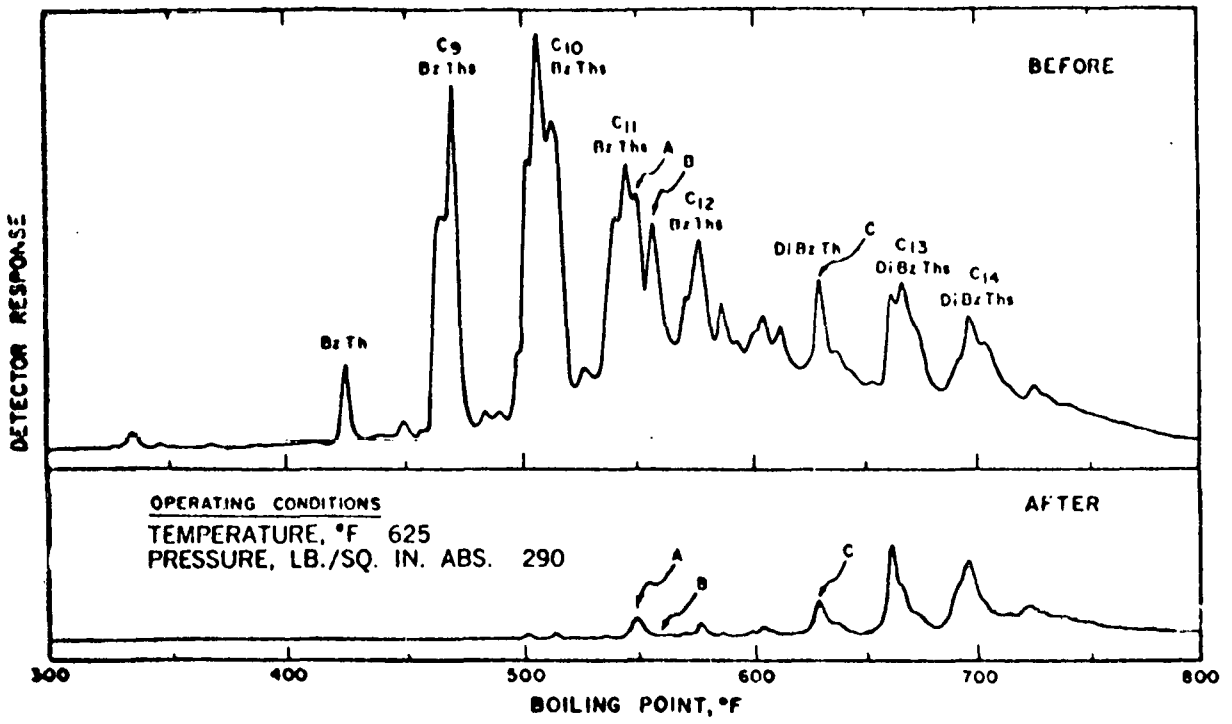


Figure 2. Gas chromatographic analyses of light catalytic cycle oil before and after hydrodesulfurization (Frye and Mosby, 1967).

Beuther (1975) reported that incorporation of methyl groups in the 4 and 6 positons of DBT (adjacent to the sulfur) leads to roughly a 100-fold decrease in the rate of desulfurization. (No reaction conditions or catalyst specifications were reported in this work, however.)

Jewell et al. (1975), in their study of isolation and characterization of sulfur-containing compounds in petroleum, concluded that within the class of alkyl-substituted dibenzothiophene the position of the alkyl group R relative to the sulfur has more effect on the rate of desulfurization than the size of R.

Carruthers (1955) observed that 4,6-diMeDBT (designated incorrectly by him as 1,8-dimethyldibenzothiophene) could not be desulfurized with Raney nickel in boiling ethanol, although dibenzothiophene itself at these conditions was converted into BPh in 5% yield. Kruber and Raeithel (1954) were, likewise, unable to desulfurize this methyl-substituted compound. Moreover, 4-methyldibenzothiophene has been found to be equally resistant to hydrodesulfurization with Raney nickel (Carruthers, 1955).

A more thorough study of the reactivities of methyl-substituted benzothiophenes has been reported by Givens and Venuto (1970). Their observations can be summarized as follows:

Methyl substitution of benzothiophene leads to a decrease in the reactivity for sulfur removal (Table 2). The drop in reactivity is more pronounced when the methyl group is on the thiophene ring, especially in the 3-position:

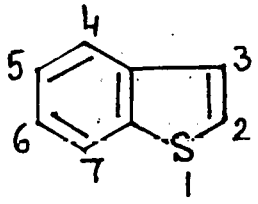


BENZOTHIOPHENE.

It must be recalled that the data of Givens and Venuto were determined only at high conversions, and may therefore not be a good indication of relative reactivities; furthermore, their results were obtained at atmospheric pressure and not under practical industrial conditions, and their catalyst was not presulfided.

TABLE 2

CONVERSION AND HYDRODESULFURIZATION SELECTIVITY
OF METHYL- AND POLYMETHYL-BENZO[B]THIOPHENES

| Position (Me group) | none | 7 | 2 | 2,7 | 3 | 3,7 | 2,3 | 2,3,7 |
|---|---|---|---|---|---|---|---|---|
| Conversion[a-1] | 91-99 | 60 | 74 | 54 | 43 | 47 | 39 | 47 |
| Hydrodesulfurization[a-2] | 91-99 | 57 | 66 | 43 | 32 | 24 | 15 | 16 |
| Selectivity (%)[b] | 100 | 95 | 89 | 80 | 75 | 51 | 38 | 34 |

[a]Reported as % reactant -1 converted and -2 desulfurized.
[b]Hydrodesulfurization/conversion x 100

Based on this literature review, it is clear that there is a need to undertake a relative reactivity study of methyl-substituted dibenzothiophenes using the aforementioned flow reactor especially suited to high-pressure hydroprocessing reactions.

## 2. Experimental

### a. Apparatus

Relative reactivity studies were carried out using the high-pressure flow microreactor. The design and operation of the reactor are described in the literature (Eliezer et al., in press). The reactor operates with solid particles of catalyst and a liquid reactant phase saturated with hydrogen.

### b. Operating Conditions

Catalyst: Commerical Co-Mo/$\gamma$-$Al_2O_3$ (American Cyanamid) (HDS 16A)
Mass: 0.025g diluted with alundum
Particle size: 149-178 μm
Volume of catalyst bed: 0.325 $cm^3$
Length of bed: 4.1 cm

Catalyst Pretreatment: Sulfided in situ with 10% $H_2S$ in $H_2$ for 2 hours at 400°C

Hydrogen Saturation Pressure: 1000 psig

Reactor Pressure: 1500 psig

Reaction Temperature: 300°C

Liquid Flowrate: 1.2 to 7.2 $cm^3/hr$

Reaction Mixture: The following reaction mixtures were studied:

| | | |
|---|---|---|
| (0.0663 wt %) | DBT - 4-methylDBT | (0.0637 wt %) |
| (0.0582 wt %) | DBT - 4,6-dimethylDBT | (0.075 wt %) |
| (0.0601 wt %) | DBT - 3,7-dimethylDBT | (0.0659 wt %) |
| (0.053 wt %) | DBT - 2,8-dimethylDBT | (0.056 wt %) |

The carrier oil was n-hexadecane

## 3. Materials

- Dibenzothiophene available from Aldrich, 95%
- 4-MeDBT was synthesized according to the method of Campaigne et al. (1964)

- The dimethyl-substituted DBT's were prepared according to the procedure of Gerdil and Luchen (1965).

- n-hexadecane was supplied by Columbia and Humphrey (purity 99%)

The reactant structures are as follows:

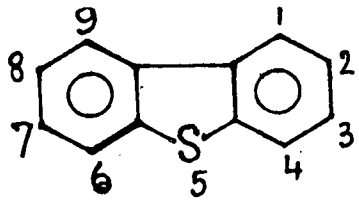


DBT.

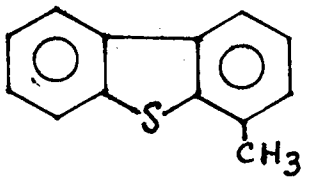


4-Me DBT.

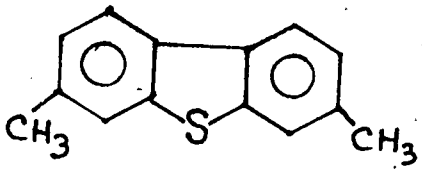


3:7 Di-Me.DBT.

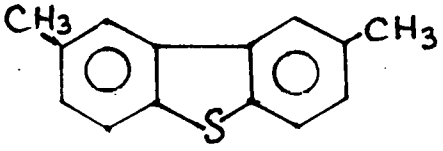


2:8-Di-Me DBT.

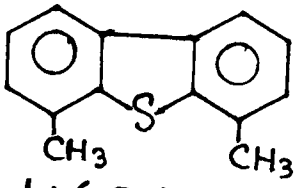


4:6 Di Me.DBT.

## 4. Experimental Procedures

In a typical run, after sulfiding of the catalyst in the reactor for two hours with 10% $H_2S$ in $H_2$ at 400°C, the reactant mixture (purged and saturated with hydrogen) was supplied to the syringe pump. After the desired flow rate was set, the liquid feed flowed through the catalyst bed, maintained at 300°C, to a dead-volume cylinder. The product was sampled every several hours and analyzed with an Antek glc (440L) with an FID. The glc column was Sp. 400 DB held at 150°C. Detection of sulfur compounds among the products was carried out on a Perkin-Elmer 3920B glc equipped with a sulfur-specific detector.

## 5. Results and Discussion

### Blank Reaction

To ensure that the hydrodesulfurization activity observed was mainly catalytic, a run was carried out with a reactor filled with the inert material used to dilute the catalyst (alundum, 90 mesh). The reactant mixture contained 0.122 wt % DBT in $\underline{n}$-$_{16}$ carrier oil. The feed flow rate was 1.2 $cm^3/hr$, and reaction temperature was 300°C. The reactor was subjected to the same pretreatment used in the catalytic experiments

(2 hrs at 400°C with 10% $H_2S$ in $H_2$). Figure 3 shows that the hydrodesulfurization activity of the reactor filled with alundum under our experimental conditions corresponds to less than 1% conversion of dibenzothiophene. Under the same conditions, a run with 25 mg of catalyst gave 80% sulfur removal.

Relative reactivities of methyl-substituted dibenzothiophenes

The conversion of four mixtures of methyl-substituted DBT was measured at different flow rates, ranging from 1.2 to 7.2 $cm^3/hr$. In all these runs, the reported conversion is based on disappearance of the sulfur-containing compound. Correspondingly, product analysis with the sulfur-specific detector showed no sulfur-containing compounds other than the reactants.

Figures 4-7 illustrate the effects of increasing L.H.S.V. on sulfur removal for four different mixtures, each containing DBT and a methyl-substituted DBT. The hydrogen contents of the liquid feeds were determined from Figure 8, which shows the calculated solubility of hydrogen in n-hexadecane at room temperature (the temperature at which the feed solutions were prepared).

To ensure useful kinetic measurements, the runs were performed with a $H_2S$ mole ratio around 24. Assuming a hydrogen consumption of 2 molecules per molecule of sulfur-containing compound and 100% sulfur removal, the hydrogen partial pressure remains nearly constant, declining by only 8%.

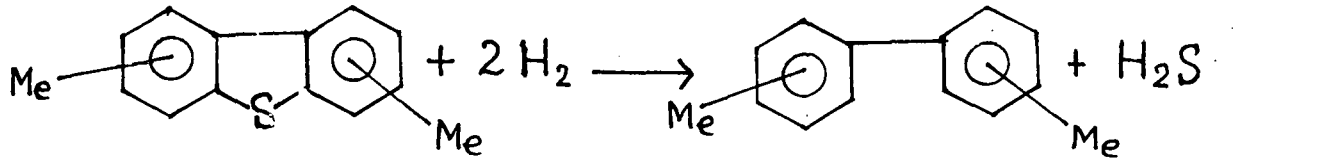


DBT OR Me-SUBSTITUTED DBT.

BIPHENYL OR METHYL SUBSTITUTED BIPHENYL.

For the piston-flow operation of the flow microreactor, we can write:

(1) $$\frac{W}{F} = \int \frac{dx_s}{(-r)}$$ where

W = weight of catalyst in g
F = flow rate of solution, $cm^3/hr$
$X_s$ = fractional conversion of the organic reactant
r = reaction rate per unit weight of catalyst

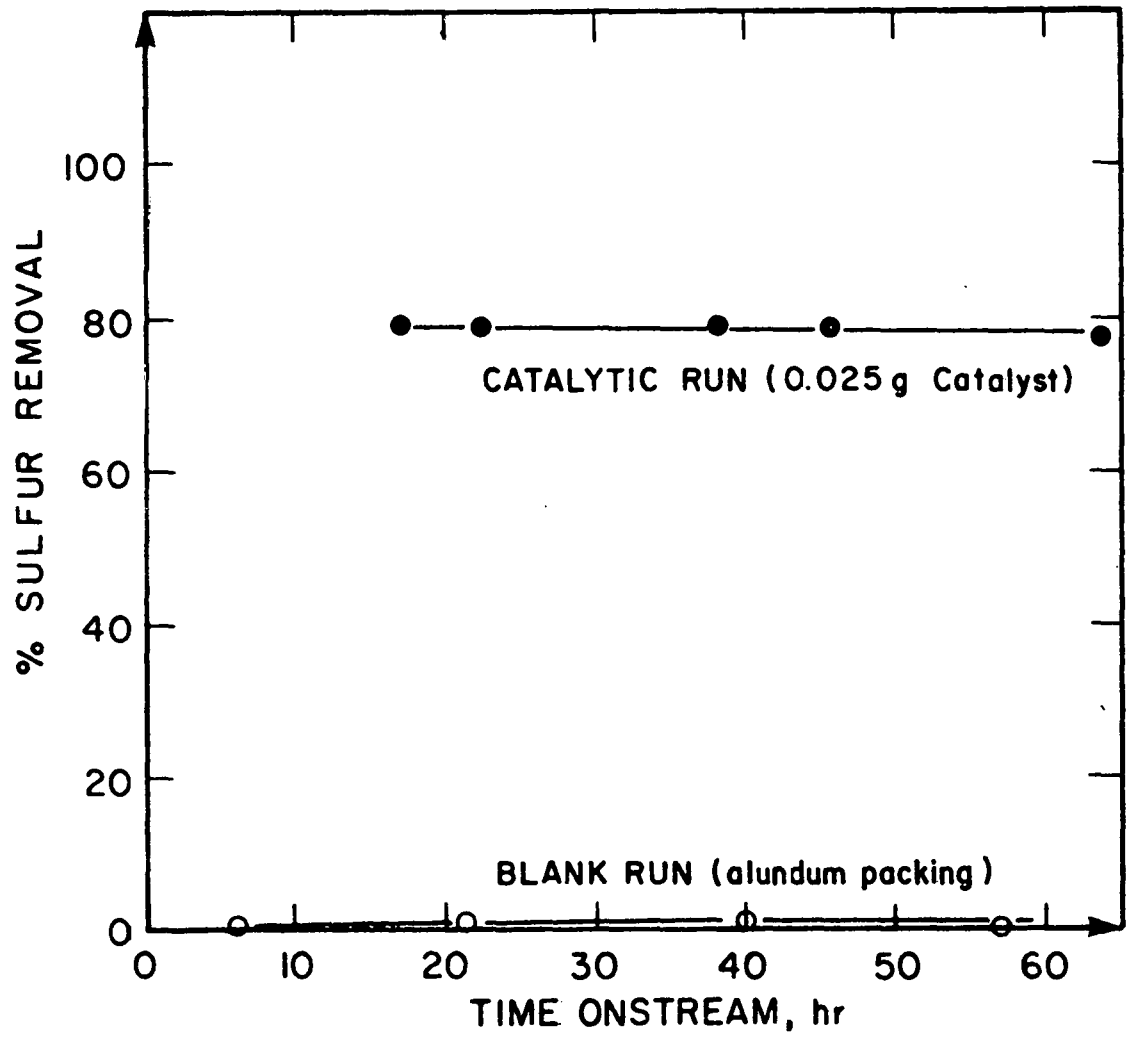


Figure 3. Blank and Catalytic runs for HDS of dibenzothiophene. Run conditions were T=300°C, 1000 psig hydrogen saturation pressure and reactant mixture, 0.123 wt% of DBT in n-hexadecane.

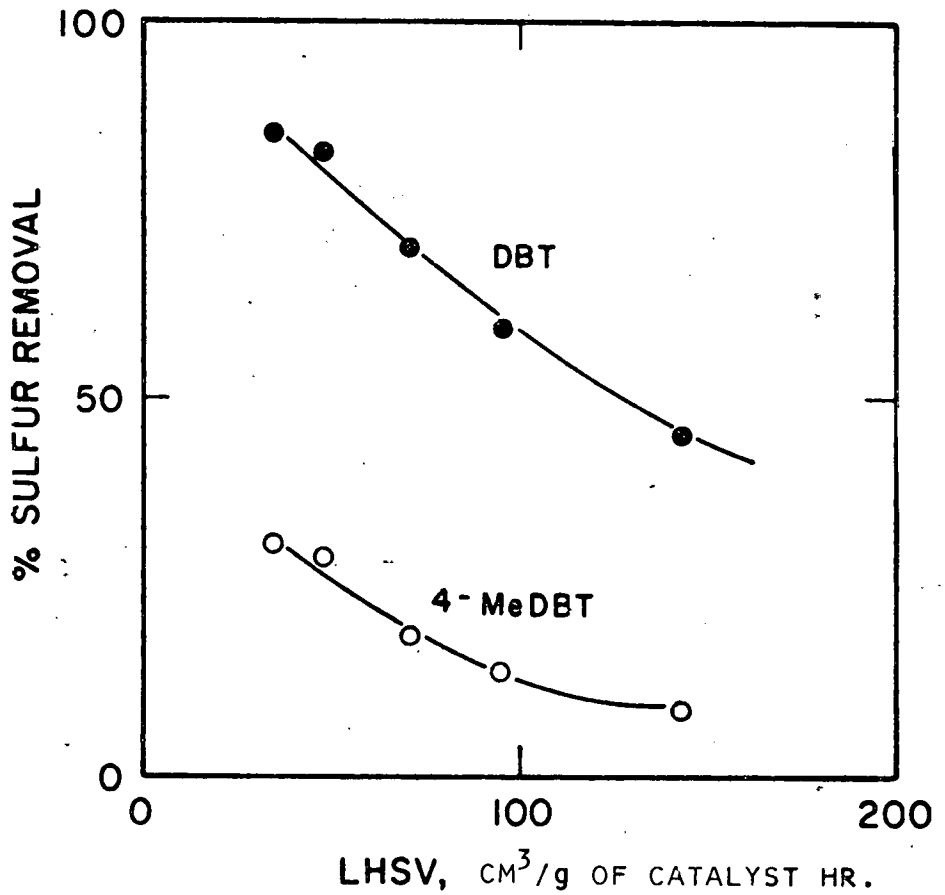


Figure 4. Sulfur removal activity of Co-Mo/$\gamma$-$Al_2O_3$ catalyst from a mixture of DBT and 4-MeDBT in n-hexadecane. See text for experimental conditions.

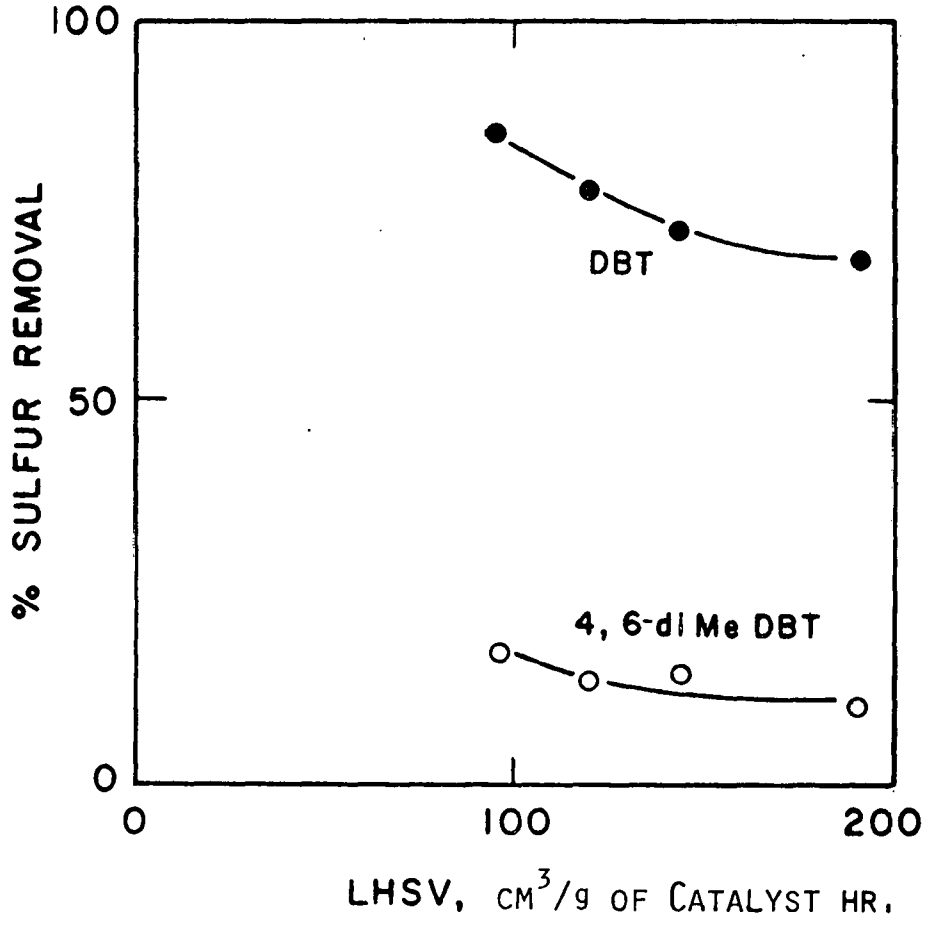


Figure 5. Sulfur removal activity of Cc-Mo/$\gamma$-$Al_2O_3$ catalyst from a mixture of DBT and 4,6-di-Me-DBT in n-hexadecane.

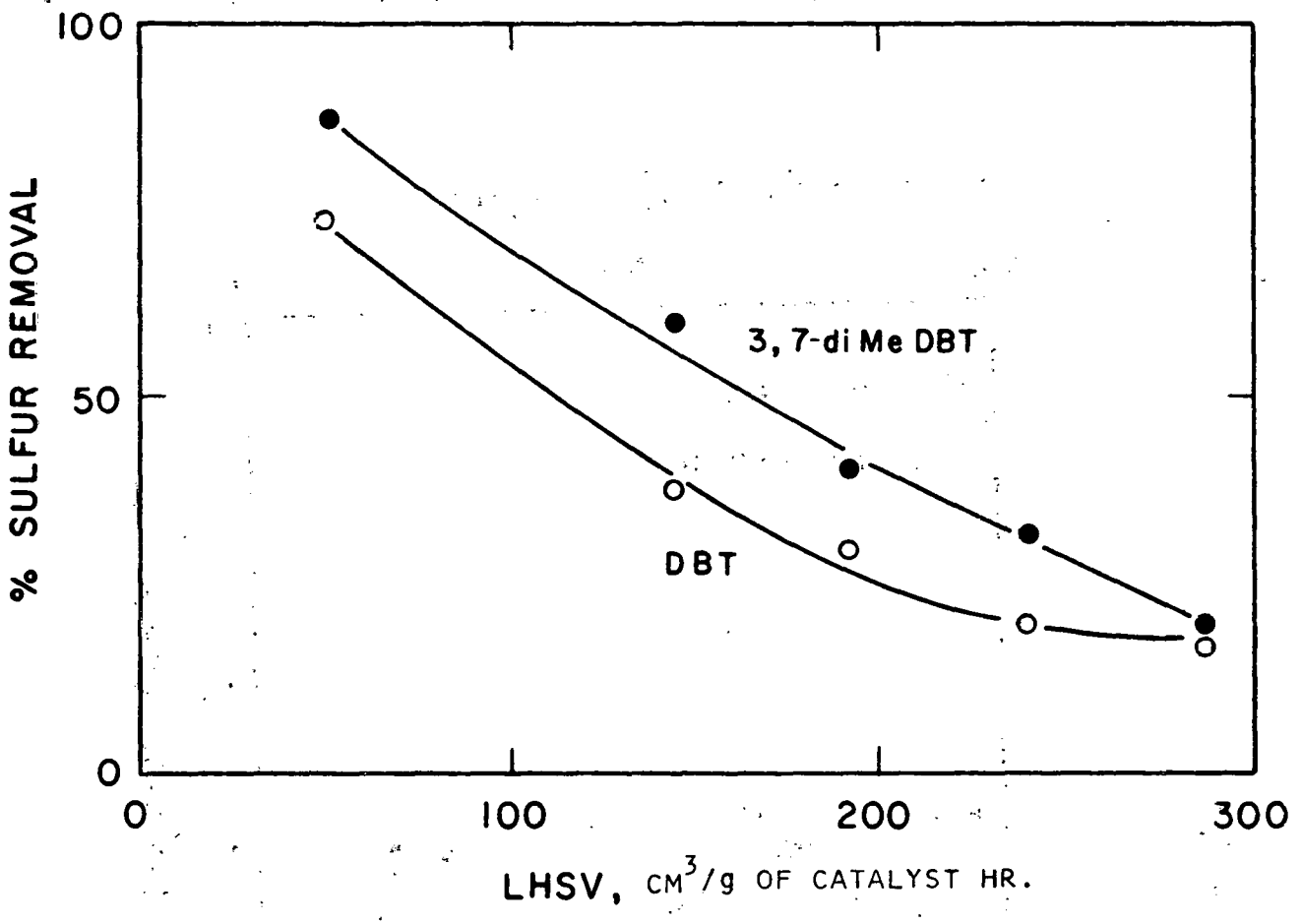


Figure 6. Sulfur removal activity of Co-Mo/$\gamma$-$Al_2O_3$ catalyst from a mixture of DBT and 3,7-diMeDBT in n-hexadecane.

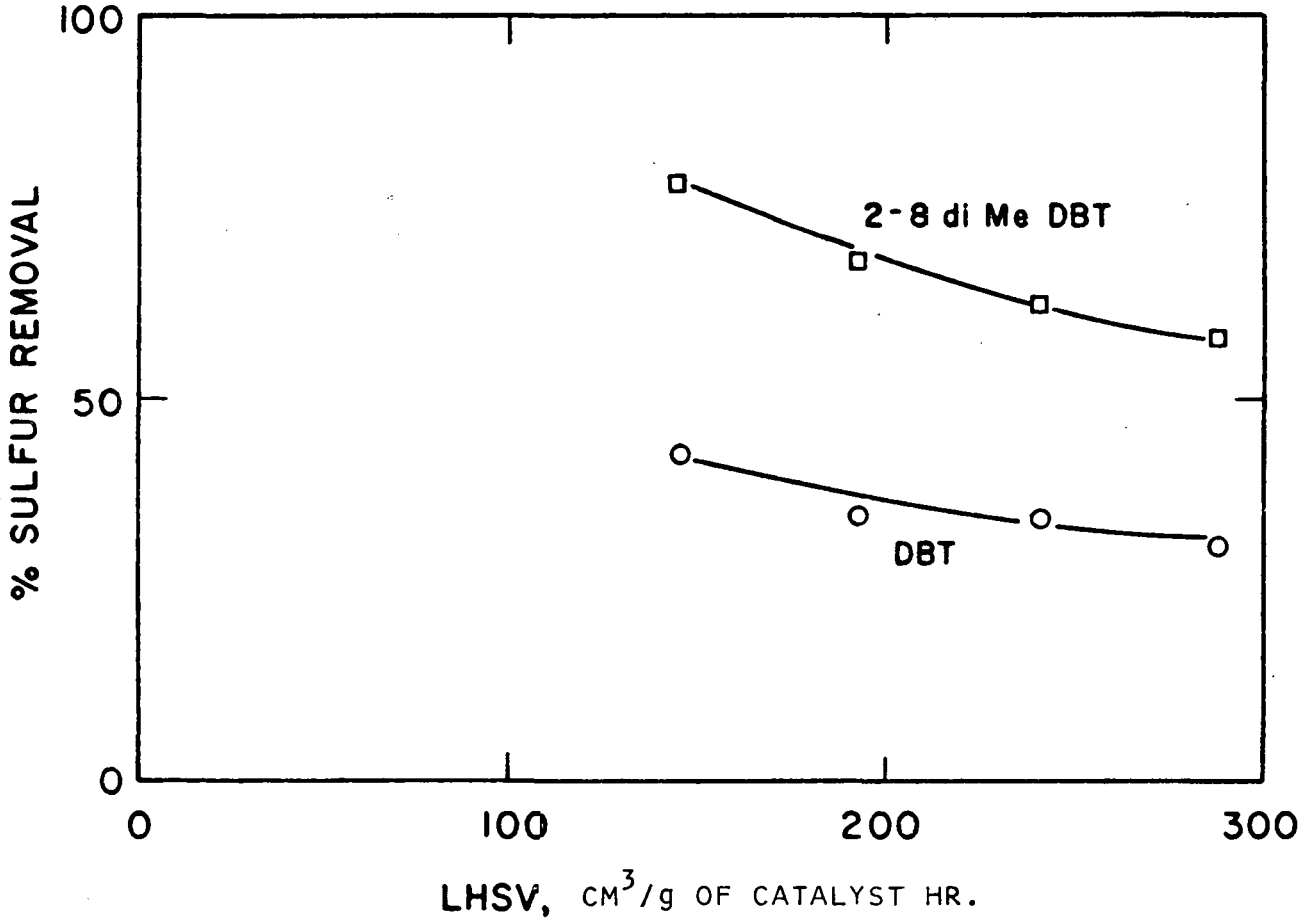


Figure 7. Sulfur removal activity of Co-Mo/$\gamma$-$Al_2O_3$ from a mixture of DBT and 2,8-di-Me-DBT in n-hexadecane.

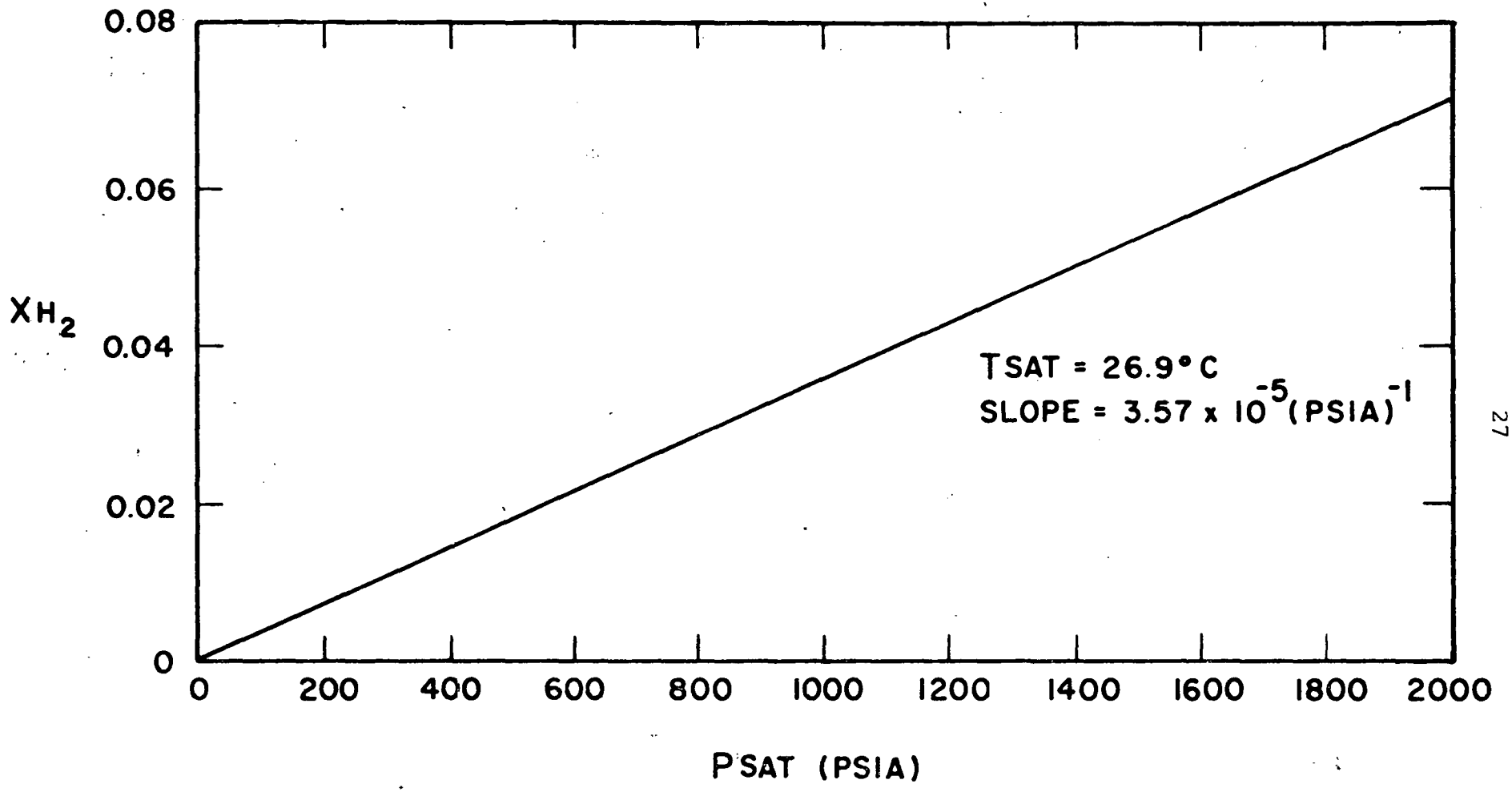


Figure 8. Calculated equilibrium mole fraction of hydrogen ($x_{H2}$) dissolved in n-hexadecane at 26.9°C.

The reaction rate per unit weight of catalyst can be written as follows, provided that simple power-law kinetics are valid:

$$r = kC_s^{\alpha}C_{H_2}^{\beta}C_{HC}^{\gamma} \qquad (2)$$

where k is the rate constant and $C_s$, $C_{H_2}$, $C_{HC}$ are, respectively, the concentrations of sulfur-containing compounds, hydrogen, and carrier oil. Taking into account the facts that the concentrations of sulfur compounds are low and the concentrations of hydrogen and carrier oil are so high that they hardly change this equation (see above)

$$r = k_1 C_s^{\alpha} \qquad (3)$$

Assuming a constant density of the reactants, we can write:

$x_s = 1 - \frac{C_s}{C_{so}}$, where $C_s$ is the concentration of DBT (or methyl-substituted DBT) remaining unconverted.

Equation (1) becomes:

$$\frac{W}{F} = -\frac{1}{k_1 C_{so}} \int \frac{dC_s}{C_s^{\alpha}} \qquad (4)$$

For $\alpha = 1$ (first-order), $\frac{W}{F} = \frac{1}{k_1 C_{so}} [\ell_n C_{so} - \ell_n C_s]$ (5)

or $k_1 \frac{W}{F} = -\ell_n(1-X)$. $1 - X$ is the fraction of sulfur compound remaining unconverted.

Assuming that there is no interaction between dibenzothiophene and substituted dibenzothiophene, the first-order kinetics can be tested for each sulfur-containing compound.

Examination of Figures 9-12 shows that first-order kinetics with respect to DBT and substituted DBT fit the experimental results very well. The ratio of the slope of the first-order plot for the methyl-substituted DBT and the slope of the plot for DBT gives a direct measure of the ease of sulfur removal from methyl-substituted DBT as compared to dibenzothiophene.

The results are summarized below:

| Reactant Compounds | 4-MeDBT | 4,6-Di-MeDBT | 3,7-Di-MeDBT | 2,8-di-MeDBT |
|---|---|---|---|---|
| $\frac{k_{MeDBT}}{k_{DBT}}$ | 0.16 | 0.10 | 1.54 | 2.6 |

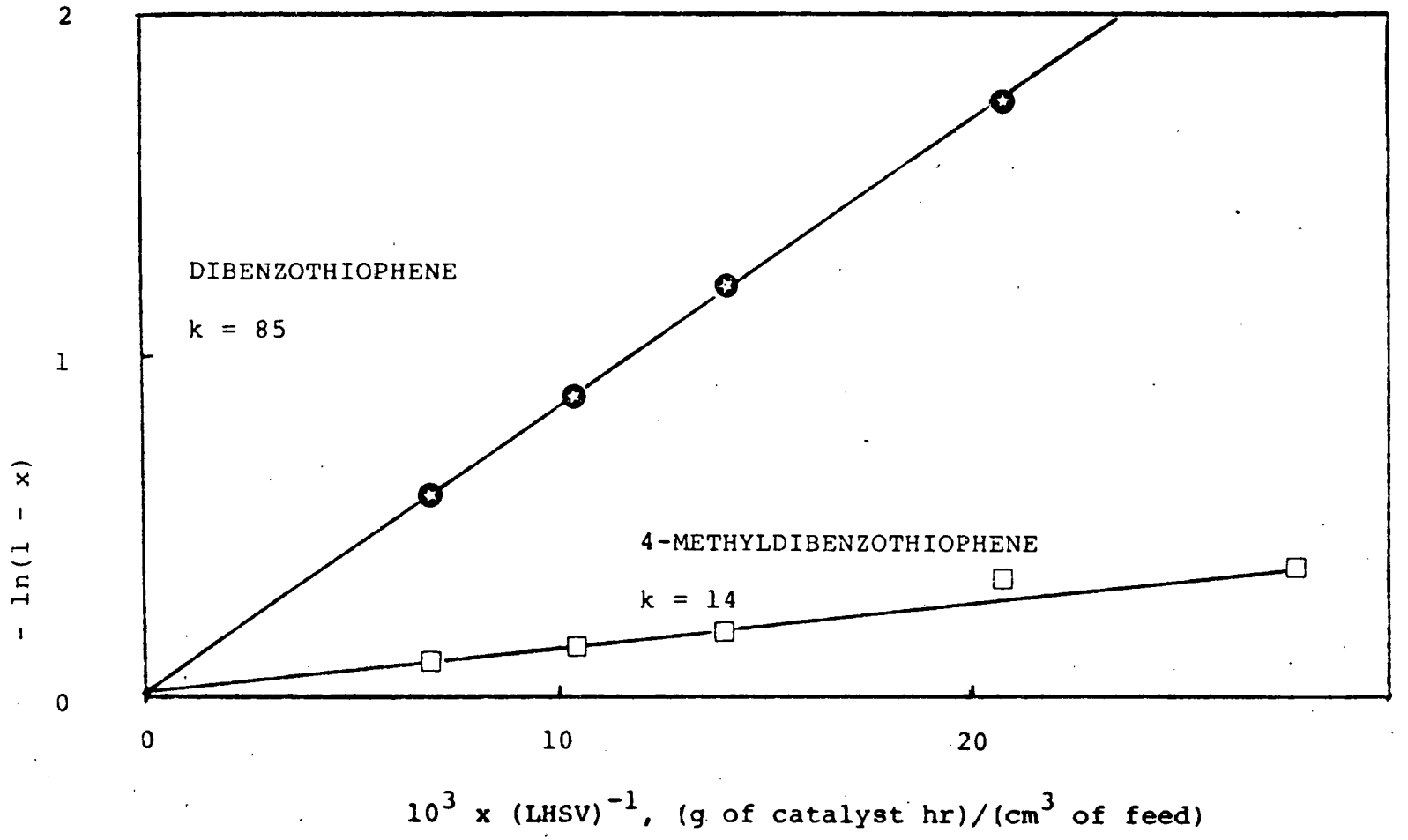


Figure 9. Pseudo first-order kinetics of hydrodesulfurization of dibenzothiophene and 4-methyldibenzothiophene; x is the fraction of the sulfur-containing compound converted. LHSV is liquid hourly space velocity; and k is a first-order rate constant in units of ($cm^3$ of feed/hr g of catalyst).

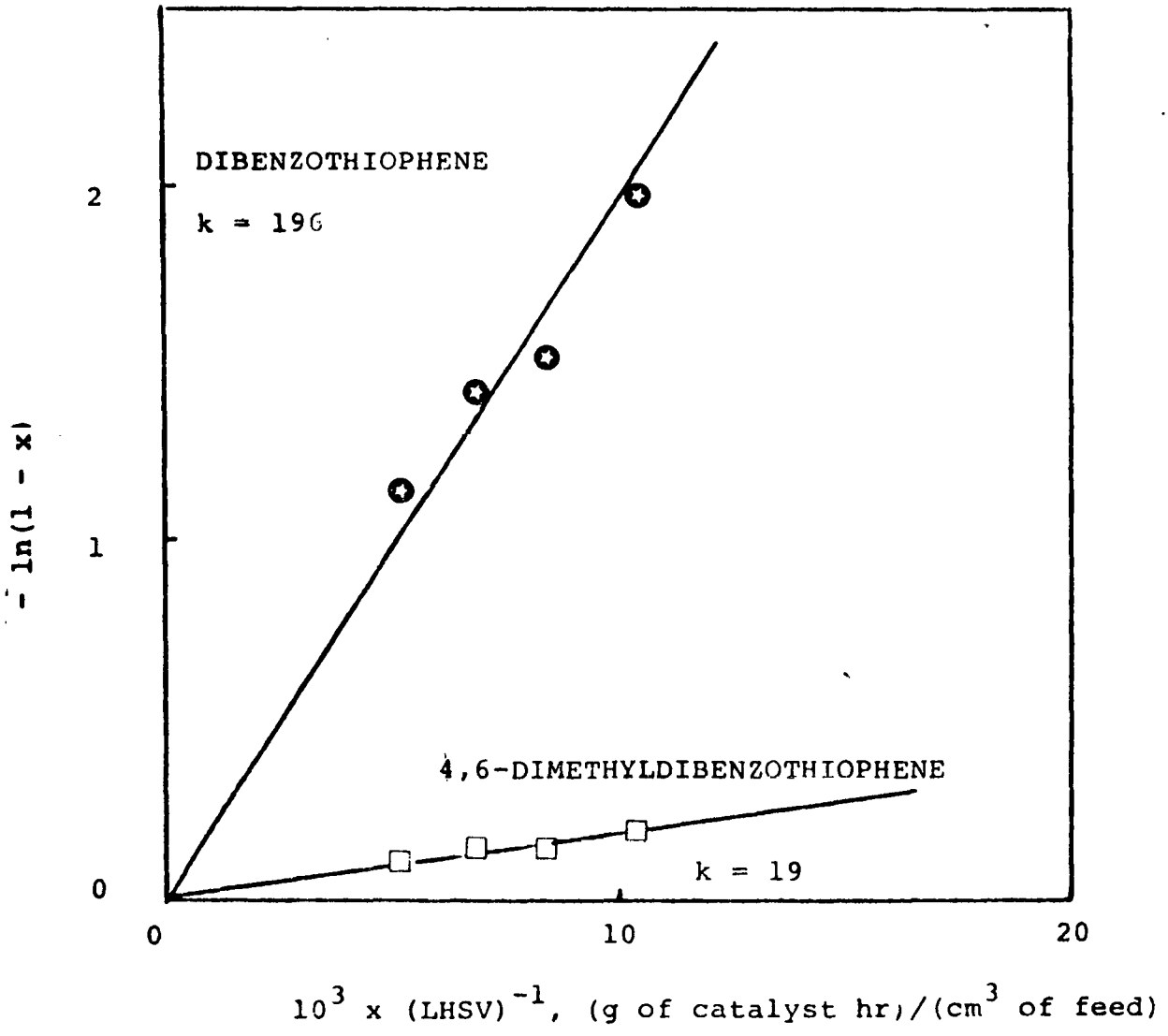


Figure 10. Pseudo first-order kinetics of hydrodesulfurization of dibenzothiophene and 4,6-dimethyldibenzothiophene.

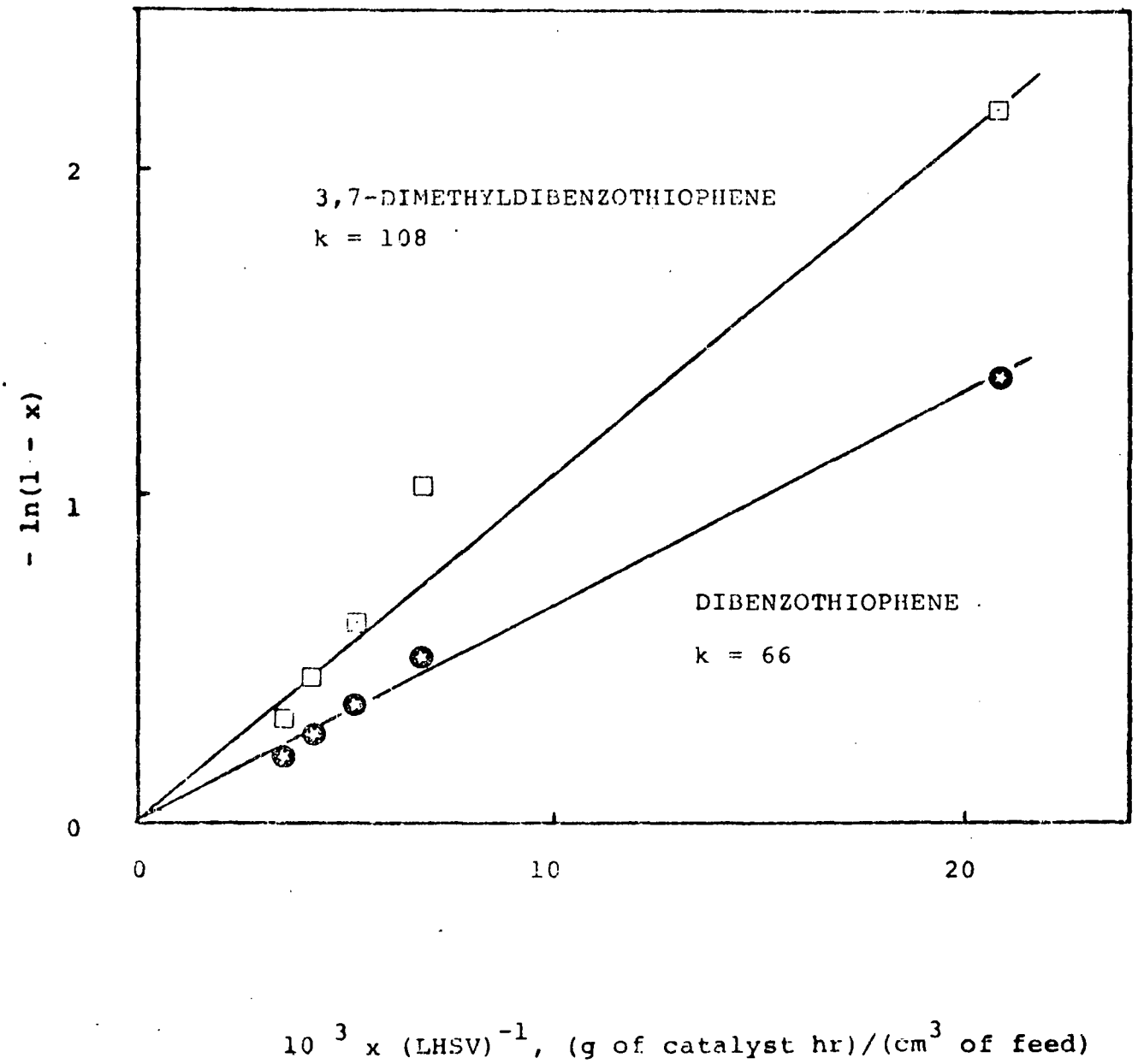


Figure 11. Pseudo first-order kinetics of hydrodesulfurization of dibenzothiophene and 3,7-dimethyldibenzothiophene.

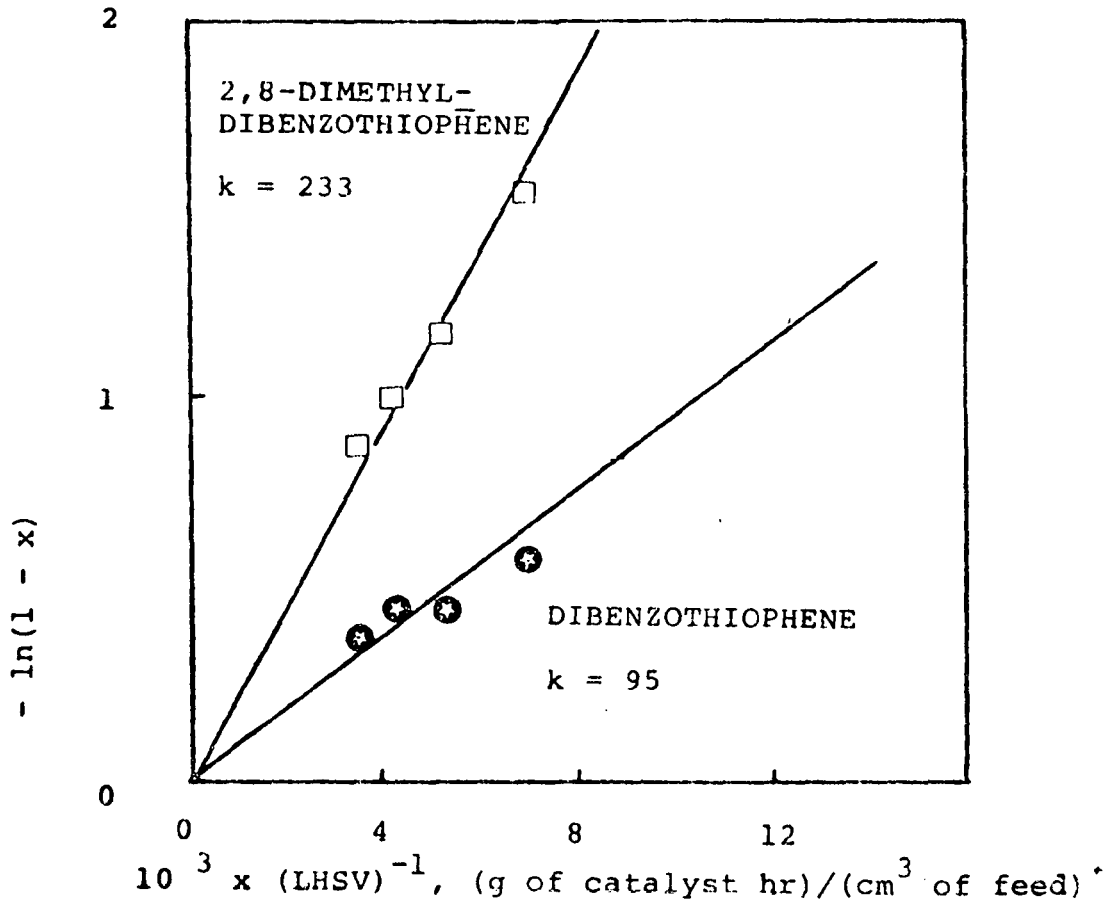


Figure 12. Pseudo first-order kinetics of hydrodesulfurization of dibenzothiophene and 2,8-dimethyldibenzothiophene.

We can conclude from these results that effects of the positions of the methyl groups are responsible for a wide range in the reactivities of DBT and methyl-substituted DBT. Before attempting to explain the substituent effects, we point out briefly a possible mechanism of HDS proposed by Amberg et al. (1961-1966) [and reviewed by de Beer and Schuit, 1975] using thiophene as a model compound. According to this mechanism, hydrodesulfurization proceeds through the following steps:

- Adsorption of thiophene on the surface, presumably as its sulfur atom interacts with an anion vacancy.

- Hydrogen donation to the carbon atoms contiguous to the sulfur atom with breaking of the C-S bonds.

- Desorption of the sulfur by addition of another pair of H atoms:

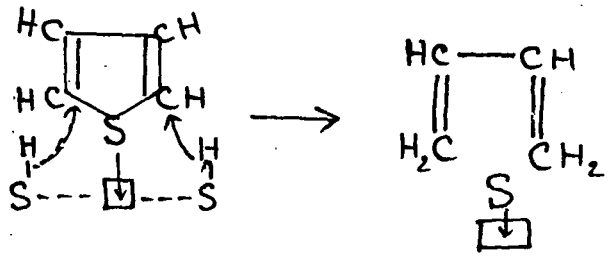

H probably has acidic character.

Assuming that the first step in hydrodesulfurization of DBT is also the adsorption via bonding of the sulfur atom with an anion vacancy, it is reasonable to expect a decrease in reactivity upon incorporation of a methyl group with the 4-position. Its presence in a position adjacent to the sulfur atom restricts its access to the active site on the catalyst surface. The steric hindrance caused by this methyl substitution is expected to be even more pronounced in case of 4,6-diMeDBT: The experimental results show, indeed, that 4,6-diMeDBT is 10 times less active than DBT, whereas 4-MeDBT is about six times less reactive.

The high reactivity of 2,8-diMeDBT compared to DBT can be explained in terms of hyperconjugation effects associated with the presence of methyl groups on the aromatic ring (March, 1968). The hyperconjugation forms that contribute to the structure of 2,8-diMeDBT are shown below:

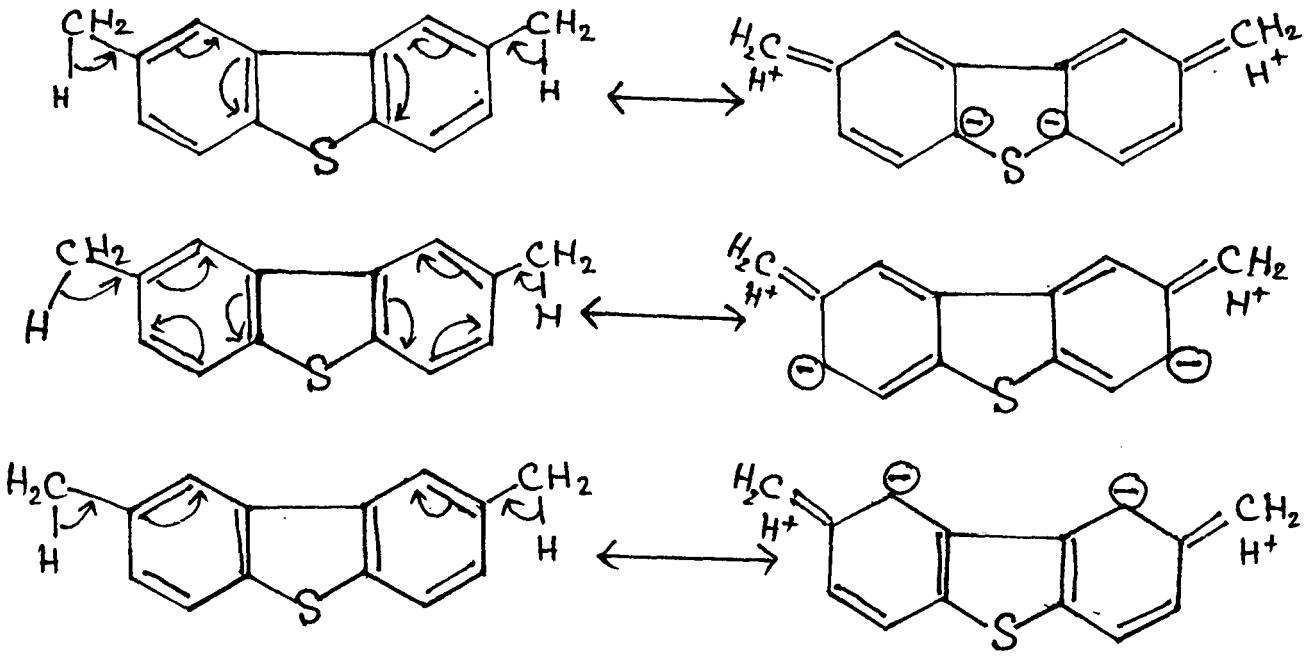

Because of the appearance of a partial negative charge on the αC, the nucleophile attack on the C-S bond by an acidic hydrogen is favored. Adsorption of S at the anion vacancy is also favored because of the higher electron density around the sulfur atom.

The reactivity of 3,7-diMeDBT would be expected to be less than that of 2,8-diMeDBT by this reasoning, since no negative charge appears on the αC in its hyperconjugated forms:

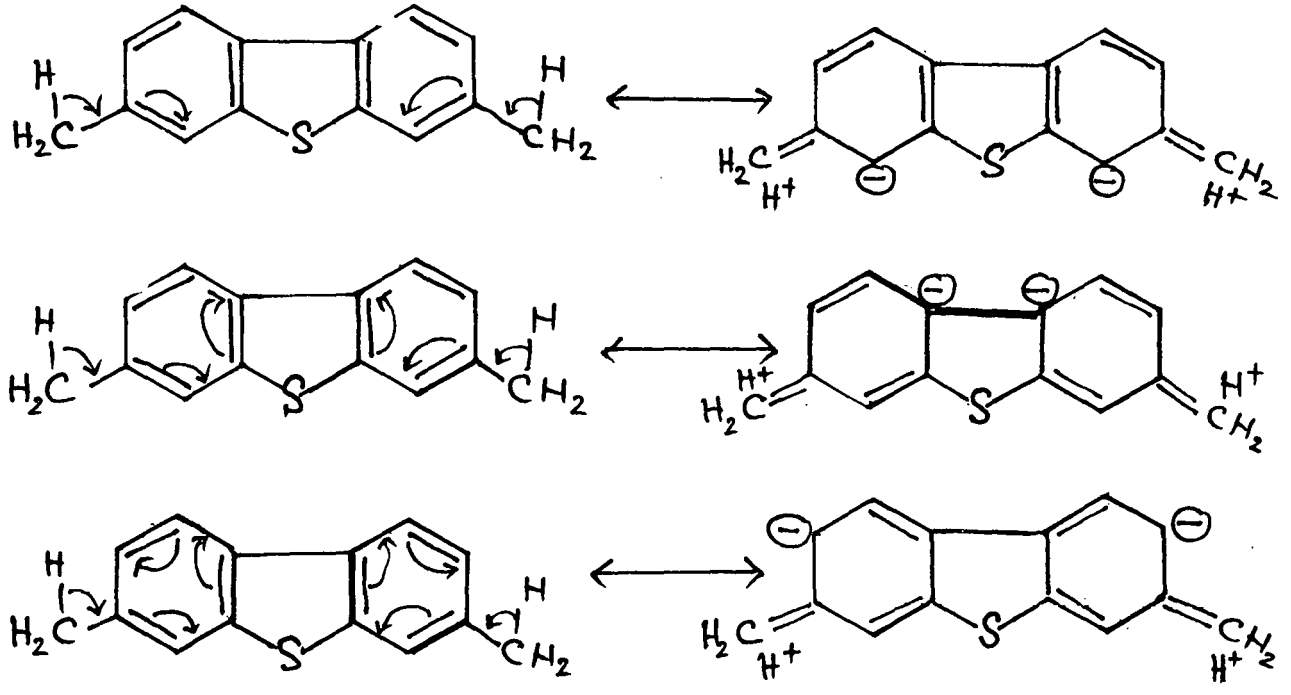

The reactivity of 3,7-diMeDBT remains higher than that of DBT because of the negative charge on the βC.

C. PROGRESS IN SYNTHESIS AND CHARACTERIZATION OF SULFUR- AND NITROGEN-CONTAINING COMPOUNDS

3,7-Dimethyldibenzothiophene has been synthesized by the following route:

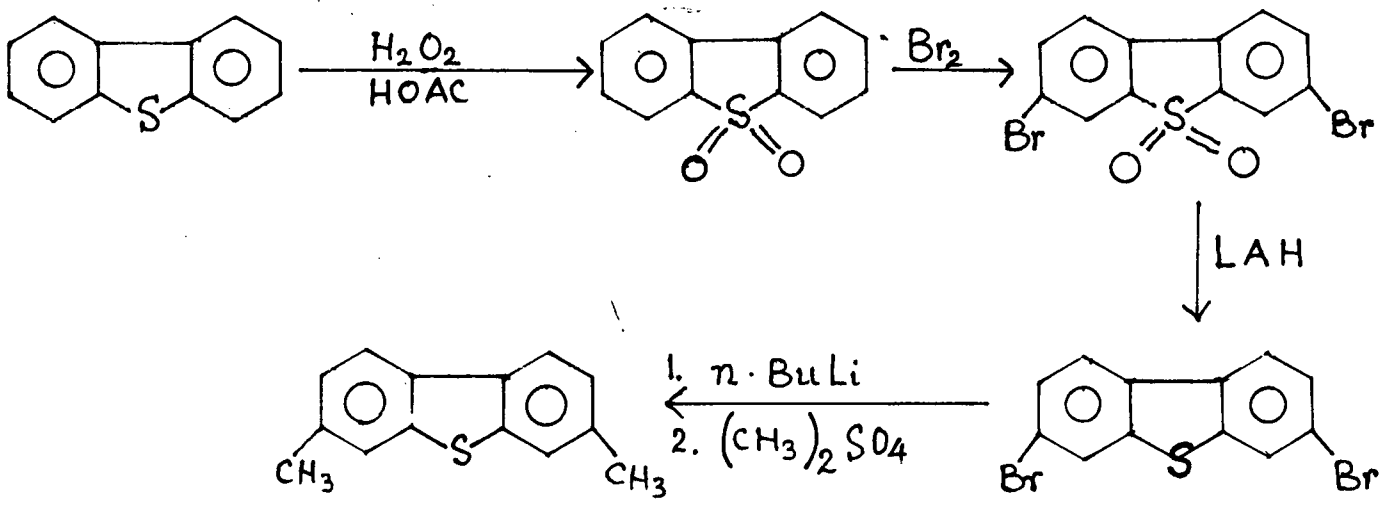


4,5-Dimethylacridine was obtained by the following sequence of reactions:

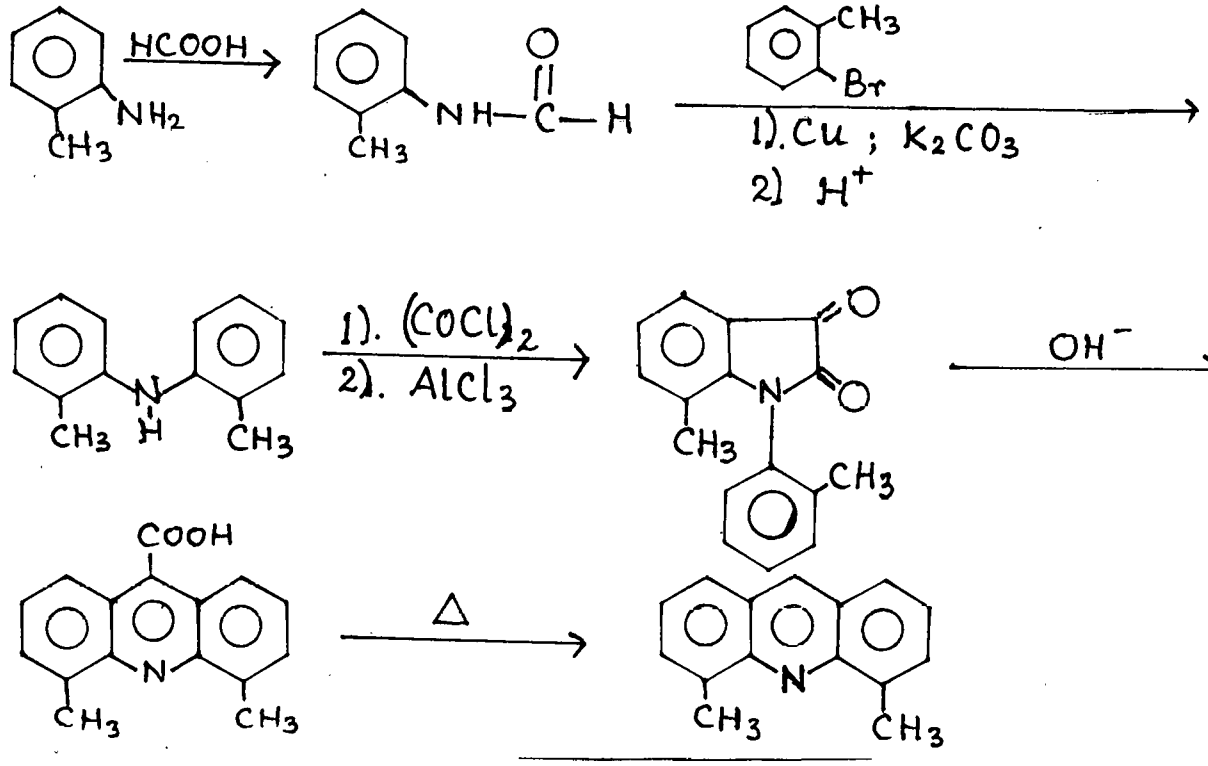

2,5,8-Trimethyl-1,4,7,9btetrazaphenalene was obtained from crotonaldehyde and ammonia via the following sequence of reactions:

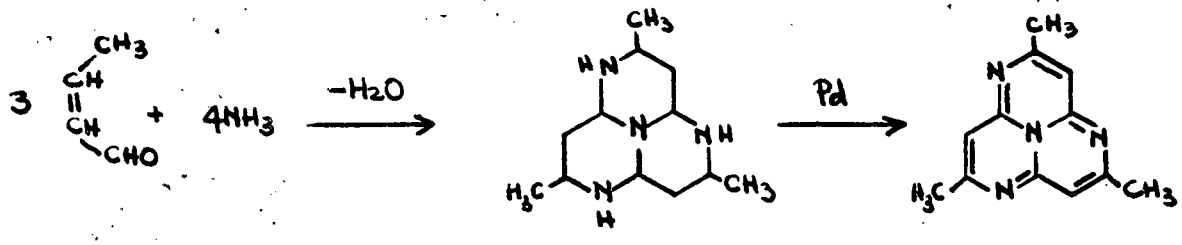


Perhydroacridine has been obtained by reduction of octahydroacridine:

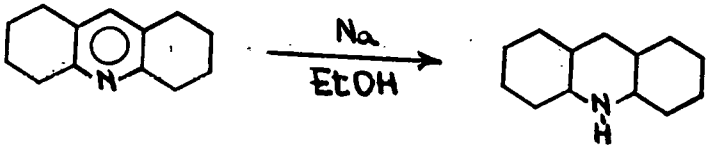


Benz[c]acridine has been prepared from 1-naphthol and o-toluidinehydrochloride:

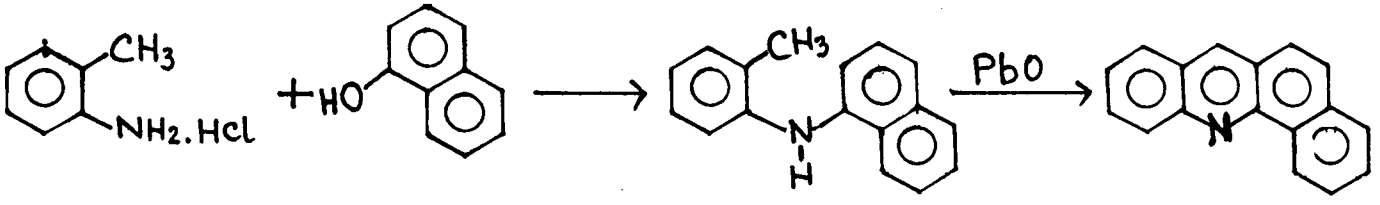


Thus far only a crude product has been isolated which is in the process of purification.

The synthesis of 3-methyldibenzothiophene is underway by the following route:

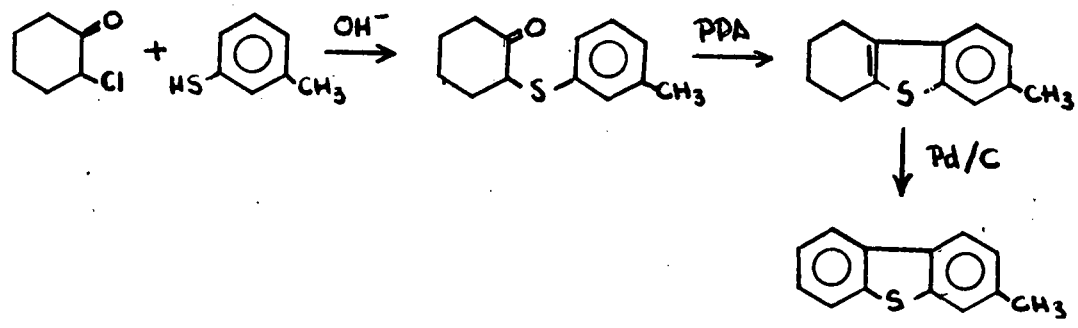


The following compounds will be synthesized, after completion of the schemes delineated above.

Benz[a]acridine:

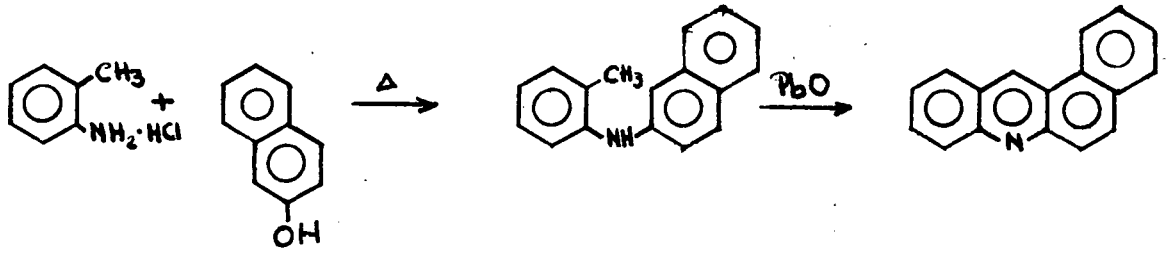


Dibenz[c,h]acridine:

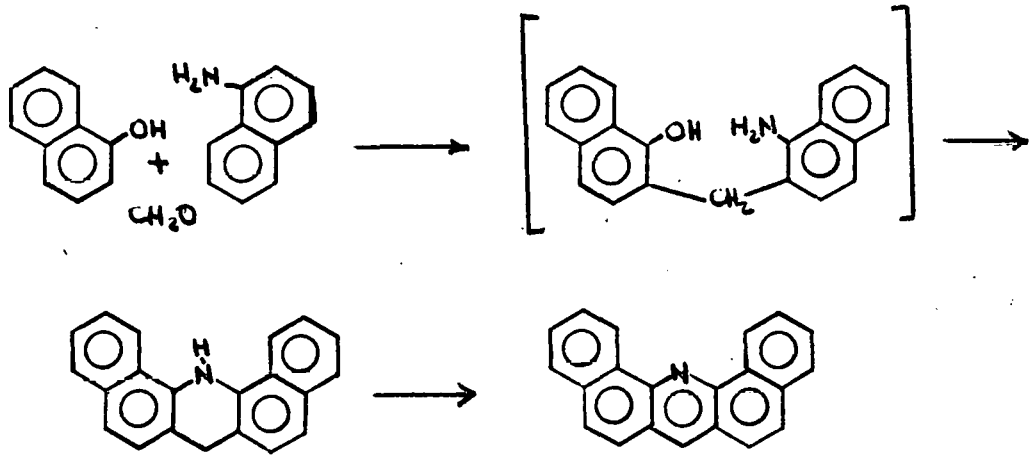

1,2-Benzocarbazole:

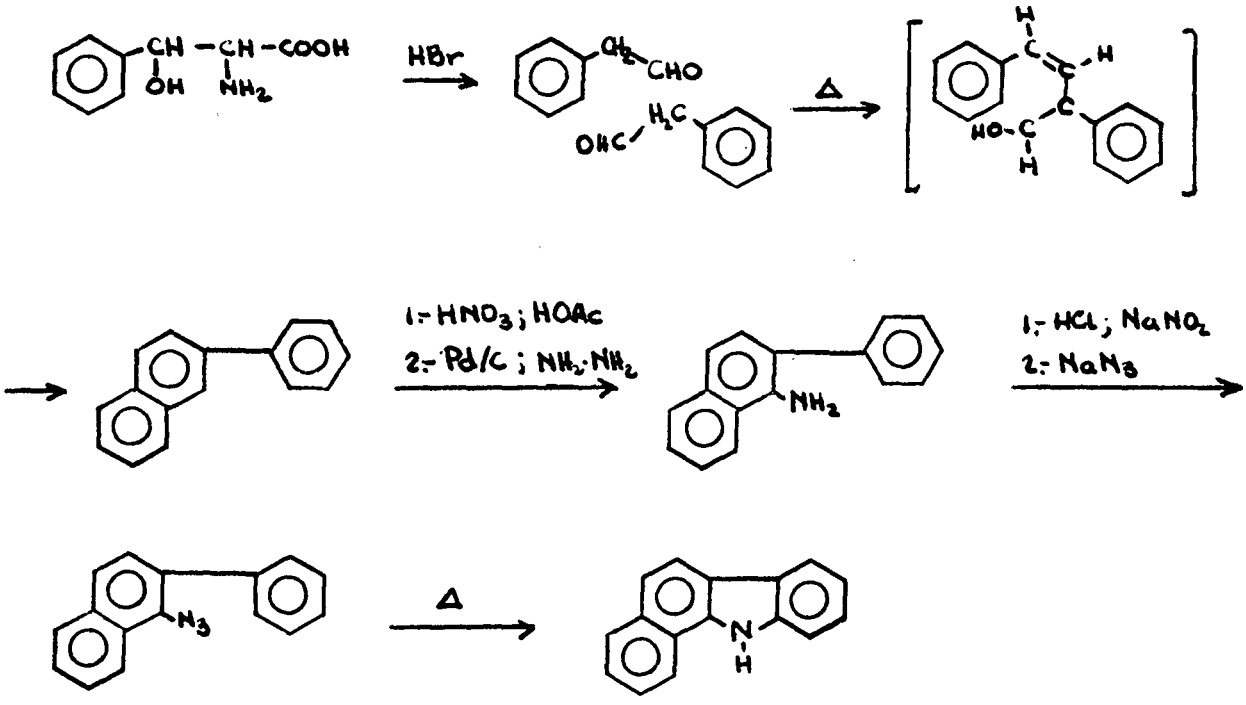


Benzo[b]naphtho[2,3-d]thiophene:

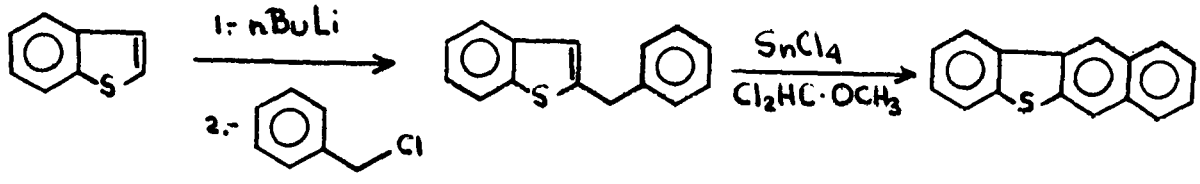

## D. CATALYTIC HYDRODENITROGENATION

### 1. Quinoline

#### a. High-pressure and high-temperature quinoline conversion catalyzed by Ni-Mo/$Al_2O_3$ and Co-Mo/$Al_2O_3$

The following abbreviations are used for the different compounds throughout this report:

Q = Quinoline
THQ = 1,2,3,4-tetrahydroquinoline
5THQ = 5,6,7,8-tetrahydroquinoline
DAQ = Decahydroquinoline
OPA = o-propylaniline
HC = Hydrocarbon

Two runs were made using two different catalysts at high temperature and pressure in the one-liter autoclave reactor. The first-order conversion plots for total nitrogen removal are shown in Figure 13. A break is observed in each straight line, and it corresponds to a cross-over point in the concentration vs. time profiles for tetrahydroquinoline and decahydroquinoline as seen in Figure 14. An explanation for this behavior is as follows, if one assumes a rate expression for total nitrogen removal as:

$$\frac{dCN_2}{dt} = k_1 C_{THQ}(t) + k_2 C_{DHQ}(t)$$

where $k_1$ and $k_2$ are the rate constants and $C_{THQ}(t)$ and $C_{DHQ}(t)$ the respective concentrations of 1,2,3,4-tetrahydroquinoline and decahydroquinoline. As the concentration of the former decreases with time, the second term becomes the predominant one accounting for the overall rate of nitrogen removal. Thus total nitrogen conversion depends strongly on how the concentration of decahydroquinoline changes with time towards the end of the run. This argument applies to both catalysts studied with the break occurring earlier for the Ni-Mo catalyst, which is not surprising since it is more active than the Co-Mo catalyst.

Table 2-A lists the rate constants for both catalysts; the schematic diagram at the bottom of the figure gives the ratios of rate constants, those for Ni-Mo relative to Co-Mo.

Ni-Mo under these conditions is the more active catalyst. Higher temperature favors the cracking of the C-N bond in THQ in accordance with results of previous reports; however, higher

TABLE 2-A

HIGH-PRESSURE AND HIGH-TEMPERATURE HDN OF QUINOLINE: COMPARISON OF Co-Mo AND Ni-Mo CATALYSTS

| REACTION | Rate Constant, $min^{-1}$ (American Cyanamid HDS 9A) Ni-Mo | (American Cyanamid HDS 16A) Co-Mo |
|---|---|---|
| Q → 5THQ | 4.5 | 0.67 |
| THQ → DHQ | 3.8 | 2.2 |
| 5THQ → DHQ | 9.7 | 3.0 |
| DHQ → HC | 9.0 | 3.3 |
| THQ → OPA | 0.5 | 0.5 |
| OPA → HC | 3.3 | 2.0 |

CONDITIONS

367°C, 2000 psig
Initial reactant concentration, $7.6 \times 10^{-5}$ $\frac{g\ mole}{g\ oil}$
Catalyst concentration 0.5 wt %
Total volume, 400 ml in white oil

SULFIDING

Both catalysts were sulfided at 325°C for two hrs under a 10% $H_2S$ in $H_2$ gas mixture.

Relative reaction rate constants; normalization is with respect to the $Co\text{-}Mo/Al_2O_3$ catalyst.

$$\begin{array}{ccccccc} Q & \rightleftarrows & THQ & \xrightarrow{1.0} & OPA & \xrightarrow{1.77} & HC + NH_3 \\ {\scriptstyle 6.7}\downarrow & & \downarrow{\scriptstyle 1.8} & & & & \\ 5THQ & \xrightarrow[3.4]{} & DHQ & & \xrightarrow[2.7]{} & & HC + NH_3 \end{array}$$

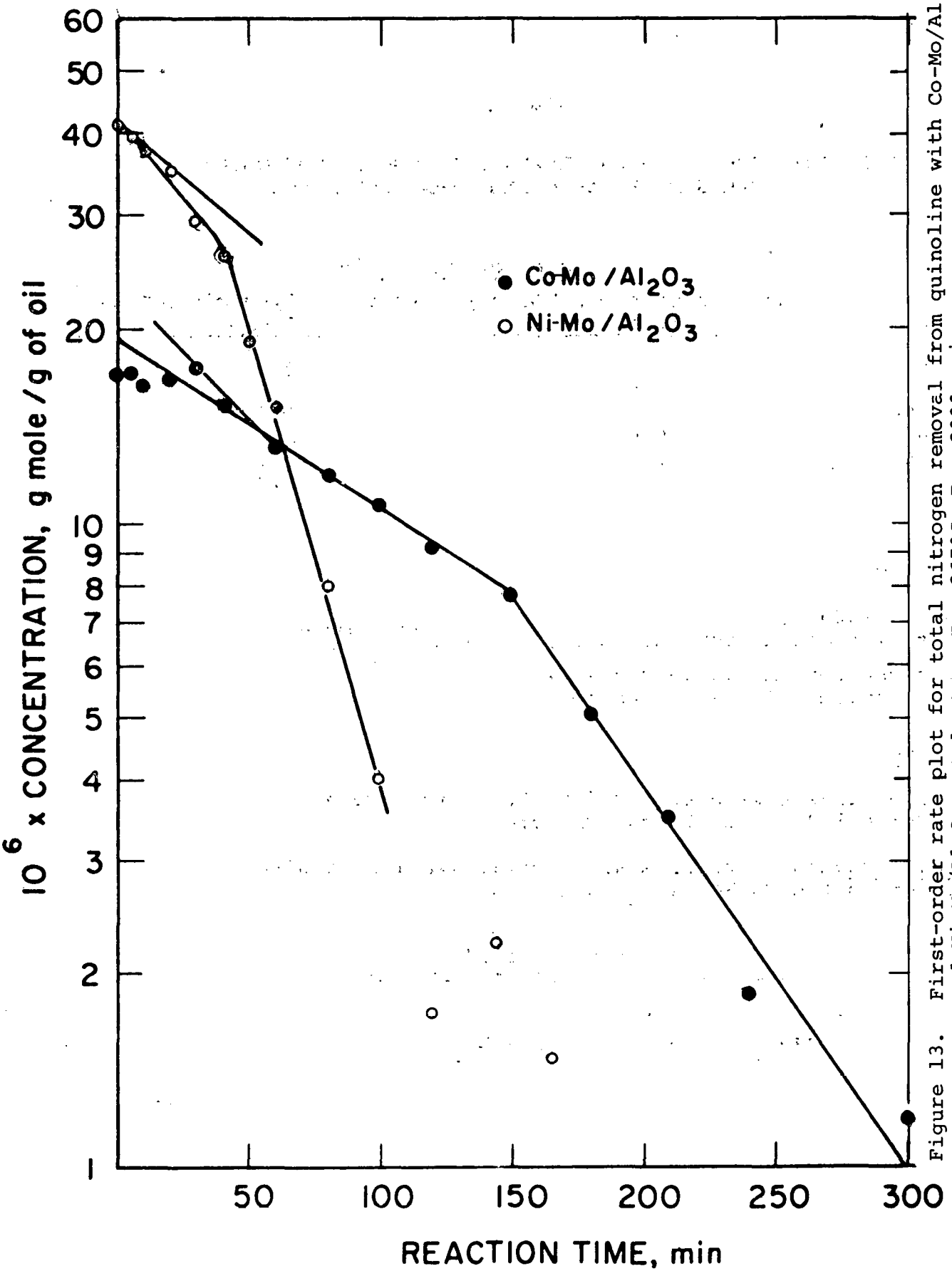


Figure 13. First-order rate plot for total nitrogen removal from quinoline with Co-Mo/$Al_2O_3$ and Ni-Mo/$Al_2O_3$ catalysts. T = 367°C, P = 2000 psig.

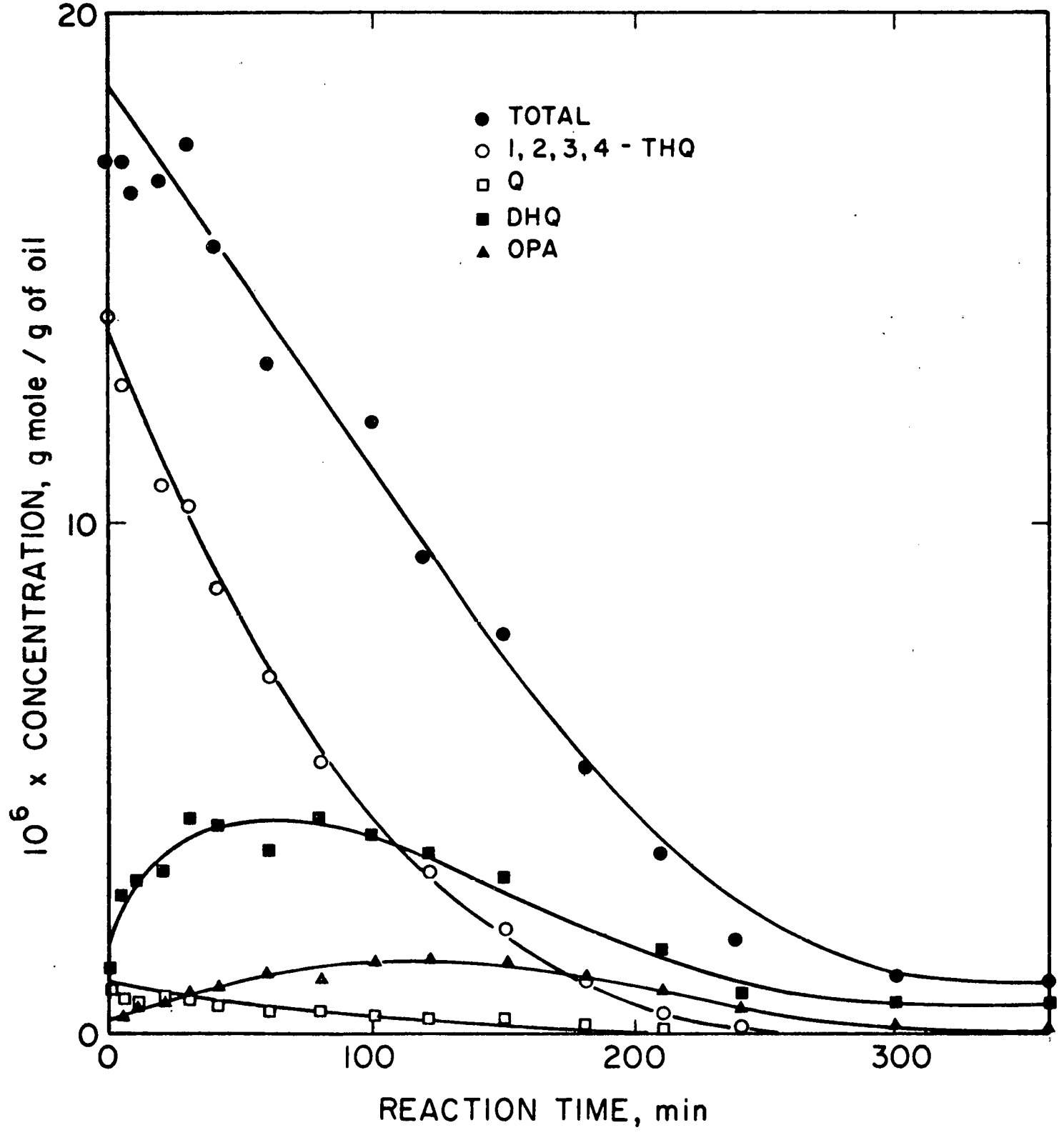


Figure 14. HDN of quinoline catalyzed by Ni-Mo/$\gamma$-$Al_2O_3$.

pressure does not favor this reaction. The relative disappearance of OPA with the two catalysts is consistent with independently determined results derived from experiments carried out with OPA as the reactant with each of these two catalysts. Co-Mo favors the formation of THQ, since comparatively very little S-THQ was observed during this run, whereas with the Ni-Mo catalyst, quinoline is present in a much higher concentration.

b. Effect of $H_2S$ on the quinoline network

As a continuation of the catalyst evaluation study of the third quarterly progress report in this series, a set of runs was carried out in the one-liter autoclave, in order to allow a comparison of the performance of three catalysts in the presence and absence of carbon disulfide. Table 3 lists the physical properties of the catalysts. Table 4 shows the results for catalyst comparison purposes. Since there was an abnormal instability of the glc detector during these experiments, a 20% increase has to be assigned to the rate constants. The rate constants were estimated by fitting the data; the computer program is outlined in an article by Himmelblau et al. (1967).

The effect of sulfiding the catalyst is evident as a 100% increase in the total nitrogen removal rate for the Ni-Mo catalyst. Similar effects are evident for each individual reaction at the network. These results are in accord with the reports in the literature that treatment of catalysts with $H_2S$ enhances their HDN activity. In order to summarize more clearly the effect of adding $CS_2$ on the individual reaction, Figure 15 was prepared showing the relative rate constants for the Ni-Mo catalyst for three different sets of run conditions.

It is clear that $H_2S$ inhibits the hydrogenation of the aromatic ring. The effect is more pronounced for the Ni-Mo catalyst than for the Co-Mo catalyst. These results are generally in accord with literature results for the hydrogenation of benzene and naphthalene. In the hydrogenolysis (cracking) reactions, the effect of $CS_2$ ($H_2S$) depends on the type of reaction. $H_2S$ promotes the cracking of DHQ by the same relative amount for all three catalysts: there is an increase by a factor of 2 in the values for the rate constant for cracking of THQ for all three catalysts. This result supports the argument that cracking requires protonic acidity on the catalyst, as has been postulated in earlier reports in this series (cf. the fifth quarterly report). The postulated reaction mechanisms seem to concur with this explanation. Interestingly, the addition of $H_2S$ to the reaction system seems to have a negative effect on the disappearance of OPA. This result is tentatively explained by the negative action of $H_2S$ on straight aromatic hydrogenation. Another possible interpretation is that since OPA is formed in low concentration, competitive adsorption and reaction of other bases in

TABLE 3

CATALYST PROPERTIES

| | Cyanamid HDS-9A | NALCO NT-550 | Cyanamid HDS-16A |
|---|---|---|---|
| Composition, wt % | NiO 3.0-4.0 | $WO_3$ 22.0 | $MoO_3$ 12.2 |
| | $MoO_3$ 17.5-18.5 | NiO 5.1 | CoO 5.7 |
| | $Na_2O$ 0.04 | $Al_2O_3$ | $Na_2O$ 0.03 |
| | Fe 0.05 | | Fe 0.04 |
| Surface area, $m^2/g$ | -- | 250 | -- |
| Pore volume, $cm^3/g$ | -- | 0.5 | -- |

TABLE 4

EFFECT OF $CS_2$ ON CATALYST PERFORMANCE IN QUINOLINE HDN

First-Order Rate Constants, $min^{-1}$

| Reaction | Co-Mo/$Al_2O_3$ No $CS_2$ a) | Co-Mo/$Al_2O_3$ b) | Ni-Mo/$Al_2O_3$ No $CS_2$ a) | Ni-Mo/$Al_2O_3$ b) | Ni-Mo/$Al_2O_3$ c) | Ni-W/$Al_2O_3$ No $CS_2$ a) | Ni-W/$Al_2O_3$ b) |
|---|---|---|---|---|---|---|---|
| Q ⇄ THQ | 5.51 | 5.84 | 5.7 | 6.3 | 6.1 | 5.7 | 6.3 |
| Q → 5THQ | 1.25 | 1.36 | 3.47 | 2.6 | 0.7 | 2.4 | 1.7 |
| 5THQ → DHQ | 1.07 | 1.3 | 1.3 | 1.3 | 0.66 | 0.78 | 1.25 |
| THQ → DHQ | 0.23 | 0.21 | 0.67 | 0.29 | 0.17 | 0.37 | 0.21 |
| THQ → OPA | 0.065 | 0.143 | 0.08 | 0.12 | 0.02 | 0.07 | 0.13 |
| OPA → HC | 1.4 | 0.37 | 0.65 | ? | 0.74 | 0.38 | 0.22 |
| DHQ → HC | 2.6 | 3.1 | 2.9 | 3.25 | 2.0 | 1.65 | 3.05 |
| Total Nitro-Removal | 0.2 | 0.4 | 0.3 | 0.6 | 0.17 | 0.2 | 0.6 |

Reaction Conditions: 342°C

500 psig

Catalyst particle size: 150-200 mesh

Initial quinoline concentration: $\sim 6.6 \times 10^{-5} \frac{\text{g mole}}{\text{g oil}}$

All catalysts were presulfided for 2 hr at 325°C with 10% $H_2S$ in $H_2$ gas mix.

Carrier: white oil

Catalyst concentration: $\sim 4.8 \times 10^{-3} \frac{\text{g catalyst}}{\text{g oil}}$

---

a) No $CS_2$ added to the white oil

b) $CS_2$ loaded concentration $\sim 7.7 \times 10^{-6} \frac{\text{g mole}}{\text{g oil}}$

c) No $CS_2$ added and the catalyst was not presulfided

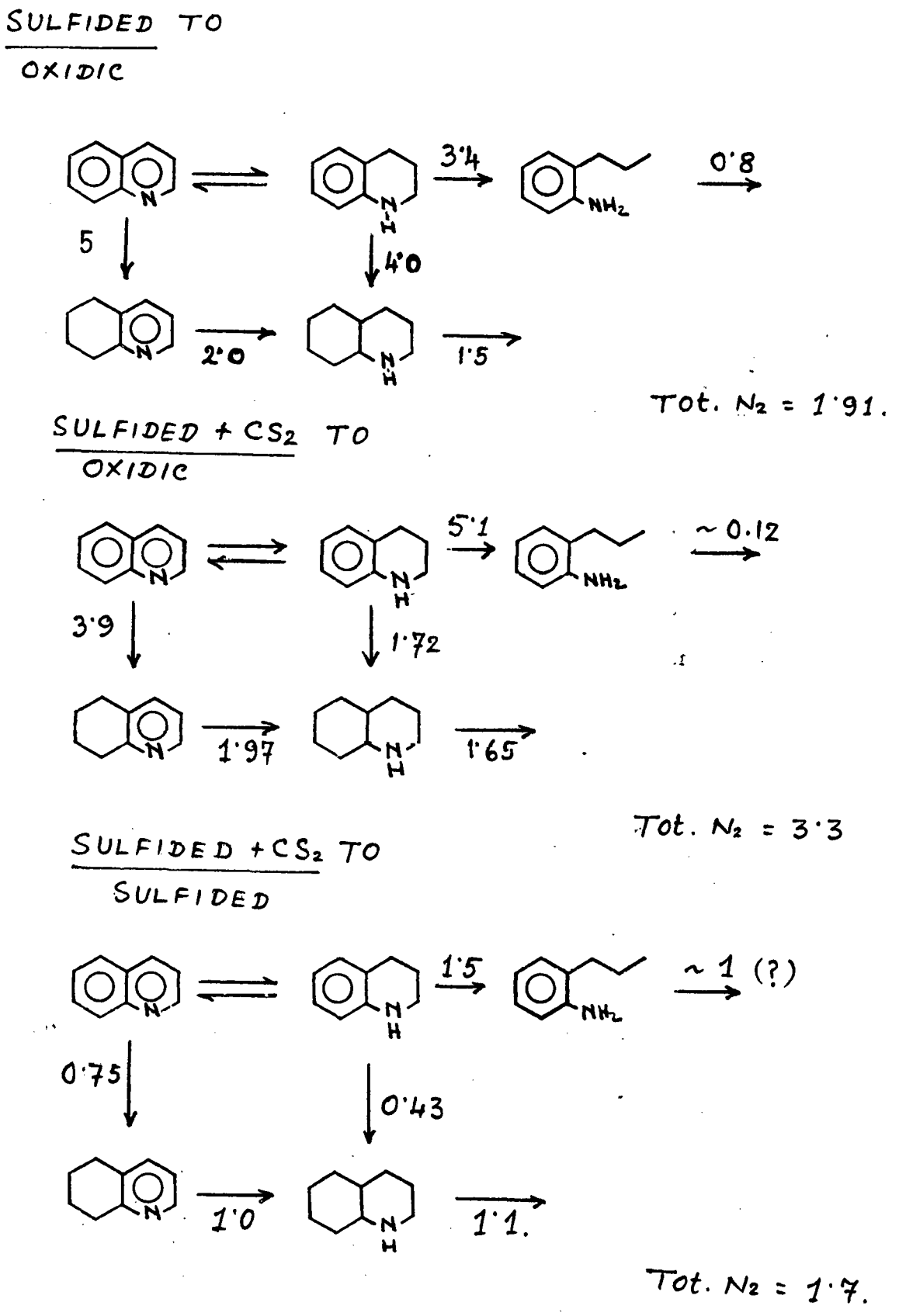


Figure 15. Effect of presulfiding and of $CS_2$ inhibitor on the Ni-Mo catalyst for quinoline HDN. (The numbers represent relative first-order rate constants.)

the system cause a reduction on the HDN rate of OPA.

c. Relative catalytic activities for the hydrogenation reactions of the network.

The effect is seen in the transformation of Q into 5THQ and of THQ into DHQ, being more pronounced for the Q→5THQ reaction. $H_2S$ favors heteroaromatic ring hydrogenation as indicated by the conversion of 5THQ to DHQ. An explanation for these trends is that the increased protonic acidity of the catalyst surface facilitates the adsorption of the base, thus hydrogenation of the heteroaromatic ring is made easier, and the hydrogenation of the aromatic ring is suppressed.

The rate constants given in Table 4 are also shown in Figure 16 in normalized form for comparison of the catalysts. In comparing the three catalysts,the rate constants have been reported relative to the values for the less active Co-Mo catalyst. In comparing the individual reactions with each catalyst, the results have been normalized to the slow DAQ cracking reaction. Since different catalysts were supplied by different manufacturers, pore volume, surface area, and preparation procedures are expected to be significantly different from one catalyst to another. Nevertheless, some significant conclusions can be drawn. For total nitrogen removal, the activity order is Ni-W $\simeq$ Ni-Mo > Co-Mo. Ni-Mo is more active in hydrogenating aromatic rings, as is implied by the observed two-fold increase in the rate constant for formation of 5THQ from Q when Co-Mo is replaced by Ni-Mo. This result accounts for the higher activity of the Ni-Mo catalyst in overall nitrogen removal. The cracking reactions seem to be unaffected by catalyst composition. For all three catalysts, the slow reaction seems to be the cracking of THQ to form OPA. As was found earlier, hydrogenation is the slow reaction in quinoline HDN under the observed experimental conditions for all the catalysts tested.

2. Acridine

a. Search for the appropriate analytical system

This work concerns the development of suitable gas chromatographic conditions (stationary phase, temperature, carrier gas flow rate) for the quantitative analysis of nitrogen-containing acridine reaction products using a Perkin-Elmer 3920B gas chromatograph with a nitrogen-specific detector. Many different stationary phases were investigated and rejected for various reasons. Table 5 presents a list of some of the stationary phases investigated and a summary of the reasons for rejection. Figures 17-22 present chromatograms obtained with several stationary phases for an acridine reaction sample.

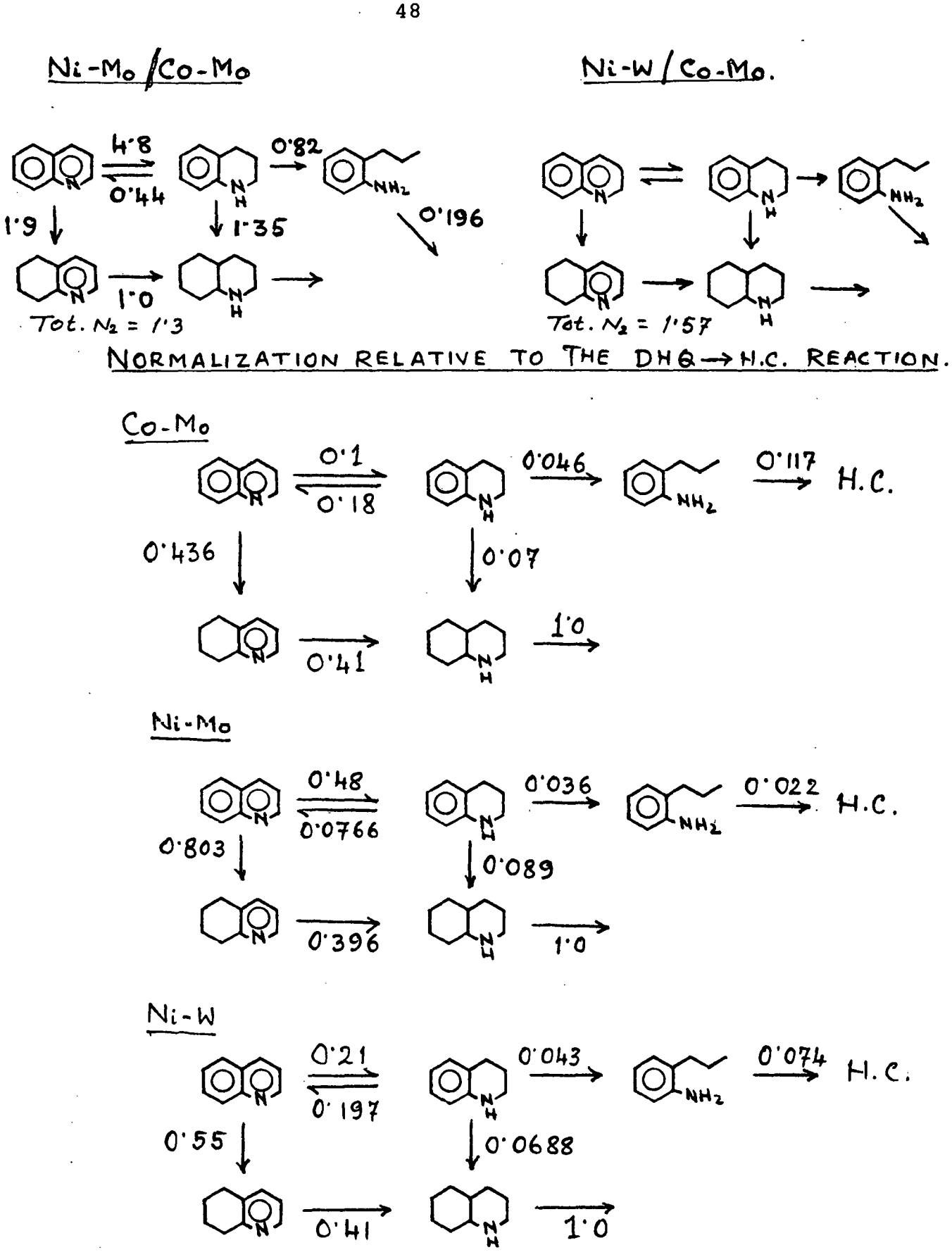


Figure 16. Quinoline HDN; normalization relative to less active catalyst.

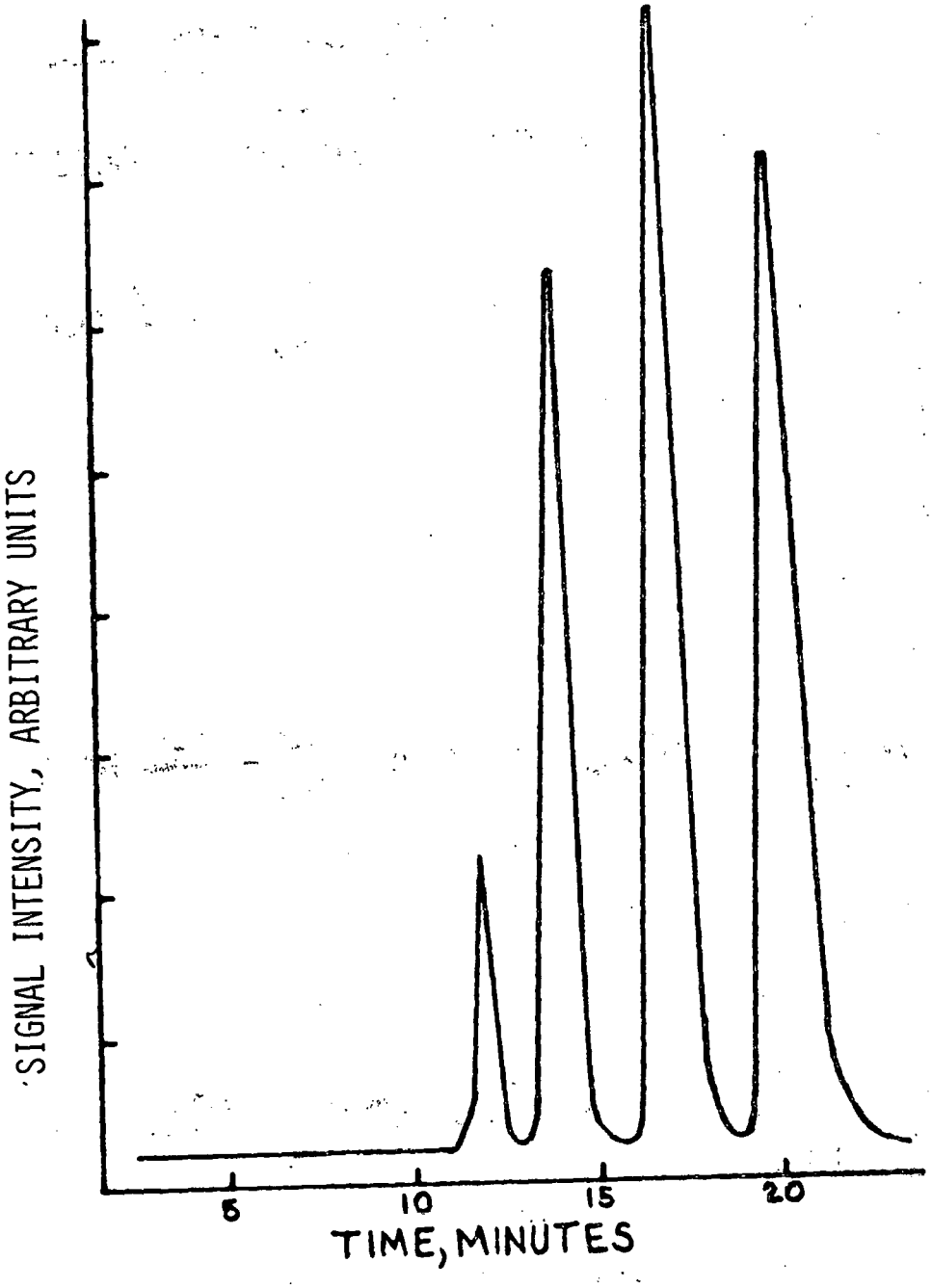


Figure 17. Chromatogram of acridine reaction sample (run 1041-10) on a 5' x 1/8" Apiezon L (2% KOH): 180°C, 30 $cm^3$/min.

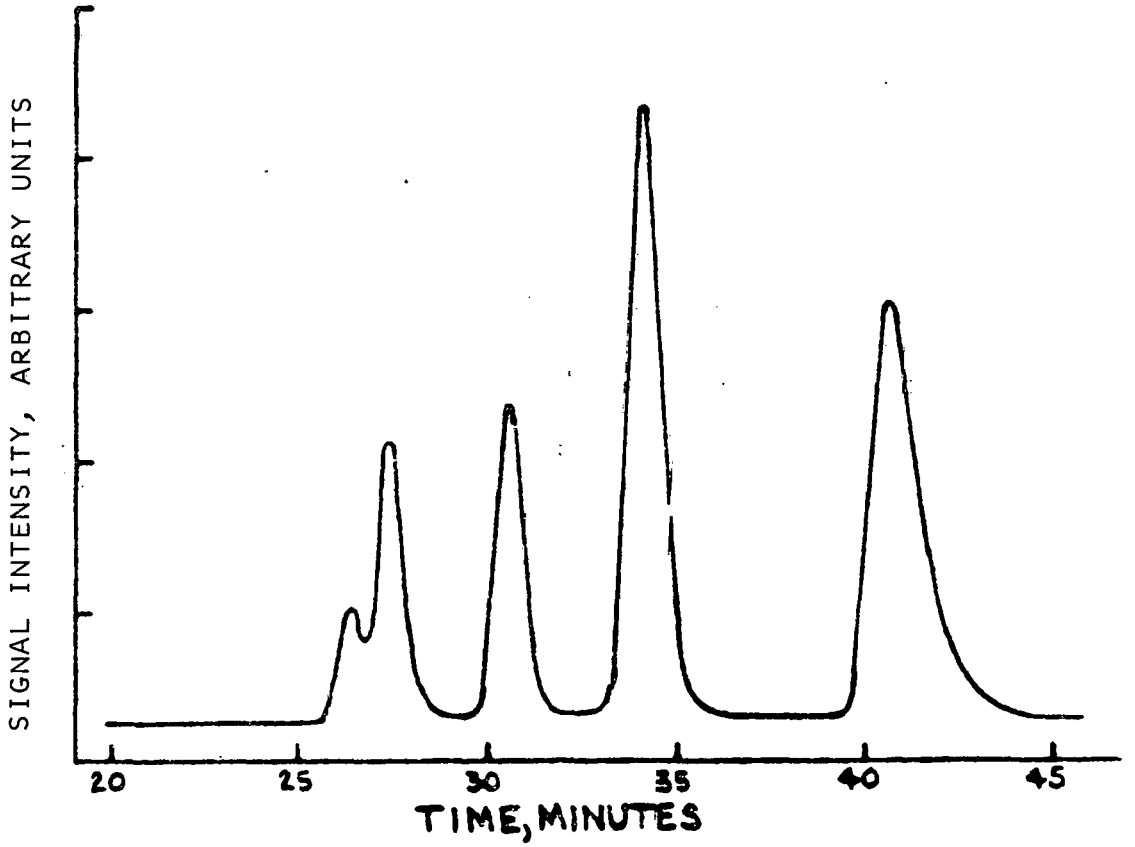


Figure 18. Chromatogram of acridine reaction sample (run 1041-10) on 17' x 1/8" SS Apiezon L (2% KOH): 200°C, 25 $cm^3$/min.

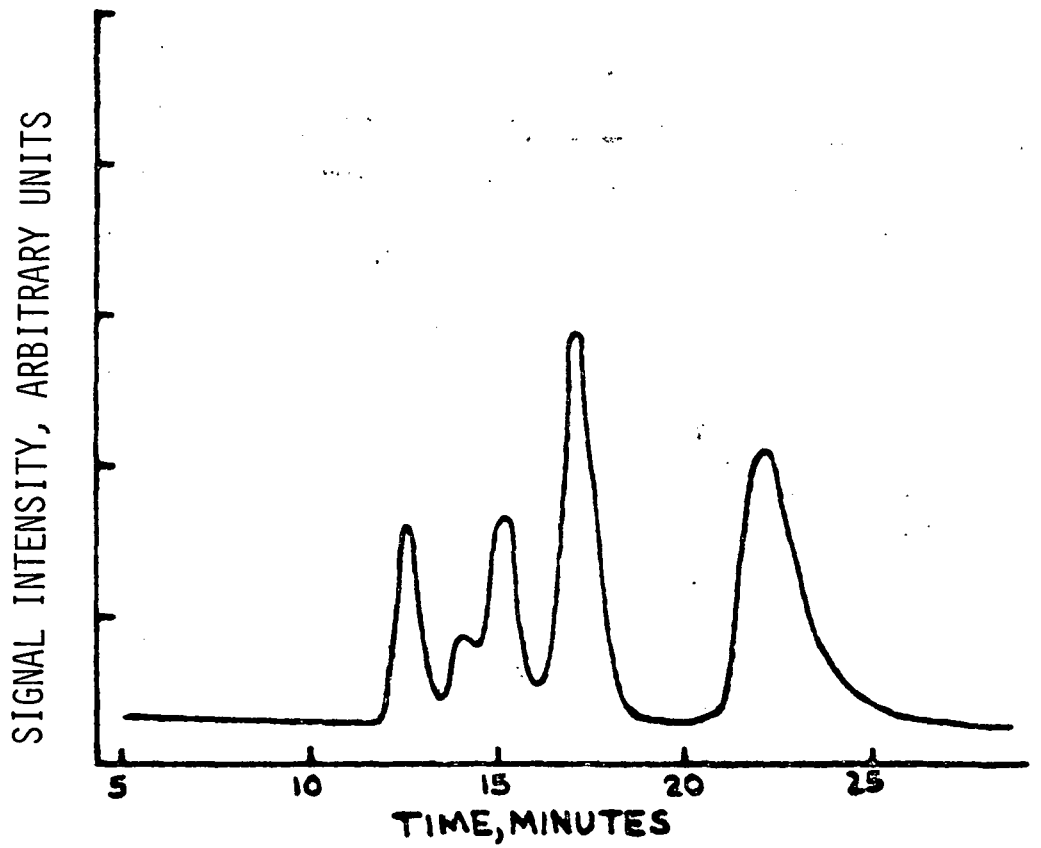


Figure 19. Chromatogram of acridine reaction sample (run 1041-10) on 6' x 1/8" Chromosorb 103: 250°C, 30 $cm^3$/min.

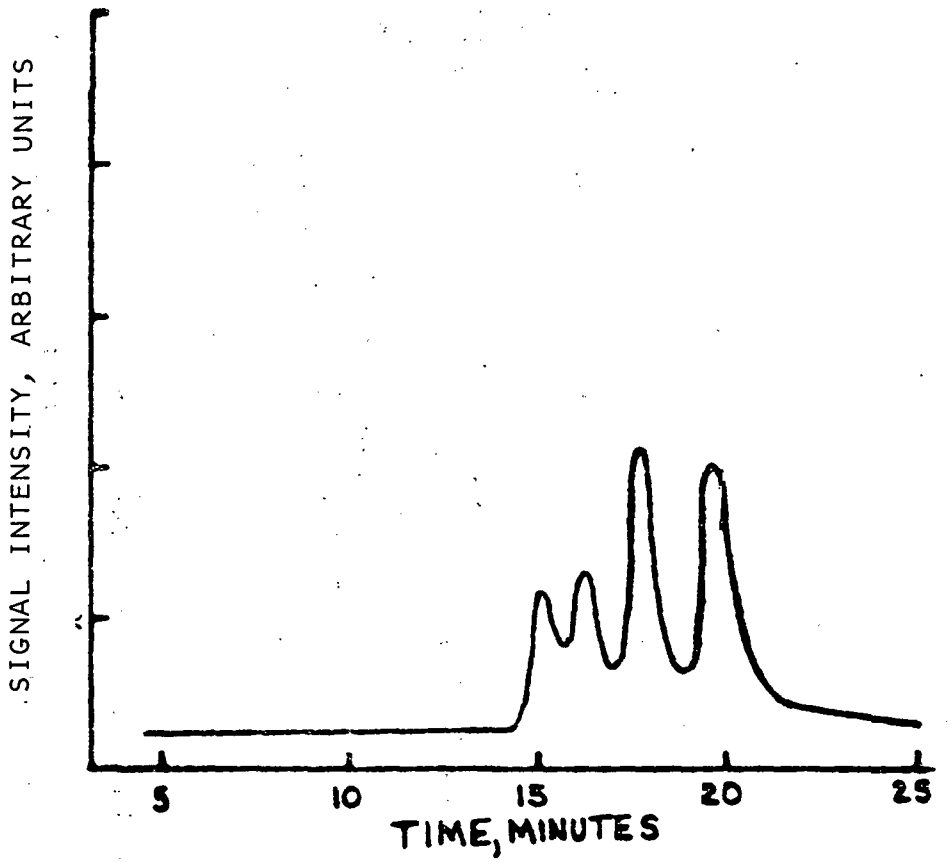


Figure 20. Chromatogram of acridine reaction sample (run 1041-10) on 6' x 1/8" SS UC-W98: 160°C, 30 $cm^3$/min.

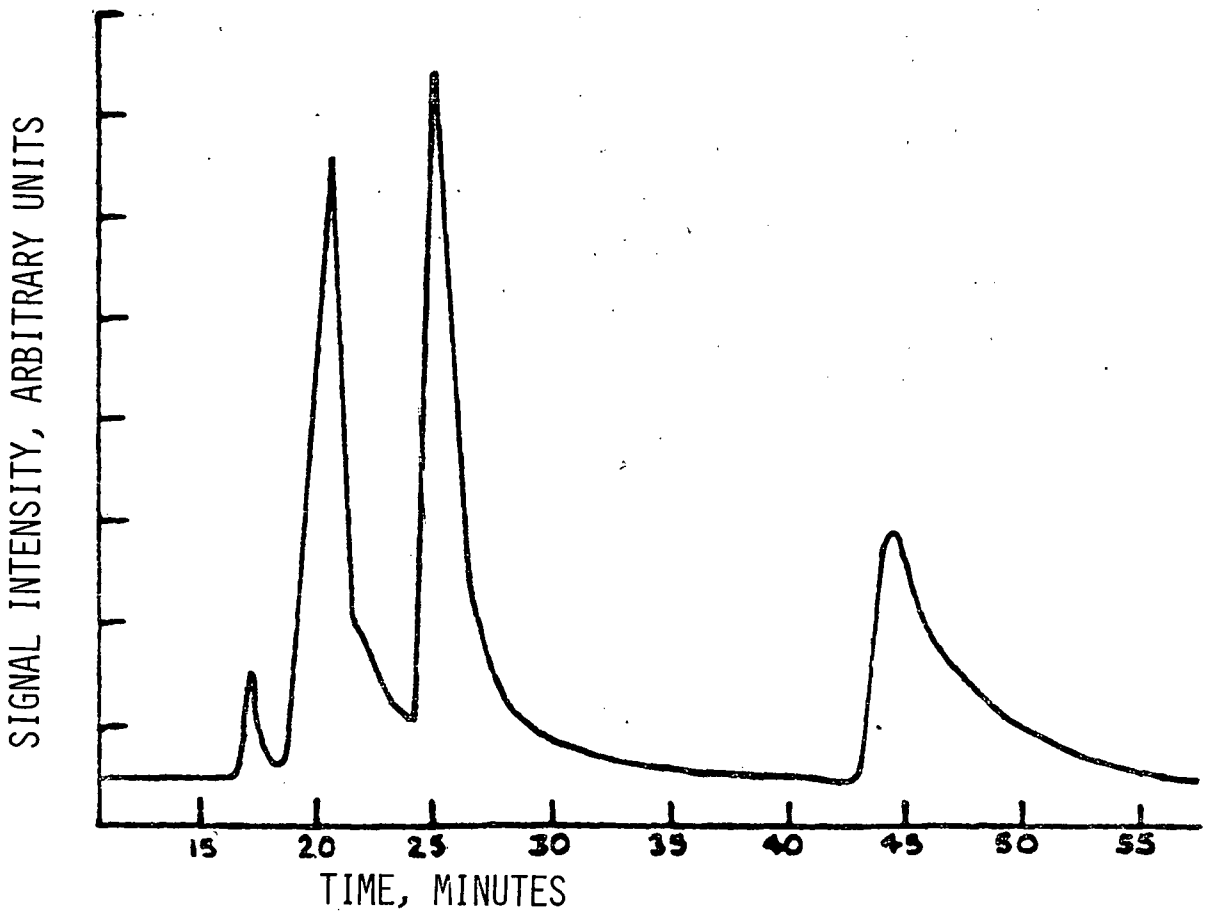


Figure 21. Chromatogram of an acridine reaction sample (1041-10) on 10' x 1/8" SS Carbowax 20M: 200°C, 21 $cm^3$/min.

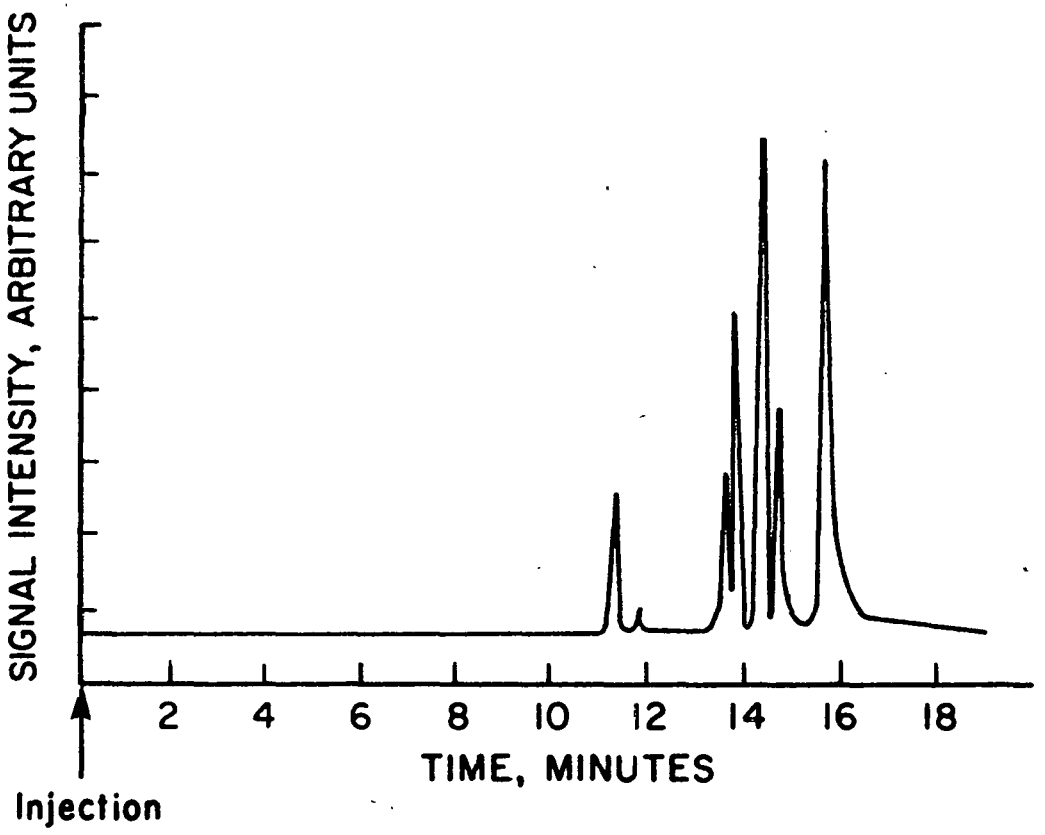


Figure 22. Chromatogram of an acridine reaction sample (R2A3-80) on a 50m OV101 WCOT column: 225°C, 1.5 $cm^3/min$.

There were several reasons for rejecting a stationary phase. First, the acridine reaction sample was known to have at least five major components, and the stationary phase should be capable of resolving these well. Second, the compound peak shapes should approach a Gaussian form and, therefore, have no severe tailing. Third, the compound retention times should not be excessively long, which was defined as greater than 1 hour. Next, the temperature required to meet the above constraints should be at least 25°C lower than stationary phase thermal stability limit, as suggested by the manufacturers. Finally, the nitrogen-specific detector is very sensitive to flow rate, and the flow rate required for the above constrainst should not be so high as to significantly decrease the detector's response. Also, it was recognized that a stainless steel column could contribute to the various problems stated above, especially resolution and tailing; however, the supply of glass columns was not sufficient to investigate every stationary phase using glass.

The analytical problem was finally solved by using a wall-coated open tubular column (WCOT) as described below:

Both internal and external standards for the acridine system calibration were tried unsuccessfully. When quinoline was used as an internal standard, non-linear response plots were obtained for concentration vs. response area for a packed glc column. When a 50m OV101 WCOT (capillary) column was used, however, the use of a calibration curve was feasible.

Several solutions of acridine in white oil were prepared. The application of such a calibration curve to compounds with differing molecular structures was confirmed using solutions of sym-octahydroacridine in white oil.

For the analysis of the reactor product samples for a given run, the curve was verified and/or regenerated before the samples were processed on the gas chromatograph.

b. Mass spectral procedures for interpretation of the acridine network

A. Procedure

1. Predetermine gas chromatographic conditions.

2. Run sample on chromatograph-mass spectrometer system.

3. As soon as a compound peak passes through the gas chromatograph thermal conductivity detector (monitored visually on the mass spectrometer oscilloscope for appearance of fragmentation pattern), monitor the total ionization until it is a maximum.

4. Record spectrum with computer software. In most cases 10 scans were taken and averaged.

B. Discussion

1. Well-resolved compounds yielded good mass spectra.

2. For fused peaks, spectra were taken over the entire area in question and then subtracted from each other to yield reasonably good mass spectra if the peaks were in about the same concentration.

3. Trace amounts of compounds appearing before or after a compound in high concentration could not be determined by mass spec.

4. Gas chromatographic preparatory work was done to isolate various fractions of the extract so that these fractions could be chromatographed at various conditions to optimize resolution.

5. Mass spectral structure assignments were made using standard literature fragmentation patterns as models. A published spectrum was available for acridine. When original compounds were available (acridine and sym-octahydroacridine), their spectra were obtained for comparison using the mass spec. direct introduction probe.

C. Limitations

1. Mass spectrometry yields information about molecular weights and compound structures; however, isomers have to be confirmed by other means.

2. If the structures of two compounds are very similar, fused peaks yield molecular weight information.

3. Many compounds do not give a molecular ion and lowering ionization voltage to retrieve this information was not always successful.

Mass Spectrometer Conditions

A Hewlett-Packard Model 5930A mass spectrometer with a 5932A data system was used for determining the fragmentation patterns. The ionization voltage was 70ev, pressure was $2 \times 10^{-6}$ torr, source temperature was 100°C, and for separation of the compounds a Hewlett-Packard 5750 gas chromatograph was used. The column was a 20' x 1/8" 10% SS Apiezon L (2% KOH) on 80/100 Chromosorb WAW operated at 200°C. The interface temperature was 200°C. Figure 23 gives the key to the assignment of the individual glc peaks in the extract, as they were passed on to the mass spectrometer. Tables 6-11 and Figures 24-27 give the computed mass spectra for the identified compounds in the extracted reaction mixture.

c. Acridine network evaluation

As part of trying to understand the nature of the catalyst, experiments were done with acridine in the presence of each of the three catalysts already mentioned in the quinoline work. The results are summarized in Table 12. The following abbreviations are used:

| | | |
|---|---|---|
| A | = | Acridine |
| THA | = | 1,2,3,4-Tetrahydroacridine |
| OHA | = | 1,2,3,4,9,10,13,14-Octahydroacridine |
| SOHA | = | 1,2,3,4,5,6,7,8-Octahydroacridine |
| PHA | = | Perhydroacridine |
| MCA | = | o(methylenecyclohexane) acridine |

Using the above-described mass spectrometric results and those pure compounds that were available, assignments were made so as to interpret the glc analyses of the autoclave reactor samples. The network for acridine was established to be the following:

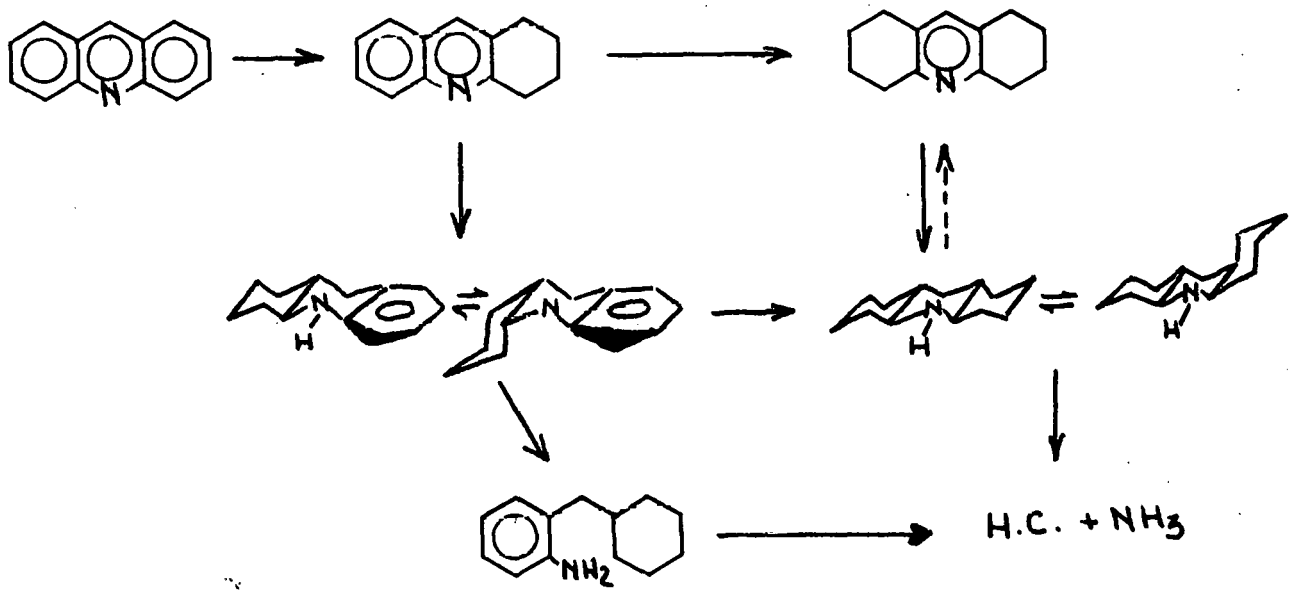

TABLE 5

STATIONARY PHASES INVESTIGATED FOR THE ANALYSIS OF NITROGEN-CONTAINING REACTION PRODUCTS

| Stationary Phase | Column* | Thermal Limit, °C | Reasons for Rejection |
|---|---|---|---|
| Apiezon L (2% KOH) on 80/100 Chromosorb WAW | 6' x 1/8" SS | 225 | Resolution |
| Same as above | 17' x 1/8" SS | 225 | Detector sensivity |
| Same as above | 5' x 1/8" G | 225 | Resolution |
| 60/80 Chromosorb-103 | 5' x 1/8" SS | 300 | Resolution, excessive retention times |
| Same as above | 6' x 1/8" SS | 300 | Same as above |
| Same as above | 5' x 1/8" G | 300 | Same as above |
| 10% UC-W98 | 6' x 1/8" SS | 250 | Resolution, slight tailing |
| Carbowax 20M (2% KOH) on Chromosorb WAW | 10' x 1/8" SS | 225 | Resolution, tailing |
| Tenax | 6' x 1/8" SS | 375 | Resolution |
| OV101 | WCOT | 250 | None |

G = Glass column
SS = Stainless steel column

# TABLE 6

## COMPOUND 7 (Perhydroacridine)

| MASS | INTENSITY | % BASEPEAK | % TOTAL IONIZATION |
|---|---|---|---|
| 27.0 | 674 | 4.05 | 0.88 |
| 28.1 | 1767 | 10.62 | 2.30 |
| 29.1 | 1633 | 9.81 | 2.13 |
| 30.1 | 783 | 4.70 | 1.02 |
| 35.0 | 2158 | 12.97 | 2.81 |
| 39.0 | 1449 | 8.71 | 1.89 |
| 41.1 | 6526 | 39.05 | 8.50 |
| 42.1 | 261 | 1.57 | 0.34 |
| 47.0 | 5029 | 30.22 | 6.54 |
| 49.0 | 2643 | 15.88 | 3.44 |
| 53.1 | 539 | 3.24 | 0.70 |
| 54.1 | 1184 | 7.11 | 1.54 |
| 55.1 | 1657 | 9.96 | 2.16 |
| 56.1 | 1142 | 6.86 | 1.49 |
| 67.1 | 1707 | 10.26 | 2.22 |
| 81.1 | 485 | 2.79 | 0.61 |
| 82.1 | 921 | 5.53 | 1.20 |
| 84.0 | 13077 | 91.34 | 17.34 |
| 86.0 | 7718 | 46.38 | 10.04 |
| 90.0 | 452 | 2.72 | 0.59 |
| 150.0 | 16642 | 100.00 | 21.66 |
| 151.1 | 4117 | 24.71 | 5.35 |
| 192.0 | 1138 | 6.84 | 1.48 |
| 193.0 | 2400 | 14.41 | 3.13 |

# TABLE 7

## COMPOUND 11 (o-(methylenecyclohexane)aniline)

| MASS | INTENSITY | % BASEPEAK | % TOTAL IONIZATION |
|---|---|---|---|
| 15.3 | 3497 | 20.36 | 1.21 |
| 25.0 | 4029 | 28.12 | 1.67 |
| 26.0 | 16717 | 97.35 | 5.78 |
| 27.1 | 16850 | 98.12 | 5.82 |
| 28.1 | 15914 | 92.67 | 5.50 |
| 29.1 | 4171 | 24.29 | 1.44 |
| 30.1 | 1592 | 9.27 | 0.55 |
| 36.0 | 3762 | 21.91 | 1.30 |
| 37.2 | 3246 | 18.90 | 1.12 |
| 38.1 | 5855 | 34.10 | 2.02 |
| 39.0 | 17120 | 99.70 | 5.92 |
| 40.2 | 5416 | 31.54 | 1.87 |
| 41.0 | 16915 | 98.50 | 5.85 |
| 42.1 | 6764 | 39.39 | 2.34 |
| 43.1 | 2276 | 13.25 | 0.79 |
| 50.0 | 5172 | 30.12 | 1.79 |
| 51.0 | 8081 | 47.06 | 2.83 |
| 52.1 | 5503 | 32.05 | 1.90 |
| 53.1 | 8256 | 48.08 | 2.85 |
| 54.1 | 8228 | 47.89 | 2.84 |
| 55.1 | 4870 | 28.36 | 1.68 |
| 56.1 | 2214 | 12.89 | 0.77 |
| 63.1 | 4337 | 25.26 | 1.50 |
| 64.1 | 1197 | 6.97 | 0.41 |
| 65.1 | 3324 | 19.36 | 1.15 |
| 66.1 | 2220 | 12.93 | 0.77 |
| 67.1 | 12914 | 75.20 | 4.46 |
| 75.0 | 2081 | 12.12 | 0.72 |
| 77.1 | 6901 | 40.19 | 2.38 |
| 78.1 | 11368 | 66.20 | 3.93 |
| 79.1 | 6182 | 36.00 | 2.14 |
| 80.1 | 1580 | 9.20 | 0.55 |
| 81.1 | 310 | 1.80 | 0.11 |
| 82.1 | 2071 | 12.06 | 0.72 |
| 83.1 | 3214 | 18.72 | 1.11 |
| 84.1 | 2109 | 12.28 | 0.73 |
| 91.0 | 2802 | 16.32 | 0.97 |
| 92.0 | 518 | 3.02 | 0.18 |
| 91.1 | 961 | 5.60 | 0.33 |
| 93.0 | 2290 | 13.34 | 0.79 |
| 104.0 | 2532 | 14.74 | 0.88 |
| 105.0 | 17172 | 100.00 | 5.93 |
| 107.0 | 16713 | 97.33 | 5.78 |
| 115.0 | 1660 | 9.67 | 0.57 |
| 130.0 | 3115 | 18.14 | 1.08 |
| 143.0 | 690 | 4.02 | 0.24 |
| 183.9 | 13261 | 77.22 | 4.58 |

# TABLE 8

## COMPOUND 12 (Sym-octahydroacridine)

| MASS | INTENSITY | % BASEPEAK | % TOTAL IONIZATION |
|---|---|---|---|
| 25.9 | 1157 | 29.69 | 4.10 |
| 27.0 | 1105 | 28.11 | 3.88 |
| 28.0 | 2320 | 59.02 | 8.14 |
| 29.0 | 270 | 32.31 | 4.46 |
| 39.0 | 1616 | 41.11 | 5.67 |
| 41.1 | 1140 | 29.00 | 4.00 |
| 42.1 | 739 | 18.80 | 2.59 |
| 51.1 | 581 | 14.78 | 2.04 |
| 52.0 | 439 | 11.17 | 1.54 |
| 53.0 | 546 | 13.89 | 1.92 |
| 53.2 | 714 | 18.16 | 2.51 |
| 63.0 | 552 | 14.04 | 1.94 |
| 65.1 | 253 | 6.44 | 0.89 |
| 77.0 | 624 | 15.87 | 2.19 |
| 78.0 | 769 | 19.56 | 2.70 |
| 79.0 | 466 | 11.85 | 1.64 |
| 107.0 | 255 | 5.49 | 0.89 |
| 108.0 | 815 | 20.73 | 2.86 |
| 117. | 586 | 14.91 | 2.06 |
| 118.1 | 289 | 7.35 | 1.01 |
| 131.1 | 431 | 10.96 | 1.51 |
| 143.1 | 493 | 12.09 | 1.70 |
| 144.1 | 435 | 11.07 | 1.53 |
| 157.0 | 610 | 15.52 | 2.14 |
| 158.0 | 915 | 23.30 | 3.21 |
| 159.0 | 422 | 10.09 | 1.52 |
| 169.0 | 1276 | 32.46 | 4.48 |
| 170.1 | 652 | 16.61 | 2.29 |
| 185.0 | 385 | 9.82 | 1.35 |
| 186.0 | 2434 | 60.53 | 9.45 |
| 187.1 | 3931 | 100.00 | 13.80 |

# TABLE 9

## COMPOUND 13 (1,2,3,4,9,10,13,14-octahydroacridine)

| MASS | INTENSITY | % BASE PEAK | % TOTAL IONIZATION |
|---|---|---|---|
| 29.0 | [illegible] | [illegible] | 6.37 |
| 37.0 | [illegible] | [illegible] | 0.50 |
| 38.0 | [illegible] | [illegible] | 0.07 |
| 39.0 | [illegible] | [illegible] | 2.84 |
| 39.1 | [illegible] | [illegible] | 0.29 |
| 40.0 | [illegible] | [illegible] | 10.52 |
| 41.1 | [illegible] | [illegible] | 1.59 |
| 42.1 | [illegible] | [illegible] | 10.62 |
| 43.0 | [illegible] | [illegible] | 2.52 |
| 50.0 | [illegible] | [illegible] | 0.42 |
| 51.0 | 4869 | 30.17 | 4.05 |
| 52.0 | 4431 | 35.77 | 4.22 |
| 53.0 | 2161 | 17.51 | 1.86 |
| 54.0 | 1699 | 13.80 | 1.47 |
| 55.0 | [illegible] | 9.70 | 1.03 |
| 56.0 | [illegible] | 12.38 | 1.30 |
| 62.0 | [illegible] | 6.75 | 0.72 |
| 63.0 | 1113 | 9.14 | 0.97 |
| 64.0 | 3385 | 27.81 | 2.95 |
| 65.0 | 768 | 6.27 | 0.67 |
| 66.0 | 1944 | 15.97 | 1.70 |
| 67.0 | 164 | 1.35 | 0.14 |
| 74.0 | 281 | 2.31 | 0.25 |
| 75.0 | 887 | 7.29 | 0.77 |
| 76.0| 1605 | 13.19 | 1.40 |
| 77.0 | 839 | 6.86 | 0.73 |
| 78.0 | 4363 | 35.85 | 3.81 |
| 79.0 | [illegible] | [illegible] | 1.31 |
| 80.0 | [illegible] | [illegible] | 0.75 |
| 90.0 | 1698 | 13.21 | 1.40 |
| 91.1 | 1951 | 16.03 | 1.70 |
| 102.0 | 1171 | 9.62 | 1.02 |
| 103.0 | 530 | 4.34 | 0.45 |
| 104.0 | 655 | 5.38 | 0.57 |
| 106.0 | 961 | 7.90 | 0.84 |
| 115.0 | 936 | 7.69 | 0.82 |
| 116.0 | 2441 | 20.06 | 2.13 |
| 117.0 | 709 | 5.83 | 0.62 |
| 118.0 | 1741 | 14.30 | 1.52 |
| 120.0 | [illegible] | [illegible] | 1.24 |
| 130.0 | [illegible] | [illegible] | 1.34 |
| 131.0 | [illegible] | [illegible] | 8.58 |
| 142.0 | 2292 | 18.83 | 2.00 |
| 143.0 | 409 | 3.36 | 0.36 |
| 144.0 | 1435 | 12.04 | 1.28 |
| 145.0 | 5065 | 41.62 | 4.42 |
| 154.0 | 493 | 4.05 | 0.43 |
| 155.0 | 511 | 4.20 | 0.45 |
| 156.0 | [illegible] | [illegible] | 0.14 |
| 183.0 | [illegible] | [illegible] | 0.70 |
| 196.1 | [illegible] | [illegible] | 0.19 |
| 197.1 | [illegible] | [illegible] | 1.22 |
| [illegible] | [illegible] | [illegible] | 1.05 |

# TABLE 10

## COMPOUND 14 (1,2,3,4-tetrahydroacridine)

| MASS | INTENSITY | % BASEPEAK | % TOTAL IONIZATION |
|---|---|---|---|
| 25.8 | 1881 | 25.08 | 3.79 |
| 26.8 | 7269 | 100.00 | 14.65 |
| 27.9 | 3354 | 45.14 | 6.76 |
| 29.9 | 1470 | 19.67 | 2.96 |
| 34.0 | 673 | 9.13 | 1.36 |
| 37.0 | 421 | 5.79 | 0.85 |
| 38.0 | 1570 | 21.60 | 3.16 |
| 39.0 | 6133 | 84.37 | 12.36 |
| 40.0 | 782 | 10.76 | 1.58 |
| 41.0 | 2304 | 31.70 | 4.64 |
| 42.1 | 900 | 12.33 | 1.81 |
| 50.0 | 2418 | 33.68 | 4.85 |
| 51.0 | 3413 | 46.95 | 6.88 |
| 52.0 | 506 | 6.96 | 1.02 |
| 57.0 | 748 | 10.30 | 1.51 |
| 61.0 | 332 | 4.57 | 0.67 |
| 62.0 | 681 | 9.37 | 1.37 |
| 63.0 | 1745 | 24.01 | 3.52 |
| 64.0 | 627 | 8.63 | 1.26 |
| 65.0 | 463 | 6.38 | 0.91 |
| 74.0 | 1631 | 22.44 | 3.29 |
| 75.0 | 1580 | 21.74 | 3.18 |
| 76.0 | 781 | 10.74 | 1.57 |
| 77.0 | 331 | 4.55 | 0.67 |
| 78.0 | 209 | 2.88 | 0.58 |
| 88.0 | 656 | 9.05 | 1.33 |
| 89.0 | 466 | 6.41 | 0.94 |
| 90.0 | 167 | 2.31 | 0.34 |
| 91.0 | 74 | 1.02 | 0.15 |
| 102.0 | 1025 | 14.10 | 2.07 |
| 103.1 | 140 | 1.93 | 0.28 |
| 115.0 | 684 | 9.41 | 1.38 |
| 116.0 | 716 | 9.85 | 1.44 |
| 128.0 | 1343 | 18.50 | 2.71 |
| 129.0 | 720 | 9.91 | 1.45 |
| 130.1 | 1336 | 18.38 | 2.69 |

# TABLE 11

## COMPOUND 15 (Acridine)

| MASS | INTENSITY | % BASEPEAK | % TOTAL IONIZATION |
|---|---|---|---|
| 25.9 | 441 | 10.72 | 3.22 |
| 25.9 | 500 | 12.16 | 3.65 |
| 27.0 | 590 | 14.34 | 4.31 |
| 28.0 | 1112 | 27.04 | 8.12 |
| 38.9 | 220 | 5.35 | 1.61 |
| 50.0 | 621 | 15.10 | 4.53 |
| 62.0 | 474 | 11.52 | 3.46 |
| 63.0 | 430 | 10.45 | 3.14 |
| 73.0 | 396 | 9.63 | 2.89 |
| 74.0 | 514 | 12.50 | 3.75 |
| 75.0 | 591 | 14.37 | 4.31 |
| 88.0 | 350 | 8.51 | 2.55 |
| 88.5 | 348 | 8.46 | 2.54 |
| 126.0 | 407 | 9.90 | 2.97 |
| 127.0 | 455 | 11.01 | 3.31 |
| 151.0 | 349 | 8.49 | 2.55 |
| 178.0 | 835 | 20.29 | 6.24 |
| 179.0 | 4113 | 100.00 | 30.03 |
| 180.0 | 937 | 22.78 | 6.84 |

TABLE 12

ACRIDINE NETWORK FOR SEVERAL CATALYST COMPOSITIONS

| | Rate Constant, $min^{-1}$ | | |
|---|---|---|---|
| REACTION | Ni-W | Ni-Mo | Co-Mo |
| A → THA | 48 | 58 | 20.5 |
| THA → SOHA | 10.7 | 11.2 | 4.4 |
| THA → OHA | ? | 15.15 | 8.1 |
| OHA → PHA | 2.9 | 9.0 | 3.4 |
| SOHA → PHA | 1.2 | 5.1 | 4.05 |
| PHA → SOHA | 0.3 | 2.7 | 2.8 |
| PHA → HC | 0.8 | 2.2 | 0.8 |
| OHA → MCA | 0.4 | 1.2 | 0.46 |
| MCA → HC | 0.74 | 2.2 | 0.78 |

CONDITIONS:

367°C

2000 psig

Initial acridine concentration: $3 \times 10^{-5} \frac{\text{g mole}}{\text{g oil}}$

Catalyst particle size: 150-200 mesh

Initial $CS_2$ concentration: $7.6 \times 10^{-6} \frac{\text{g mole}}{\text{g oil}}$

Catalyst concentration: $4.4 \times 10^{-3} \frac{\text{g catalyst}}{\text{g oil}}$

All catalysts were sulfided at 400°C for 2 hr using a 10% $H_2S$ in $H_2$ gas mixture.

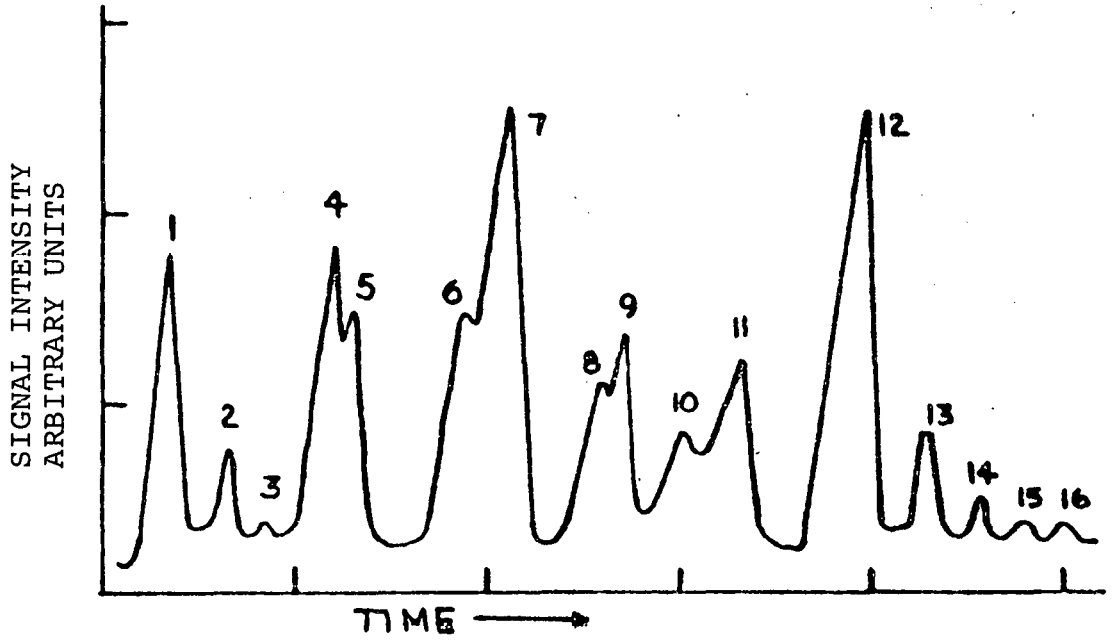


| PEAK | MOLECULAR WEIGHT | STRUCTURE |
|---|---|---|
| 1 | 152 | |
| 2 | 153 | |
| 3 | 153 | |
| 4 | 174 | |
| 5 | 153 | |
| 6 | 193 | PERHYDROACRIDINE |
| 7 | 193 | PER-HYDROACRIDINE |
| 8 | 187 | |
| 9 | 193 | |
| 10 | 187 | 1,2,3,4,9,10,13,14-OCTAHYDROACRIDINE |
| 11 | 189 | o-(METHYLENECYCLOHEXANE)ANILINE |
| 12 | 187 | SYM-OCTAHYDROACRIDINE |
| 13 | 187 | 1,2,3,4,9,10,13,14-OCTAHYDROACRIDINE |
| 14 | 183 | 1,2,3,4-TETRAHYDROACRIDINE |
| 15 | 179 | ACRIDINE |
| 16 | 201 | |

Figure 23. Chromatogram of the extracted nitrogen-containing reaction products for the acridine experiment run at 353°C and 2000 psig (run 1052); Ni-Mo/$Al_2O_3$ (American Cyanamid HDS-9A) catalyst. 20' x 1/8" 10% Apeizon L 5% NOH on Chromosorb WAW at 220°C column temperature.

# ACRIDINE AND 1,2,3,4-TETRAHYDROACRIDINE

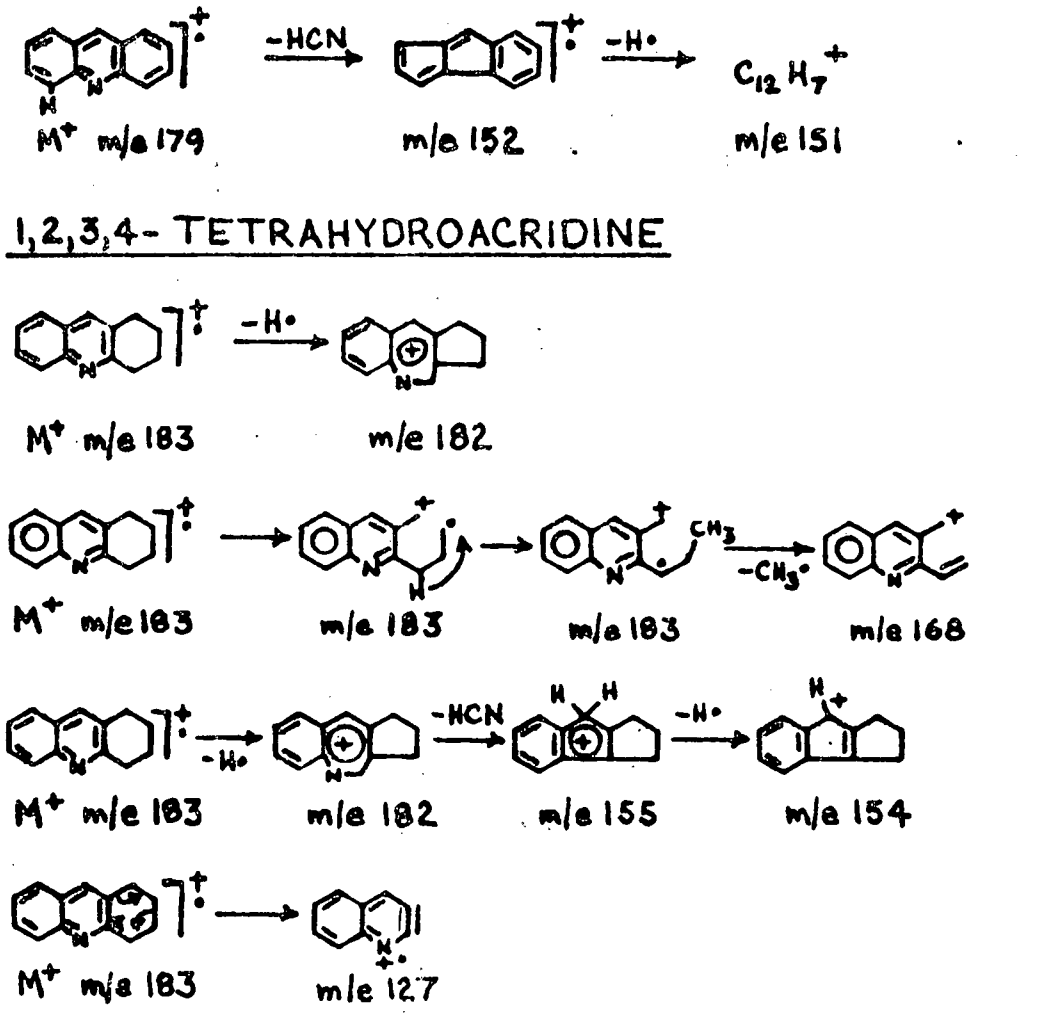


m/e 179,180,181 ACCOUNT FOR THERMAL DEHYDROGENATION

Figure 24. Mass spectral fragmentation patterns for acridine and 1,2,3,4-tetrahydroacridine nitrogen-containing reaction products.

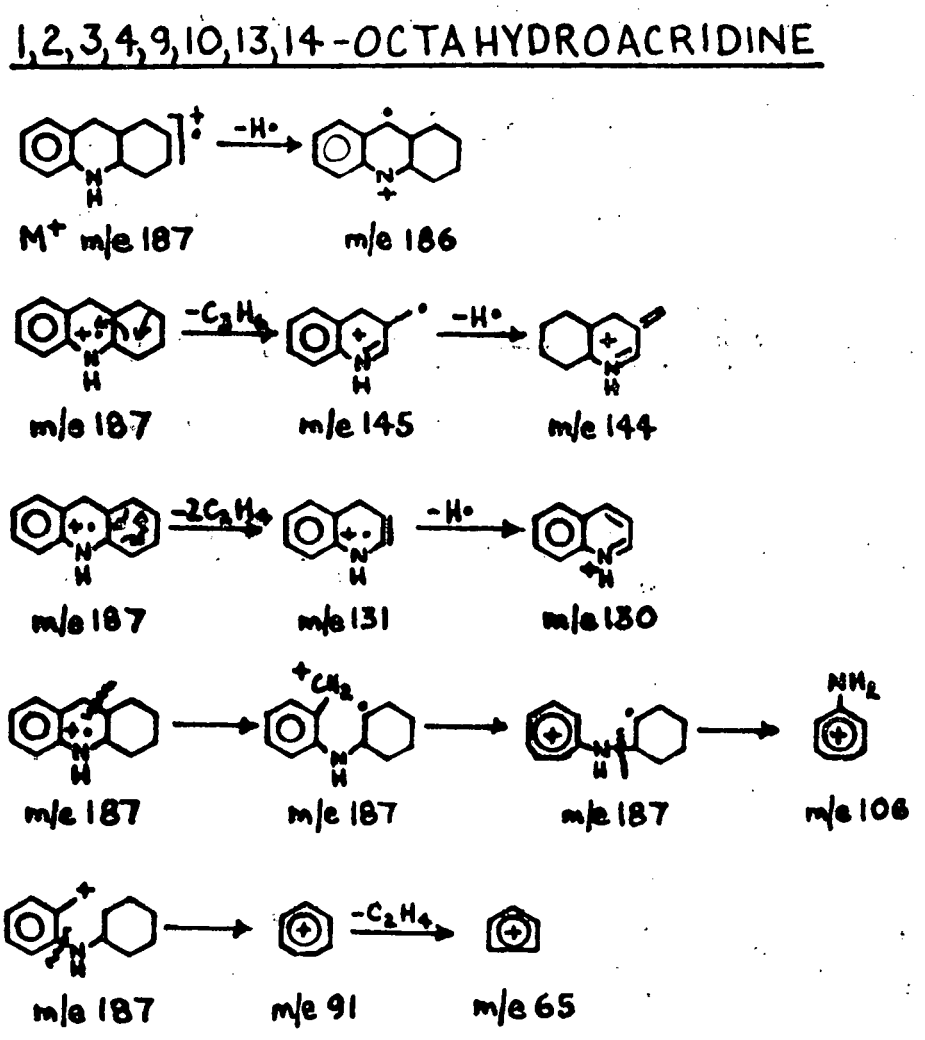


ANILINE TYPE STRUCTURES UNDERGO ∝ CLEAVAGE OF SIDE CHAIN AS DOMINANT PROCESS YIELDING THE AMINOTROPYLIUM ION AND ALSO FRAGMENTATION OF THE AROMATIC NITROGEN BOND

Figure 25. Mass spectral fragmentation pattern for 1,2,3,4,9, 10,13,14-octahydroacridine.

## 1,2,3,4,5,6,7,8-OCTAHYDROACRIDINE

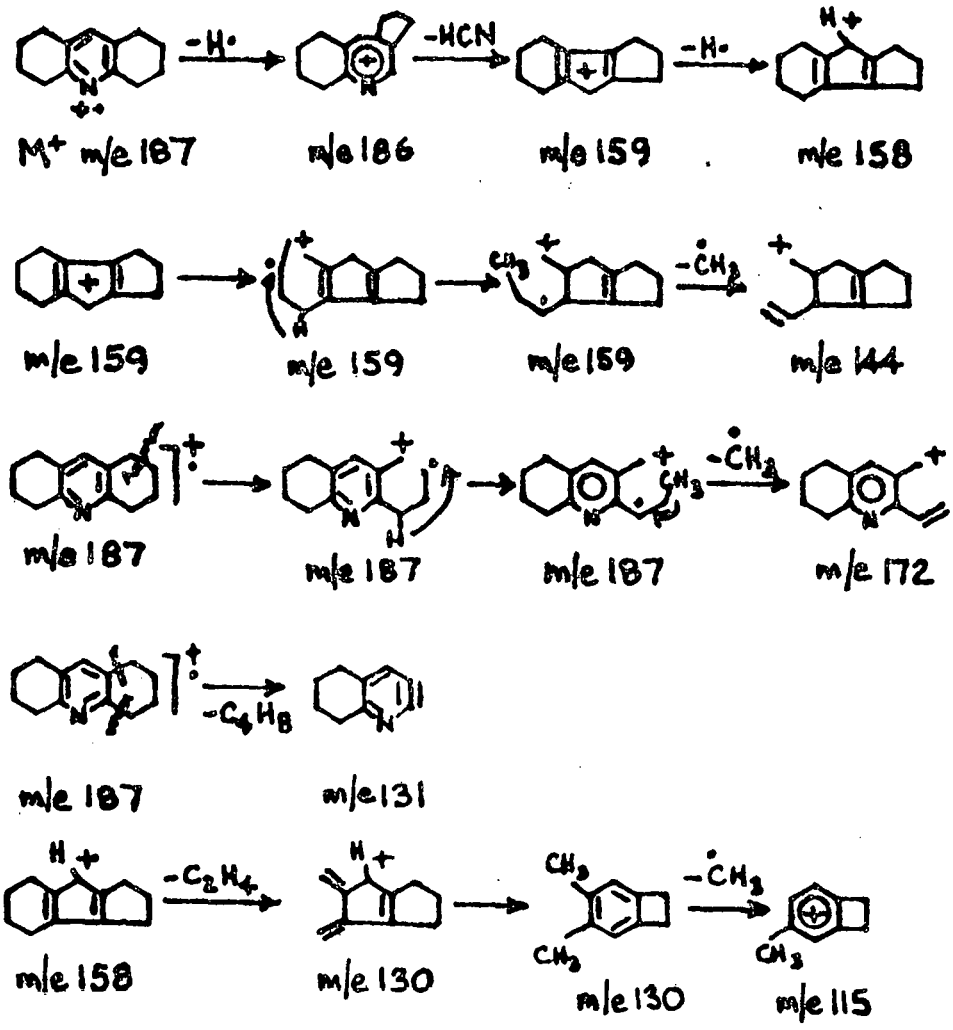


PYRIDINE TYPE STRUCTURES LOSE HYDROGEN RADICAL TO FORM AN AZATROPYLIUM ION. IN SUBSTITUTED PYRIDINES $\beta$ CLEAVAGE IS IMPORTANT. NO $\alpha$ CLEAVAGE CAN OCCUR.

Figure 26. Mass spectral fragmentation for 1,2,3,4,5,6,7,8-octahydroacridine.

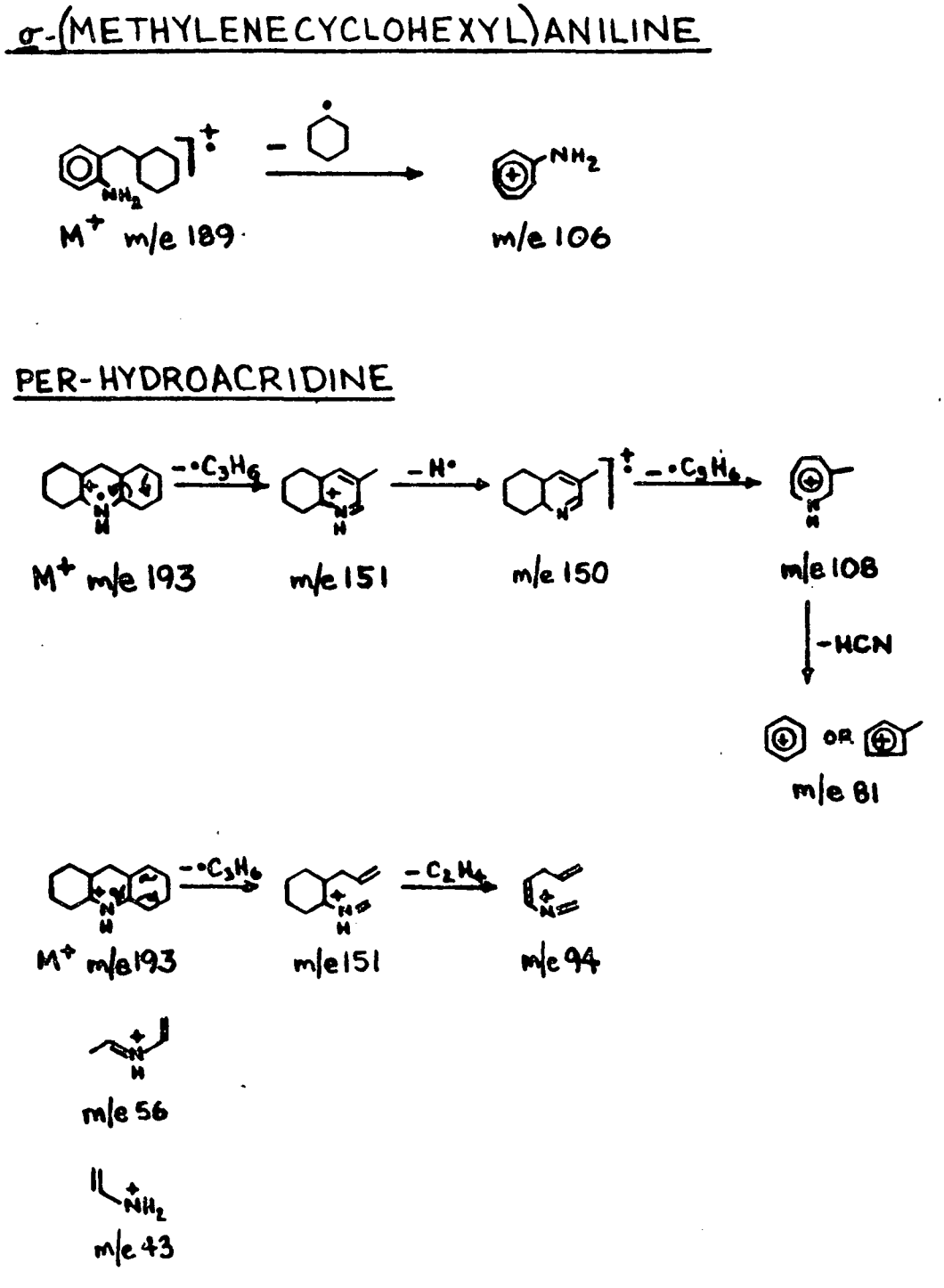


Figure 27. Mass spectral fragmentation pattern for o-(methylenecyclohexyl)aniline.

The presence of cis and trans OHA was determined by mass spectrometric means; the isomers presented two distinct glc peaks that have the same molecular ion and fragment peaks. Only those compounds observed in the glc analysis of the reactor samples were included in the network. Other compounds that were seen in the extract were present in more measurable quantities in the reactor samples with present analytical techniques.

The acridine network shows some similarity to the quinoline network in that hydrogenation of the aromatic ring has to be effected before nitrogen removal can occur. Acridine undergoes a very rapid hydrogenation to THA. Independent experiments confirmed the first-order rate constant for disappearance of A. These experiments were conducted at lower temperatures, and the rate constants are of the same magnitude as the runs determined with the aid of the numerical integration (computer) program.

A blank (no catalyst added) run was made in the autoclave, using a glass liner under the same conditions as the standard runs. The results showed that the reactor itself has hydrogenating activity but, for all reactions, was at most 10% of the same activity in the presence of any catalyst. During a 12-hr run, no hydrodenitrogenation activity could be detected in the blank experiment.

Since the operating pressure was high compared to the value in the quinoline runs, and since the hydrogenation reactions have generally been found to exhibit a positive reaction order with respect to hydrogen partial pressure, it follows that hydrogenation is no longer the slow reaction in the HDN network when the reactant is acridine. The rate constant for cracking, at the relatively high temperature and pressure, is roughly the same as that for quinoline at one-fourth of the pressure and a temperature 25°C lower. It is clear that acridine is much less reactive than quinoline.

Total nitrogen removal does not follow the simple first-order kinetics. This result can be seen in Figure 28. The formation of SOHA predominates and the rate is high even for early samples, whereas tetrahydroacridine and octahydroacridine appears and disappears very rapidly. The formation of PHA predominates at the later stages of the conversion. A concentration vs. time profile for the reaction was given in the sixth quarterly report.

In order to test the network for reversibility of any of the individial reactions, a run was made using sym-octahydroacridine as the reactant, and the experimental conditions were the same as for the acridine run using the Ni-Mo/$Al_2O_3$ cat. Only two major species could be detected in analysis of

reactor samples, SOHA and PHA. SOHA hydrogenated rapidly to form the completely hydrogenated species; no dehydrogenation could be detected as would have been indicated by the presence of OHA and THA, although the reversible step to form SOHA from PHA could not be ruled out. Further work, using the completely hydrogenated compound should provide a suitable answer.

The rate parameters are as follows:

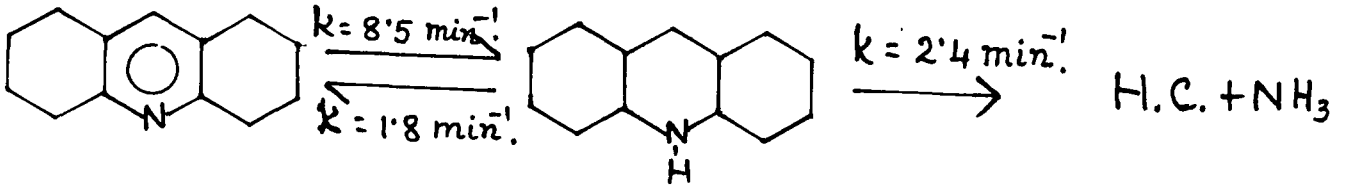


The agreement between the calculated rate parameters and the runs for the complete network is fairly good as can be seen from Table 4.

SOHA could possibly present a great amount of steric hindrance towards dehydrogenation due to the presence of the two puckered rings attached to the quinoline ring, thus making the energy requirement for the reverse reaction to occur unaccessible under the experimental conditions.

The results of contacting acridine with three differenct catalysts are summarized in Figure 28. Again, the normalization for the catalyst comparison was with respect to the least active Co-Mo/$Al_2O_3$ catalyst. To account for the effect on the network, rate constants were normalized with respect to that for cracking of OHA. The rate constant for the reaction THA → OHA for the Ni-W catalyst is questionable. The reason for the uncertainty is not clear and is presently under investigation. One explanation could be that, due to the difference in physical properties, the network might undergo small changes. The Co-Mo and Ni-Mo catalysts are more uniform in properties and the discussion will be centered on these two catalysts hence.

The Co-Mo and Ni-Mo catalysts have similar effects on the individual reactions of the network. Ni-Mo is more active by a factor of at least two in both hydrogenation and hydrogenolysis (cracking). Both catalysts affect the network in similar ways, hydrogenation of A to THA is done with the same relative ease; the same is approximately true for the cracking reaction. In the nitrogen ring hydrogenation (i.e., THA → OHA and SOHA → PHA), the Co-Mo catalyst appears to perform slightly better, thus confirming the results already suggested for quinoline. One possible explanation is that the promotor effect of Ni and Co is different on the Mo, thus giving rise to a strange adsorption of nitrogen

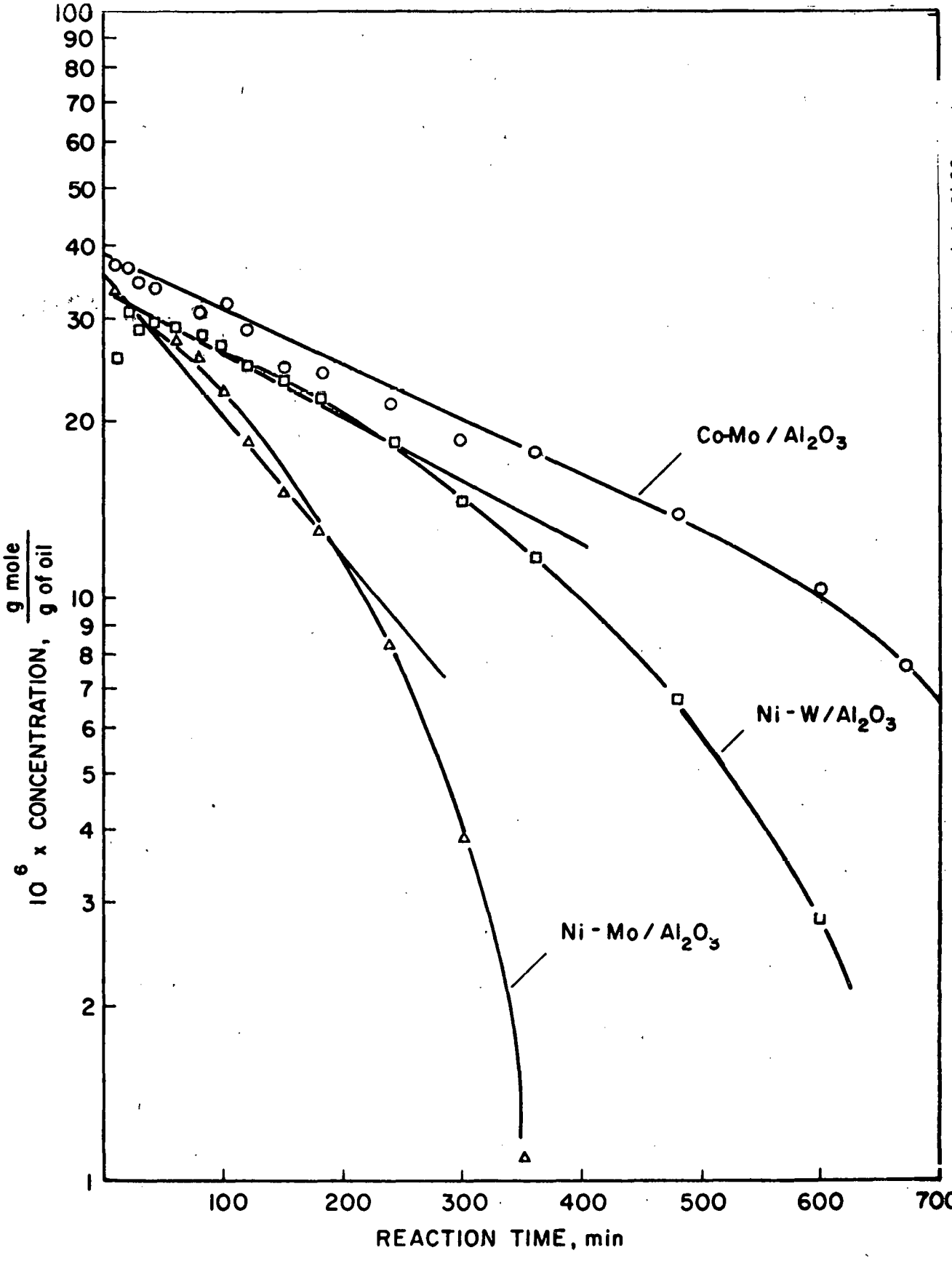


Figure 28. First-order rate plot for total nitrogen removal from acridine with different catalysts. T = 367°C, P = 2000 psig.

on the Co-Mo catalyst and therefore a more pronounced hydrogenation activity. The reason why the Ni-W catalyst is more active in HDN than Co-Mo, even though the network analysis shows little difference, is likely to be associated with the complexity of the network contributing to total nitrogen removal. As can be seen from Figure 28, the initial slopes are about equal (within experimental error), but the relatively rapid hydrogenations for the Ni-W catalyst have the effect of "pushing" the system into a condition for faster nitrogen removal earlier in time.

3. HDN of quinoline in the flow microreactor

A preliminary comparison of quinoline HDN runs carried out in a batch autoclave reactor and in a high-pressure flow microreactor was presented in the sixth quarterly report.

First-order rate constants for total nitrogen removal for these runs have been calculated as follows:

Batch Autoclave Reactor

$$k_{Total} = 1.04 \frac{\text{g oil}}{\text{g catalyst min}}$$

Flow Microreactor

$$k_{Total} = 1.41 \frac{\text{g oil}}{\text{g catalyst min}}$$

The rate calculated from flow microreactor data appears to be significantly higher than that calculated from batch reactor data, but it is still too early to comment further on the flow reactor performance with only a single comparison at hand.

It is not possible to calculate rate constants for the detailed reaction network in the case of the microreactor run, since the maxima in concentration profiles of various intermediate N-containing compounds were not observed in the range of LHSV's considered. In order to observe the maxima in product distribution curves, the flow microreactor has to be operated at LHSV's in the range 150-3000 g oil/catalyst hr, which requires still lower catalyst loadings than have been used (in the present case, 25.8 mg of catalyst was used) or much higher liquid flow rates. Furthermore, to evaluate precisely eight rate constants in the reaction network, product distribution data are probably required at 12-13 different space velocities. Data of this sort will be taken during the next quarter.

Meanwhile, three reproducibility runs have been carried out at a reduced catalyst loading (10.6 mg). Results and reaction conditions for these three runs are presented in Figure 29 and Table 13. The figure indicates that the runs are reproducible within 6% (based on total nitrogen removal).

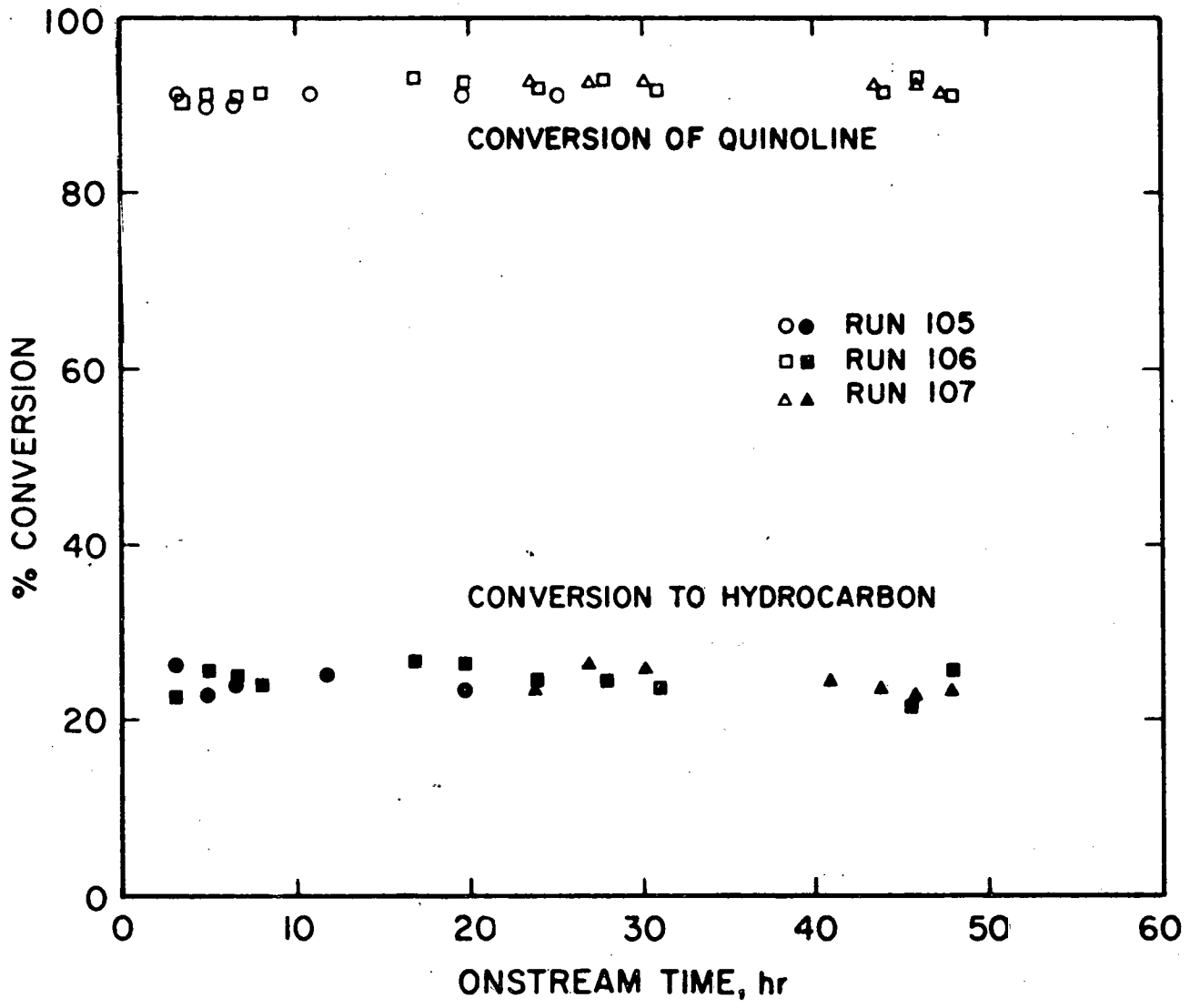


Figure 29. Reproducibility runs for HDN of quinoline in the flow microreactor.

TABLE 13

REACTION CONDITIONS FOR REPRODUCIBILITY RUNS IN A FLOW MICROREACTOR

- Reactant mixture:

  Quinoline in white oil ~$2.03 \times 10^{-5}$ $\frac{\text{g mole}}{\text{g oil}}$

- Hydrogen saturation pressure:

  ~2000 psig at 25°C with ~1% $H_2S$

- Catalyst:

  $10.6 \times 10^{-2}$g of $Ni\text{-}Mo/Al_2O_3$

  In situ sulfided with 10% $H_2S/H_2$ (~150 $cm^3$/min) for 2 hr at 325°C

- Reaction temperature:

  342°C

- Space velocity:

  ~220 $\frac{\text{g oil}}{\text{g catalyst-hr}}$

- Reactor pressure:

  ~2200-2500 psig

## E. POISONING REACTION ENGINEERING

This section reports a continuation of study of the aged catalysts from pilot plants for hydrogenation of coal or coal-derived liquids. In the sixth quarterly report, both the heterogeneous surface properties and the spatial distributions of deposited mineral matter observed by SEM and EDAX were discussed. In the present report, data for the same samples of H-Coal catalyst (Run No. 130-73) are reported for both hydrodesulfurization and hydrodenitrogenation activity in a batch autoclave reactor; dibenzothiophene (DBT) and quinoline were used as the typical sulfur- and nitrogen-containing compounds. In the DBT experiment, the aged catalyst was first (partially) regenerated by burning off the deposited hydrocarbon poison (coke) with ~27% oxygen at 450°C with a total gas flow rate of 100 $cm^3$/min (air and helium). The data are shown in Figures 30-33.

The burning process was continued for about 24 hours at which time the weight of residual catalyst became constant. The total loss of catalyst weight using the "burn off" process was about 11%; and therefore it is concluded that there had been coke laydown during the hydrotreating process.

The rate constants of both the aged and (partially) regenerated catalysts in HDS and HDN experiments are compared to those of fresh catalysts operated under similar conditions given in the sixth quarterly report. The results are shown in Table 14. The loss of activity of the aged catalyst thus can be evaluated. Some remarks about the data follow.

In Table 14, the activity of aged catalyst is shown to be very low in both HDN and HDS experiments. In the HDS experiment, the data for (partially) regenerated catalyst shows that only 10% of the original catalyst was recovered. Thus most of the catalyst deactivation (85% in this case) was contributed by permanent poisoning deposits of mineral matter. Although the deposition of carbon contributed only about 10% of the poisoning in the specific experiment examined, the total volume of carbon deposition on the catalyst (as it was mentioned earlier that 11 wt % loss was found in the burning off process) presents a serious problem since the pores of catalyst may be either blocked or plugged.

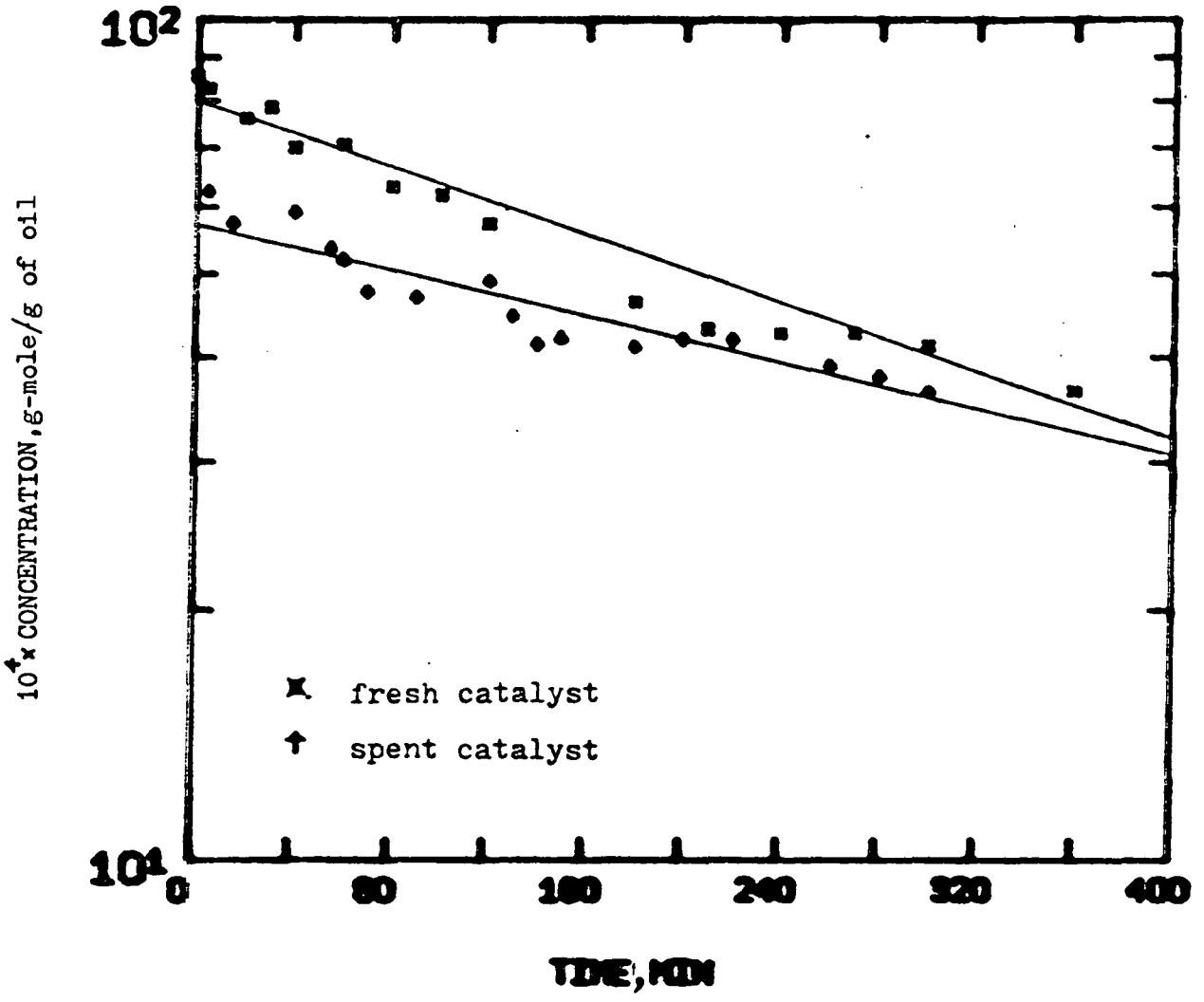


Figure 30. HDN of quinoline with aged catalyst (American Cyanamid HDS-1442A). Run No. 130-73 from hydrocarbon research; the run duration was 534 hours at approximately 445°C and with a coal slurry density of 70 lbs/cu.ft. The throughput was 3,066 lb of dry coal/lb of catalyst. There was an 80% reduction in catalyst activity.

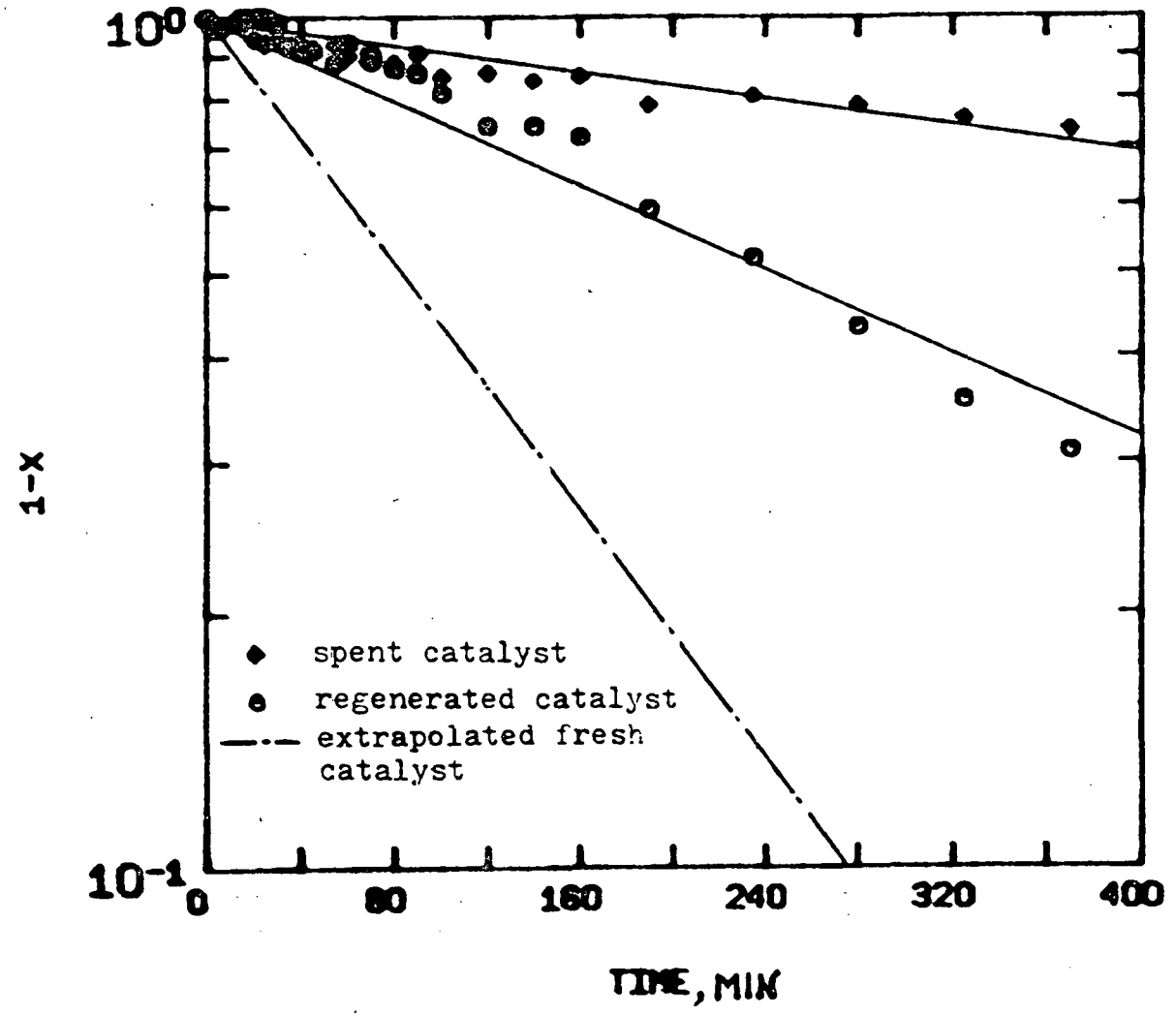


Figure 31. HDS of DBT with aged spent catalyst. Regeneration by burning yielded only a partial recovery of the catalyst activity, and therefore simple burning does not appear to be attractive.

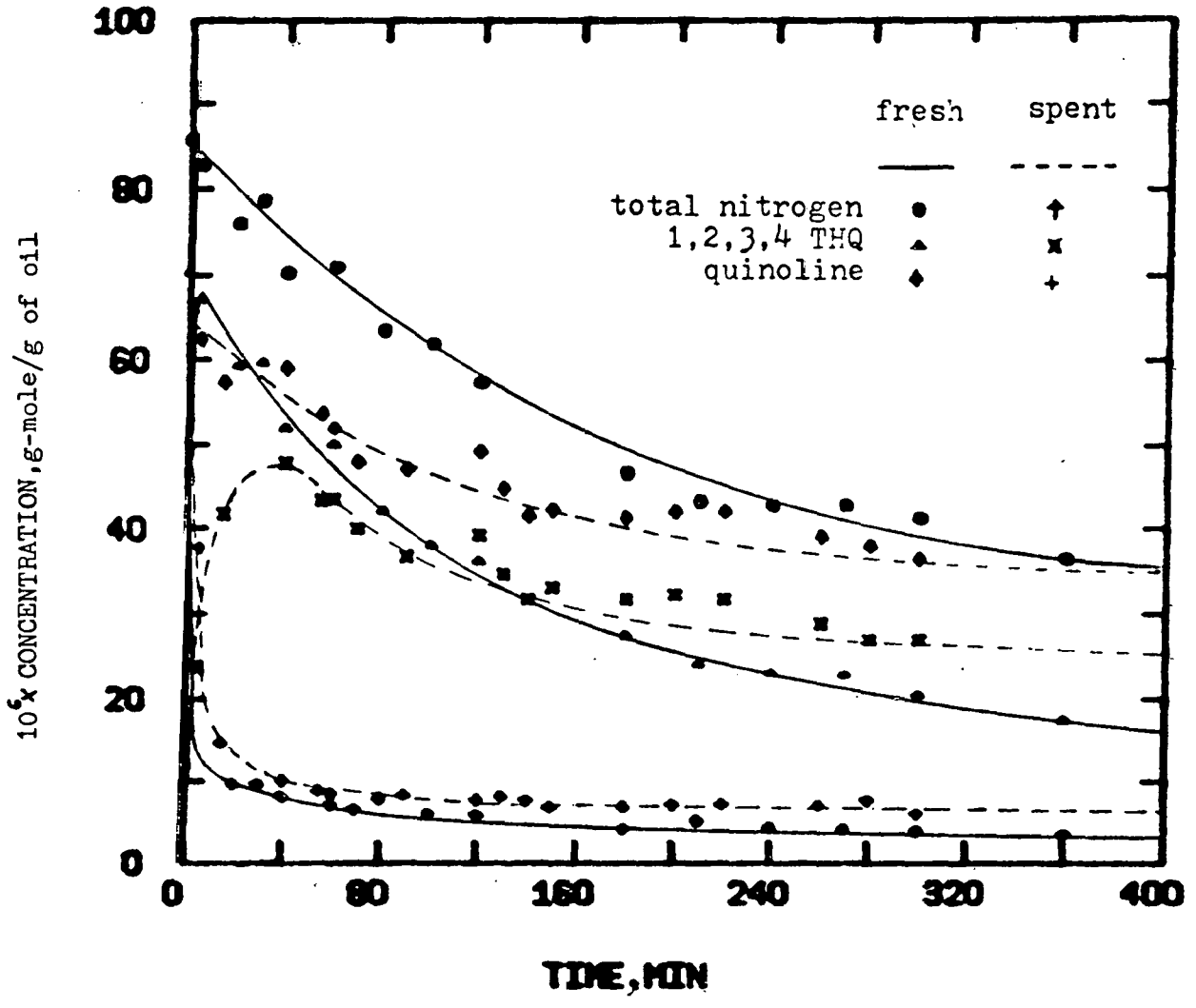


Figure 32. HDN of quinoline with aged catalyst, major component. In contrast with the fresh catalyst, the equilibrium between quinoline and tetrahydroquinoline is not established until a relatively long time (30 min. of operation).

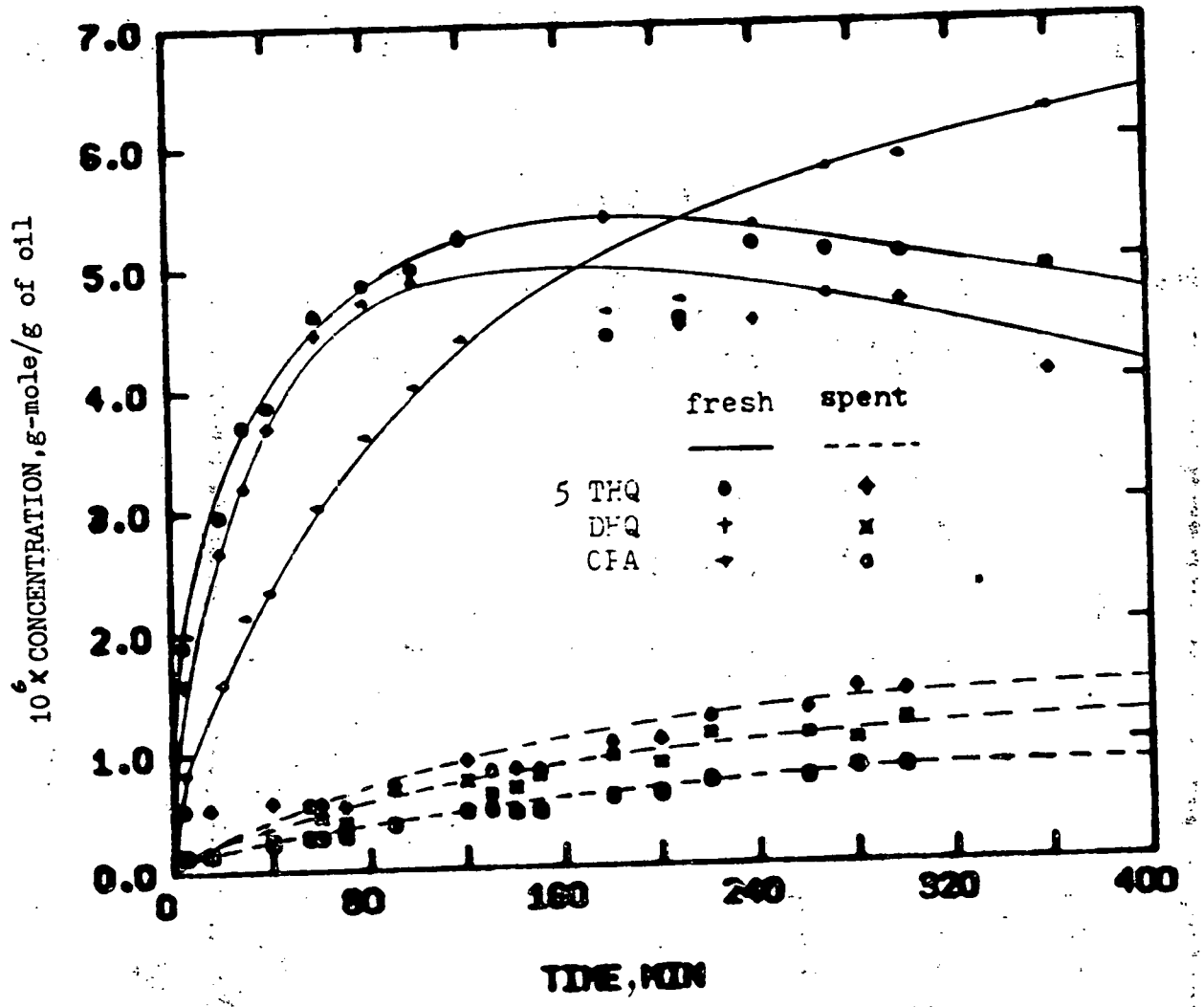


Figure 33. HDN of quinoline with aged catalyst, minor components. The hydrogenation rates in the spent catalyst were reduced by about a factor of ten, and consequently the secondary and tertiary reaction products were found in very low concentration when the aged catalyst was used.

TABLE 14
CATALYTIC ACTIVITIES OF FRESH AND USED CATALYSTS

| | HDN | | HDS | | |
|---|---|---|---|---|---|
| Reactant | Quinoline | | Dibenzothiophene | | |
| Classification of catalyst | Aged | Fresh | Aged | Regenerated | Fresh |
| Operating conditions | 344.5°C<br>500 psig | 344.5°C<br>500 psig | 320°C<br>1000 psig | 320°C<br>1000 psig | 320°C<br>1000 psig |
| First-order reaction rate ($\frac{\text{g of oil}}{\text{g of catalyst/min}}$) | ( " ) | ( " ) | ($\frac{\text{cm}^3}{\text{g of catalyst/hr}}$) | ( " ) | ( " ) |
| Constant, k | 0.112 | 0.608 | 4.9 | 15.6 | 104.0 |
| Activity | 18.4% | 100% | 4.7% | 15% | 100% |

The rate constants tabulated for HDN and HDS are referred to total nitrogen and DBT, respectively.

# V. CONCLUSIONS

1. In the presence of sulfided $CoO-MoO_3/\gamma-Al_2O_3$ catalyst at 300°C and 104 atm, dibenzothiophene (DBT) reacts to give $H_2S$ and biphenyl in high yield. Methyl-substituted dibenzothiophenes react similarly. Each HDS reaction is first order in the sulfur-containing compound. The relative rate constants for the various reactants are the following: BT, very large; DBT, 1; 4-MeDBT, 0.16; 4,6-diMeDBT, 0.10; 3,7-diMeDBT, 1.7; and 2,8-diMeDBT, 2.6. These results are largely explained by steric effects. Groups located near the S atom restrict its interaction with a surface anion vacancy and lower the reactivity. Inductive effects explain the higher reactivities of the compounds having methyl substituents where they exert no steric influence.

2. In hydrodenitrogenation of acridine, a large amount of hydrogenation precedes nitrogen removal, and the carbon-nitrogen bond breaking is the rate-determining process. In the presence of $Co-Mo/\gamma-Al_2O_3$ catalyst, heteroaromatic ring hydrogenation is favored, and with a $Ni-Mo/\gamma-Al_2O_3$ catalyst, aromatic ring hydrogenation is favored. For both acridine and quinoline, little effect of replacing Co with Ni could be detected in the nitrogen removal reactions, although $Ni-Mo/\gamma-Al_2O_3$ is twice as active as $Co-Mo/\gamma-Al_2O_3$ for acridine.

3. The activity of aged catalyst from the H-Coal$^R$ process has been measured in batch experiments with dibenzothiophene and with quinoline. The activity was reduced 20-fold for HDS of dibenzothiophene and 5-fold for HDN of quinoline. Burning off of carbonaceous deposits increased the activity of the aged catalyst only three-fold for dibenzothiophene HDS, which implies that irreversibly deposited inorganic matter was responsible for most of the loss of catalytic activity.

## VI. LITERATURE CITED


1. Akhtar, S., Sharkey, A. G., Schultz, J. C., Yavorsky, P. M., Abs. 167th Meeting, ACS, Los Angeles, CA., March 31-April 5, 1974.

2. Beuther, H., ACS Meeting on Coal Conversion Catalysts, Pittsburgh, PA., 1975.

3. Campaigne, E., Hewitt, L., Ashby, J., J. Heterocyclic Chem. 6, 533 (1969).

4. Carruthers, W., Nature 176, October 22, 1955.

5. de Beer, V.H.J., and Schuit, G.C.A., Annals New York Academy of Sciences, p. 61 (1975).

6. Desikan, P., and Amberg, C., Can. J. Chem. 41, 1966 (1963).

7. Desikan, P., and Amberg, C., Can. J. Chem. 42, 843 (1963).

8. Eliezer, K. F., Bhinde, M., Houalla, M., Broderick, D., Gates, B. C., Katzer, J. R., and Olson, J. H., Ind. Eng. Chem. Fundamentals, in press.

9. Frye, C. G., and Mosby, J. F., Chem. Eng. Progr. 63(g), p. 66, Sept. 1967.

10. Gerdel, R., and Luchen, E.A.G., J. Amer. Chem. Soc. 87, 213 (1965).

11. Givens, E. N., and Venuto, P. B., Symposium on Hydrogen Processing of Solid and Liquid Fuels, ACS Meeting, Division of Petroleum Chemistry, Inc., Chicago Meeting, September 13-18, 1970.

12. Himmelblau, D. M., Jones, C. R., and Bischoff, K. B., I&EC Fundamentals 6, 539 (1967).

13. Jewell, D. M., Ruberto, R. G., and Swansinger, J. T., ACS Philadelphia Meeting, Division of Petroleum Chemistry, April 6-11, 1975.

14. Kolboe, S., and Amberg, C. H., Can. J. Chem 44, 2623, (1966).

15. Kruber, O., Raeithel, A., Chem. Ber. 87, 1469 (1954).

16. March, J., "Advanced Organic Chemistry. Reactions, Mechanisms, and Structures," McGraw-Hill, 1968, p. 56.

17. Owens, P. J., and Amberg, C. H., Adv. Chem. Ser. 33, 182, (1961).

18. Owens, P. J., and Amberg, C. H., Can. J. Chem. 40, 941, 947, (1962).

19. Sharkey, A. G., Jr., Schultz, J. C., and Friedel, R. A., Advan. Chem. Ser. 55, 643, (1966).

## VII. PUBLICATIONS

1. Stanulonis, J. J., B. C. Gates, and J. H. Olson, "Catalyst Aging in a Process for Liquefaction and Hydrodesulfurization of Coal," A.I.Ch.E. Journal 19, 417 (1976).

2. Eliezer, Kenneth F., Manoj Bhinde, Marwan Houalla, Dennis Broderick, Bruce C. Gates, James R. Katzer, and Jon H. Olson, "A Flow Microreactor for Study of High-Pressure Catalytic Hydroprocessing Reactions," Ind. Eng. Chem. Fundamentals, in press.

3. Chiou, M. J., and J. H. Olson, "A Method for Determining Catalytic Kinetics in a Pulse Microreactor System," submitted to Chem. Eng. Sci.

4. Houalla, M., D. Broderick, V.H.J. de Beer, B. C. Gates, and H. Kwart, Preprints, ACS Div. Petrol. Chem., in press (Chicago meeting, August-September, 1977).

5. Shih, S. S., J. R. Katzer, and H. Kwart, ibid., in press.

## VIII. PERSONNEL

There have been two changes in personnel this quarter: Ed Reiff has completed his M.Ch.E. thesis and left the group, and Dr. N. K. Nag has joined the group, working on hydrodesulfurization; Dr. Stuart Shih is expected to leave at the end of March and Dr. Marwan Houalla at the end of April.

☆U.S. GOVERNMENT PRINTING OFFICE:1977 -740 -306/ 205 REGION NO. 4